NOTICE

The quality of this microform is heavily dependent upon the quality of the original thesis submitted for microfilming. Every effort has been made to ensure the highest quality of reproduction possible.

If pages are missing, contact the university which granted the degree.

Some pages may have indistinct print especially if the original pages were typed with a poor typewriter ribbon or if the university sent us an inferior photocopy.

Reproduction in full or in part of this microform is governed by the Canadian Copyright Act, R.S.C. 1970, c. C-30, and subsequent amendments.

AVIS

La qualité de cette microforme dépend grandement de la qualité de la thèse soumise au microfilmage. Nous avons tout fait pour assurer une qualité supérieure de reproduction.

S'il manque des pages, veuillez communiquer avec l'université qui a conféré le grade.

La qualité d'impression de certaines pages peut laisser à désirer, surtout si les pages originales ont été dactylographiées à l'aide d'un ruban usé ou si l'université nous a fait parvenir une photocopie de qualité inférieure.

La reproduction, même partielle, de cette microforme est soumise à la Loi canadienne sur le droit d'auteur, SRC 1970, c. C-30, et ses amendements subséquents.

ISBN 0-315-56385-0

Canada

PHASE BEHAVIOR OF TWO BINARY SYSTEMS CONTAINING ETHYLENE AT SUPERCRITICAL CONDITIONS

by

ADOLF S.F. CHEUNG

A Thesis

Presented to the University of Ottawa

in Fulfillment of the Thesis

Requirement for the Degree of

Master of Applied Science

in

Chemical Engineering

Department of Chemical Engineering

University of Ottawa

UNIVERSITÉ D'OTTAWA
UNIVERSITY OF OTTAWA

Acknowledgements

In presenting this thesis, I would like to express my sincere thanks to the following people and organizations for their support of this work.

Dr. Benjamin C.-Y. Lu, Professor of Chemical Engineering and my principle research director, for his encourgement, guidance, advice and full support, without which this work would not have been possible.

The technical staff of the Department of Chemical Engineering of the University of Ottawa, **Mr. J. Gasperetti**, and his assistants, **D. Lefebvre, L.G. Tremblay**, and **A. Bonaldo**, for their excellent technical assistance in the design and fabrication of the experimental equipments.

Mr. Michael M. Margerum for his help with the computational works.

Mr. Dingan Zhang for permission to use his experimental apparatus, and his invaluable suggestions in both computational as well as experimental works.

Natural Science and Engineering Research Council of Canada for awarding me a Postgraduate Scholarship.

University of Ottawa for awarding me a Graduate Research Supplementary Scholarship.

Finally, I would like to express my deepest appreciation to my parents and my family for their encouragement and love.

Abstract

The high pressure phase behavior of two binary mixtures containing ethylene was experimentally investigated. The "first freezing point" technique was used in this study to measure the pressure-temperature-composition (P-T-x) values along the three-phase coexistence curve for naphthalene-ethylene and biphenyl-ethylene systems. The T-x data of the three-phase coexistence curve was correlated using the van Laar equation. The best fitted valued of A_{12} and A_{21} were 1.9524 and 1.0492 for naphthalene-ethylene system and 3.0647 and 1.0481 for biphenyl-ethylene system, respectively.

The Peng-Robinson equation of state with one or two-parameter random mixing rules was used to correlate the P-T-x section of the three-phase coexistence curve. By treating the k_{ij} and l_{ij} in the mixing rules as temperature independent, it was found that the P-T projection of the three-phase curve can be well correlated. However, the prediction of composition values are very poor. In addition, the k_{ij} in the mixing rules was found to have a profound effect on the representation of P-T-x data. By considering the k_{ij} as a function of temperature, calculation of the equilibrium data indicate that the one-parameter temperature dependent random mixing rules were much better than the two-parameter temperature independent random mixing rules in correlating the equilibrium data, especially in the prediction of liquid-phase compositions.

Nomenclature

List of Symbols

- A_{12}, A_{21} : parameters of the van Laar equation.
- B_{12} : cross second virial coefficient.
- A,B : equation of state parameters.
- A, B, C : Antoine equation constants.
- E : enhancement factor.
- $\Delta \tilde{G}_f$: molar Gibbs free energy change of fusion, $J \cdot mole^{-1}$.
- $\Delta \tilde{H}_f$: molar heat of fusion, $J \cdot mole^{-1}$.
- LCEP : lower critical end point.
- MW : molecular weight.
- P : pressure, MPa.
- P_c : critical pressure, MPa.
- R : gas constant, $J \cdot mole^{-1} \cdot K^{-1}$.
- T : absolute temperature, K.
- T_c : critical temperature, K.
- T_m : melting temperature of heavy component, K.

- UCEP : upper critical end point.
- V : volume, cm^3.
- Z : compressibility factor.
- a(T), b, α(T) : parameters in equation of state.
- γ_i : activity coefficient of component i in the liquid mixture.
- $\hat{\phi}_i$: fugacity coefficient of component i in the mixture.
- f : fugacity.
- $\hat{f}_i$: fugacity of component i in the mixture.
- k_{ij} : binary interaction coefficient in the mixing rule.
- l_{ij} : binary interaction coefficient in the mixing rule.
- m : mass.
- n : number of moles.
- v : molar volume, $cm^3 \cdot mole^{-1}$.
- x : liquid mole fraction.
- y : vapor mole fraction.

Greek Symbols

- α, β : phases index.
- γ : activity coefficient.
- ϕ :fugacity coefficient.
- ρ : density.
- ω : acentric factor.
- Ω_{ac}, Ω_{bc} : dimensionless quantities Ω_a and Ω_b at the critical point.
- μ : chemical potential.

Superscripts

- s : solid state.
- l : liquid state.
- f : fluid state.
- o : pure state.
- sat : saturated state.
- $\bar{}$: molar property.

Subscripts

- 1 : heavy component.
- 2 : light component.
- c : critical property.
- m : melting property.
- r : reduced property.
- mix : mixture property.
- ij, ji : pertaining to the binary pair of molecules i and j.
- cal : calculated value.
- exp : experimental value.

Contents

List of Figures

List of Tables

Chapter 1

Introduction

In chemical industries, the two most widely utilized separation techniques are distillation and liquid extraction. Conventional distillation is used when relative volatilities of consitituents are different. On the other hand, if the relative volatilities between constituents are the same or if the constituents are thermally labile, then liquid extraction is the preferred separation technique. In recent twenty years, due to rapidly increasing energy costs, air pollution concerns, and increasing government regulations of traditional industrial liquid solvents used in food and drug industries, supercritical fluid extraction (SFE) technology has received much attention and has been applied to a large number of industries such as the chemical, pharmaceutical, food, and petroleum industries.

Supercritical fluid extraction combines features of both distillation and liquid extraction and is based on the experimental observation that a highly compressed gas exhibits enhanced solvating power. Due to the unusual behavior of solute dissolved in fluid under supercritical conditions, as first discovered by Hannay and Hogarth [1], this subject has been an active area of fundamental research, experimentation, and thermodynamic modelling. In this chapter, the basic concept and application of SFE are highlighted.

1.1 Definition of Supercritical Fluid

A phase is a homogeneous, physically distinct part of a system, separated from other parts by definite boundaries. For pure substance, the Gibbs phase rule specifies a maximum of two independent variables. Therefore, the phase behavior of pure substance can be represented by two convenient varibales such as pressure and temperature [2]. Figure 1.1 shows a typical pressure - temperature phase diagram for pure substance. Solid, liquid, and gas exist in the areas so indicated in the diagram. The solid lines represent the phase boundaries. The line OA represents the vapor pressure curve where liquid and vapor are in equilibrium. The line OC represents the sublimation curve and separates the solid and gas regions. Along this line solid and vapor exist in equilibrium. The line OB represents the effect of pressure on the melting point of pure substance. The slope of this line can be positive or negative. All three curves meet at the triple point, O, where all three phases coexist in equilibrium. The vapor pressure curve OA stops at the critical point, A. The coordinates of this point are the critical pressure P_c and the critical temperature T_c. These point represents the highest temperature and pressure at which a pure substance can exist in liquid-vapor equilibrium. A phase is considered to be a vapor if it can be condensed by a reduction of temperature at constant pressure, and a liquid if it can be vaporized by isothermal decompression. The fluid region, existing at higher temperature and pressure is marked off by dashed lines. As the fluid region fits neither of these definitions, the term supercritical fluid (SCF) is applied to this region.

Since supercritical fluid is neither a gas nor a liquid, its properties are therefore intermediate between those of a liquid and a gas. The diffusivity and viscosity of a supercritical fluid as shown in Table 1.1 are intermediate to that of a liquid or a gas. The density of a supercritical fluid approaching that of a liquid [3]. As pointed out by many review papers [4,5,6,7], the solvent power of a supercritical fluid can be approximated by its density. Higher density of supercritical fluid

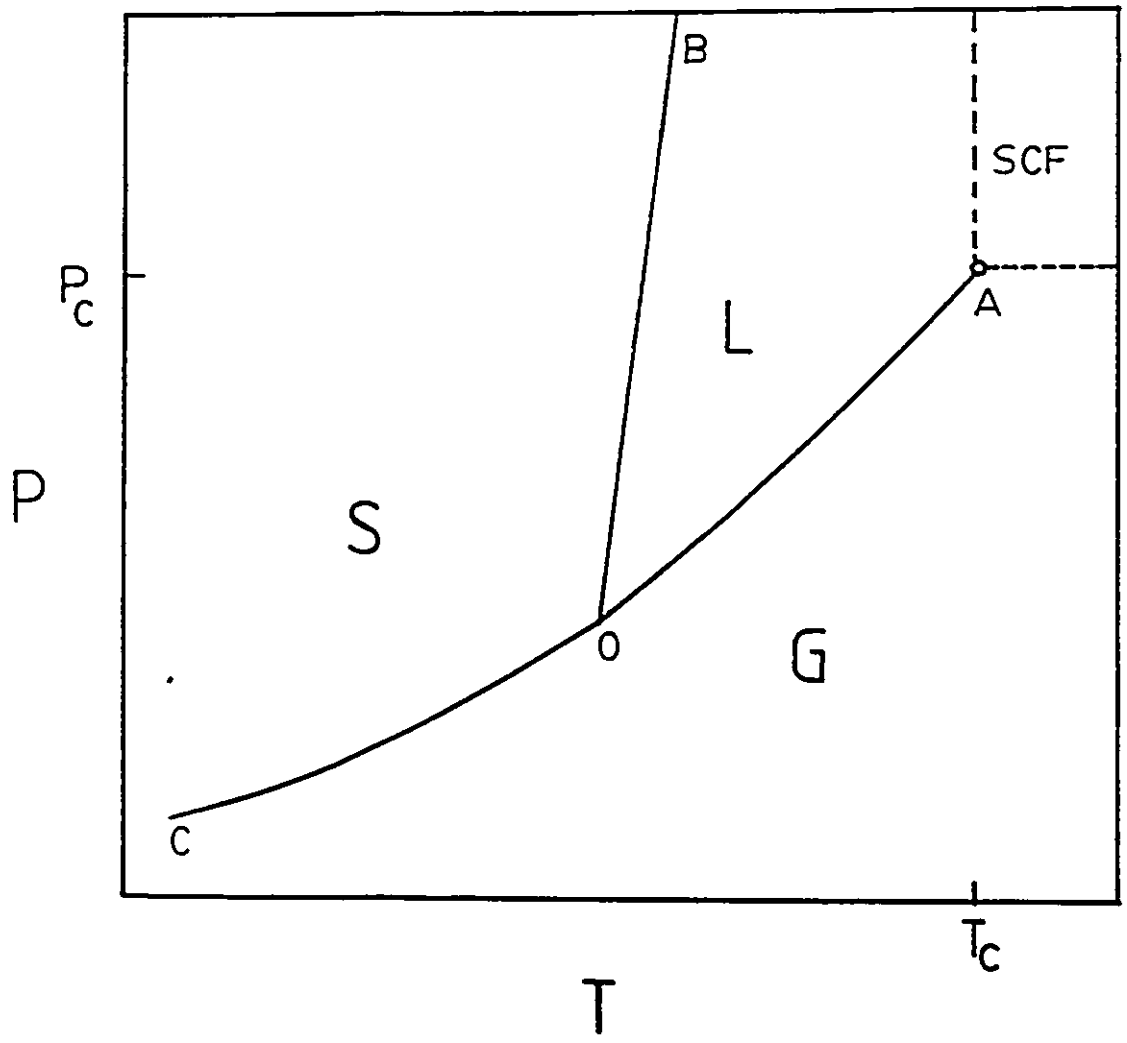

Figure 1.1 : P-T projection for a pure substance.
S : solid; L : liquid; G : gas; SCF : supercritical fluid;
A : critical point; O : triple point;
OA : vapor pressure curve; OB : melting curve;
OC : sublimation curve.

Table 1.1 : Properties of a gas, a liquid, and a supercritical fluid [3]. (order of magnitude only)

property	gas	supercritical * fluid	liquid
density ($\frac{g}{cm^3}$)	10^{-3}	0.7	1.0
diffusivity ($\frac{cm^2}{s}$)	10^{-1}	10^{-3}	10^{-5}
viscosity ($\frac{g}{cm \cdot s}$)	$10^{-3} - 10^{-2}$	10^{-2}	10^{-1}

* CO_2 at 305.15K and 14.0 MPa

indicates higher dissolving capacity for solute than a gas. These remarkable fluid characteristics, i.e. less resistance to mass transfer, large density, and hence higher solvent power make supercritical fluids a desirable solvent in separation processes.

1.2 Supercritical Fluid Extraction

Supercritical fluid extraction covers the application of fluid at supercritical or near critical conditions in separation operations. The observation that an increase in temperature or decrease in pressure is accompanied by a decrease in density and hence in the solvent power of supercritical fluid form the basis of SFE applications. The solvent power of a supercritical fluid is determined by density, and density in turn strongly depends on pressure and temperature. Beside density, other physical properties such as thermal and transport properties also play an important role in the design and development of SFE. For example, the transport properties provide the driving force and control the rates of mass transfer between the solute and solvent. The thermal properties determine the amount of energy required during the process. Therefore, a suitable supercritical solvent must have the following properties :

- Good solvent regeneration characteristics;
- High density at supercritical or near critical region;
- Low viscosity and high diffusivity.

Figure 1.2 shows the reduced density of carbon dioxide as a function of reduced temperature and reduced pressure [8]. The two phases region is bordered by the dashed curve $ABCDE$. Above the dashed curve $ABCDE$, the solvent exist in one phase. At temperature below T_c, for example, at $0.9T_r$, isothermal compression of saturated vapor B will cause the vapor to condense and result

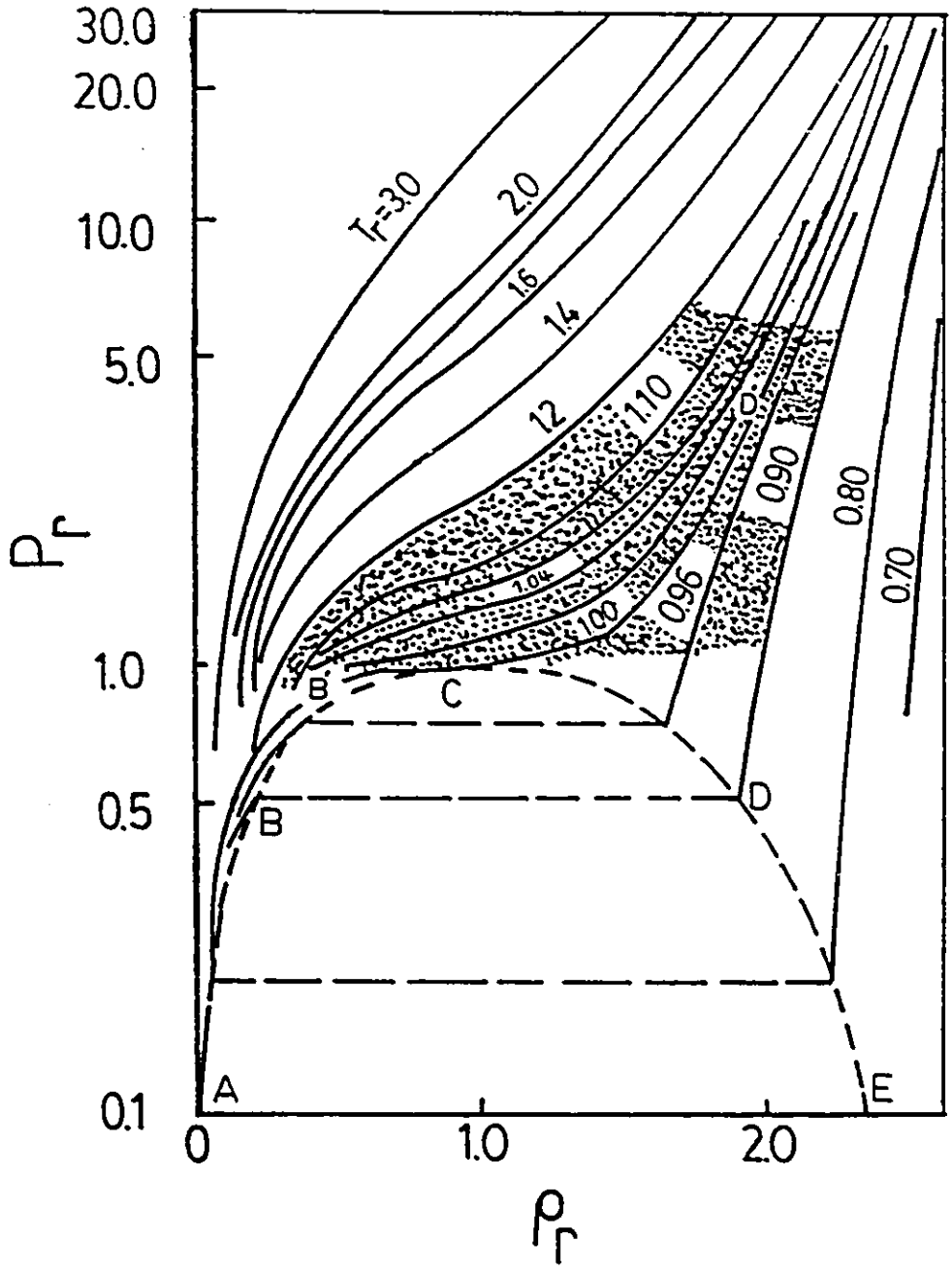

Figure 1.2 : Reduced density of CO_2 as a function of reduced pressure along lines of constant reduced temperature [8].

in the formation of a saturated liquid of density corresponding to point D. In order to obtain the liquid-like density, a phase transition must be observed. Just above the critical temperature, liquid-like density can also be achieved without crossing the phase boundary. For example at $1.04T_r$, small changes in pressure from B' to D' cause the same change in density without formation of second phase. Since the density of supercritical CO_2 at D' is the same as the density at D, supercritical CO_2 at D' could also act as a solvent. The shaded area shows the typical region of most interest for supercritical fluid extraction. At higher temperature above the shaded region, says $1.6T_r$, higher pressure is required to achieve the density. In economic and design point of views, SFE is therefore usually carried out at temperature slightly above the critical temperature.

Based on the relationship between temperature, pressure, and density in Figure 1.2, it can be easily accepted that the solvent power of the supercritical fluid should be greater the lower the temperature at constant pressure, i.e. the closer to T_c. In a similar manner, at a given temperature, the solvent power of the supercritical fluid should be greater the higher the pressure. To illustrate the relationship between the solvent power and density, the solubility of naphthalene in carbon dioxide as a function of temperature along lines of constant pressure is shown in Figure 1.3 [9]. The relationship between the solvent density and solubility is obvious. Isothermal compression from 7 to 30 MPa will enhance naphthalene solubilities in CO_2 by several order of magnitudes. Isobaric heating at low to moderate pressure will decrease naphthalene solubilities. Both phenomena are closely related to the changing density of CO_2 by varying either pressure or temperature. In the latter case, although the volatility of naphthalene increase as the temperature increase, the effect of decrease in density and hence in solvent power of CO_2 is so large that a net decrease in solubilities is observed. Therefore, as a rule of thumb, solubilities increase with increasing solvent densities at constant temperature due to an increase in solvent power. With increasing temperature, change in

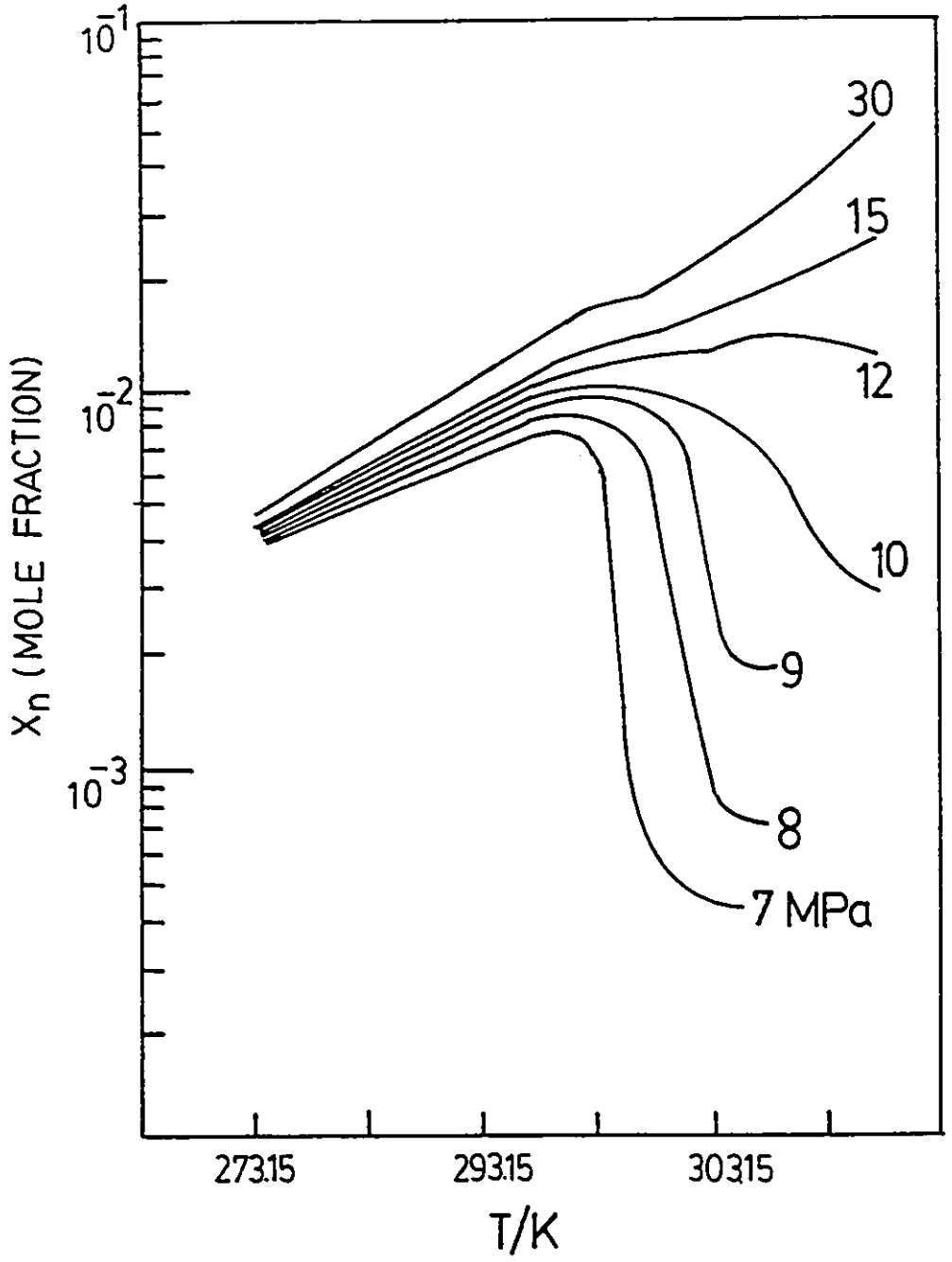

Figure 1.3 : Solubility of naphthalene in CO_2 as a function of temperature and pressure [9].

densities is relatively insignificant at high pressure and solubilities increase mainly due to increasing volatility of pure solute.

Since solvent recovery in SFE is achieved by selective manipulation of either temperature or pressure, a number of solvent regeneration schemes are developed as shown in Figure 1.4.

In Figure 1.4 A, the solute is removed from supercritical solvent by manipulating the pressure alone. This system contains two pressure units, one for extraction and the other for separation. The solvent power of the solvent is decreased by passing through a throttle valve. The extracts precipitate out of the fluid and the solvent is recompressed and recycled. An example of this type is the removal of spice extracts proposed by Vitzthum and Hubert [10].

Figure 1.4 B shows a similar process but uses temperature to manipulate the solvent power. Isobaric heating is used to achieve the separation in this case.

Unlike the above two regeneration schemes, Figure 1.4 C used absorbant to removed the solute from the mixtures. An example of this type include the removal of caffeine from supercritical CO_2 using methods such as water scrubbing or adsorption on to activated carbon.

Supercritical fluid extraction is characterized by the following features which exhibits desirable characteristics over distillation and liquid extraction :

- Properties of the supercritical fluid can be varied within a wide range of conditions by means of pressure and temperature;
- Easy recovery of solvent by decreasing the density of the supercritical phase, either by isothermal decompression or by isobaric heating;
- Thermally labile substance can be separated by supercritical fluid at mild temperature condition;

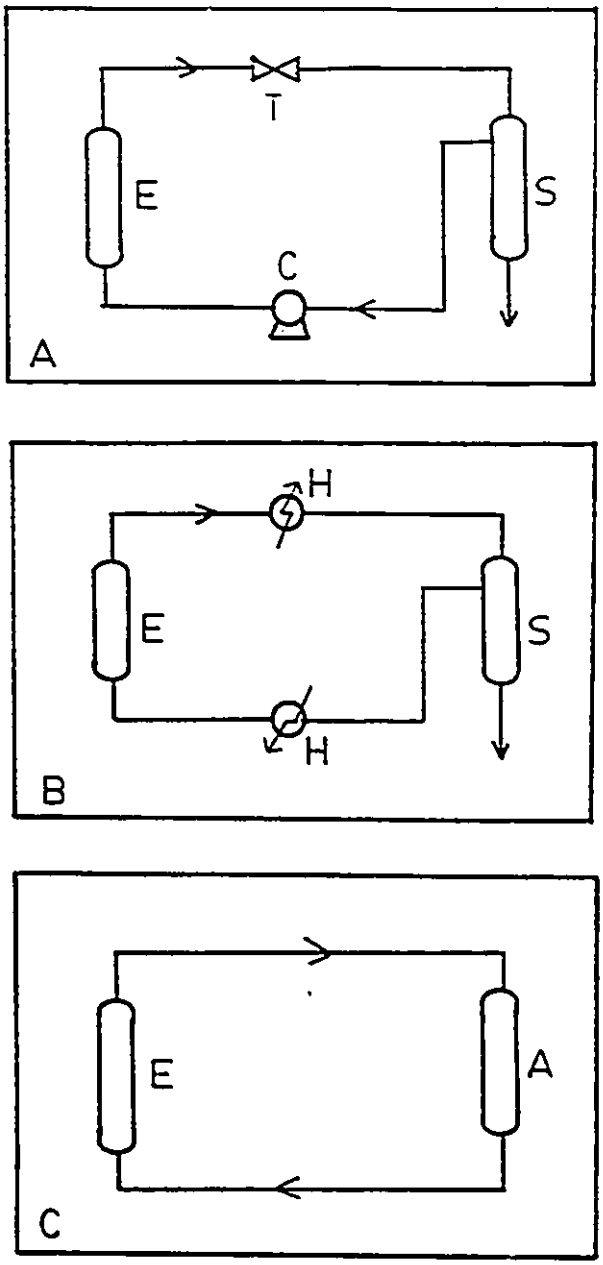

Figure 1.4 : Process schematic diagrams for supercritical extraction : ultilizing (a) pressure, (b) temperature, and (c) adsorption separation of solvent and solute.
E : extraction stage; C : compressor; T : trottle valve;
S : separation stage; H : heat exchanger; A : adsorption stage.

- Low volatility materials can be extracted by compressed gases;
- Solubilities of different substances may vary widely in supercritical fluid;
- Possibilities for fractionating extracts of complex substances by a series of pressure reduction.

High capital and operation cost are the major disadvantages of SFE processes due to the high pressure required to achieve the supercritical state. Besides, lack of experimental data, phase diagrams, and information on physical properties of complex systems further hindered the development of industrial SFE process. The above weaknesses made economics evaluation difficult and questionable which lead to a higher risk in capital investment. Therefore, SFE is usually considered as an alternative only when distillation or liquid extraction has significant weakness.

Experimental results indicated that the enhancement factor is strongly dependent on either temperature, pressure or the properties of the solvent. One ways to increase the enhancement factor is to modify the properties of solvent and hence the solvating power through the use of an entrainer [130]. An entrainer is a substance which has a volatility between the substances to be separated and the supercritical solvent. The entrainer modifies the polarizability and solvent strength (by slightly increased the molar density of solvent) of the supercritical fluid and therefore enhanced the solubility still further.

The advantages accompanying the use of an entrainer are summarized as follow :

- Improve the solubility of a low volatile solute;
- Modify the P-V-T behavior of the solvent or chemical nature (e.g polarity or relative size) of supercritical mixtures;
- Improve selectivity when extracting a mixture, i.e. separation factor;
- Save energy;

- Achieve solvent regeneration with small pressure drop.

Although an entrainer complicates the system, the solubility and separation factor are enhanced and, therefore from an energy economics point of view, one should not be restricted to using a supercritical gas alone as a solvent.

1.3 Applications of Supercritical Fluid Extraction

Within the past decade several SFE processes have been developed [11] and applied to energy, food, and chemical industries.

In energy industry, Kerr-McGee Corporation has developed a Residuum Oil Supercritical Extraction (ROSE) process for fractionating petroleum residues using a supercritical solvent such as pentane [12,13].

Petroleum residues consisting of asphaltenes, resins, and light oils are separated by a series of stagewise fractionation. It is based on the idea that high molecular weight materials are insoluble in supercritical pentane. Since asphaltenes are insoluble in pentane and therefore are separated as a bottom fraction. The next heaviest materials, resins, dissolving in pentane are precipitated out in second stage. Finally, the light oils and solvent are separated and the solvent is recompressed and recycled. The utility costs of ROSE process are estimated to be 50 per cent less than conventional distillation technique. Other advantage of ROSE process is that the impurities remain in the asphaltic fraction and the light oils can be further processed without addition treatment.

The Kerr-McGee Corporation has also developed a process called "Critical Solvent Deashing" using a supercritical solvent [14,15]. The need for an expensive filtering step is eliminated because the insoluble coal particles and ash are settled from solvent directly without the need to agglomerate or flocculate the insoluble coal particles and ash into larger particles.

In Great Britain, the use of supercritical solvent to extract the lower molecular weight components from coal is studied by the National Coal Board [16,17]. A suitable solvent such as toluene is used. The temperature of the extraction process is operated slightly greater than the critical temperature of toluene so that extensive thermal decomposition of the coal is prevented.

Another application in energy field is enhanced oil recovery (EOR) by injection of supercritical CO_2 into the oil reservoir [18]. The formation of a miscible mixture caused a large reduction in viscosity and surface tension of reservoir oil. The mobility of miscible mixture is greatly increased and therefore flow more easily.

Several other applications include the extraction of bitumen from tar sand and oil shale [19], and the fractionation of various fossil materials.

Recently, many extraction processes using supercritical solvent in food industry have been developed. The most popular cited example is the decaffeination of coffee bean by Hag AG in West Germany [20,21,22]. In this process, flavor and aroma oils are extracted from roasted coffee beans using dry supercritical CO_2. The caffeine is then extracted using wet CO_2 in second stage. In the final stage, extracted flavor and aroma oils are added back to the coffee beans. The solvent is recovered by either isothermal decompression, water scrubbing or adsorption. The use of entrainer or co-solvent has been proposed. Other supercritical fluids such as propane, butane have also been used in this kind of extraction process.

Other examples in food industry include extraction of oil from soybeans and potato chips using supercritical CO_2 [23,24,25], extraction of hops , spices, and tabacco [10,26,27], and finally extraction of flavor, aromas and drugs [28].

Examples of SFE process in the field of chemical industry include regeneration of activated carbon using supercritical CO_2 developed by Arthur D. Little inc [29], separation of isomers [30,31],

waste water treatment, and separation of organic substance from aqueous solution.

The separation of organic chemicals from dilute aqueous solution requires large energy consumption when conventional distillation is used [32]. Alternative separation method using supercritical fluid has received much attention. Elgin and Weinstock [33] reported the separation of water - organic mixtures using supercritical ethylene. Extraction of ethanol from water using both supercritical CO_2 and ethylene has also been reported. The results suggest the potential advantage of supercritical CO_2 over ethylene because of the higher ethanol solubilities in supercritical CO_2.

Besides industrial applications, a powerful analytical technique using supercritical fluid as an mobile phase is called "Supercritical Fluid Chromatography". The application of supercritical fluid as an mobile phase was first proposed by Klesper [34,35]. He pointed out that using supercritical fluid can achieve higher separation effeciencies in comparison to conventional liquid chromatography due to the more desirable transport properties of fluid than a liquid. In addition, thermally labile or high boiling substances can also be analyzed using supercritical fluid chromatography due to its low operating temperature and unusual solubilities of low volatile substances in supercritical phase.

1.4 Research Objectives

Future application of supercritical fluid extraction technique depends on our ability to understand and predict the unusual phase behavior which occurs at near critical or supercritical region. There is still a need for fundamental research because too little is known about the thermodynamics of fluid mixtures at supercritical conditions.

The possible experimental works include :

- the measurement of solubilities of heavy component (solid or liquid) in supercritical fluid;
- the effect of mixed solvent, so called "entrainer effect", on the solubility of solute in super-

critical fluid;

- the determination of phase boundaries (such as L-L-G or S-L-G three phase curve), and the critical loci (such as L=G or L=L), etc.

The solubilities of many nonvolatile components in supercritical fluid has been investigated [36 - 47]. In addition to the solubility measurements, the pressure-temperature (P-T) projection of the three phase coexistence curve has also been measured. For example, McHugh et al. [3,38,39,41] measured the three phase S-L-G coexistence curve for the binary systems such as biphenyl-CO_2, naphthalene-CO_2, and octacosane-CO_2. van Gunst et al. [48] measured the three phase S-L-G curve for naphthalene-ethylene, and biphenyl-ethylene binary systems, etc. In the study of McHuge et al., a large temperature minimum was observed in the P-T projection. Such temperature minimum was not observed in ethylene systems. Due to the temperature minimum in the P-T projection, thermodynamic correlations based on solid-fluid assumption are no longer valid in certain pressure ranges because some reported solubility data actually described a liquid-gas equilibrium [3,38,39]. Therefore the three phase coexistence curve is very important in correlation and prediction of phase behavior.

Figure 1.5 shown the P-T projection and corresponding P-x diagram for naphthalene-ethylene system [36,125]. Although the solubility increase fast near the LCEP ($T = 10.7℃, P = 52.0\ atm$), the overall loading power is still quite low. However, a large solubility enhencement was observed at 50℃ isotherm as the pressure increases to 175 atmospheres. This region is in the vicinity of the UCEP ($T = 52℃, P = 174.1\ atm$) of naphthalene-ethylene system. From the separation point of view, the advantages of operating near the UCEP are obsvious.

Experimental measurement of the three phase coexistence curve is important because the three phase curve provide a guide to the classification of the types of phase behavior, provide the

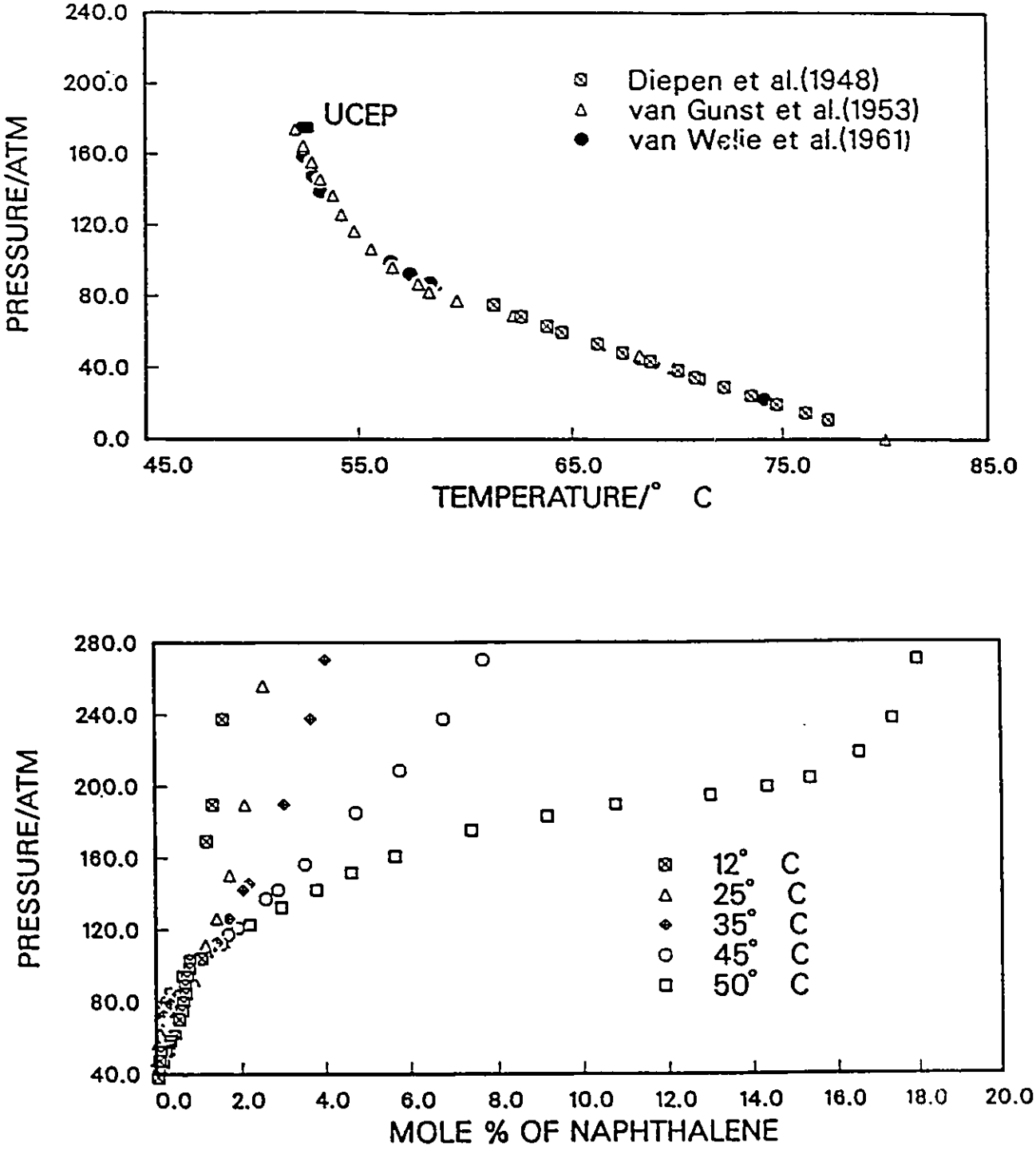

Figure 1.5 : P-T projection and superimposed P-x diagram for the naphthalene(1)-ethylene(2) system [36,125].

operating region where supercritical fluid extraction usually takes place, and the most important is that it provide information in which UCEP can be directly determined with the aid of critical loci.

The objective of this research is to study the phase behavior of naphthalene(1)-ethylene(2) and biphenyl(1)-ethylene(2) systems at supercritical conditions. The "First Freezing Point" technique was used to determine the equilibrium values along the three phase S-L-G coexistence curve. Although equilibrium pressure-temperature values for the two systems are available in the literature, equilibrium liquid compositions have not been reported for biphenyl-ethylene system. An effort was made in this work to determine the liquid composition along the three phase curve for biphenyl-ethylene system. The van Laar solution model was used to correlate the T-x data along the S-L-G coexistence curve obtained in this study. In addition, empirical equation of state such as Peng-Robinson together with one or two-parameter random mixing rules was used to correlate the equilibrium values along the three phase coexistence curve.

Chapter 2

Theoretical Background

Supercritical fluid extraction is a separation technique based on thermodynamics, predominantly on the phase equilibrium of fluid mixtures at high pressures. New applications of SFE largely depend on our understanding of phase behavior for mixtures which occurs at near critical or supercritical region. In this chapter, different types of phase behavior for binary mixtures are discussed. In addition, methods of correlation and prediction of phase behavior at supercritical conditions are also highlighted.

2.1 Description of Fluid Phase Equilibria

To understand the phase behavior is not an easy task even restricted to only binary systems. For simple systems, the locus of the critical points produced by changing compositions of mixture has a dome shape. Nonideal interaction can cause azeotropes, and formation of separate liquid, or gas phase at equilibrium. Also, the constituents may be solid through part of the temperature range. Differ in molecular size, shape, structure, and polarity of mixture components influence the shape on the continuity of the critical locus and hence make the phase behavior more complex.

Therefore, in order to explore the phase behavior for complex mixtures, it is better to understand the phase behavior for some well defined simple binary mixtures first. Several review articles [49,50,51,52,53,54] and books with extensive references to the relate literature provide more detailed descriptions of the phase behavior. Examples for other highly asymmetric mixtures are also given by Schneider [54].

Gibbs phase rule specifies a maximum of three independent variables for a binary system. Phase diagram for binary mixtures are usually represented by pressure-temperature-composition plots. Since pressure-temperature-composition plots require three dimensional graphic approach, one convenient way to presenting information is to illustrate the phase behavior in P-T projections and P-x diagrams at various temperatures. This kind of plots show the critical lines, liquid-gas phase boundaries, etc. For highly asymmetric mixtures, liquid-liquid and gas-gas equilibria together with complex critical behavior and a variety of end-points may offen occur [55].

In this chapter, two classes of supercritical phase behavior are discussed, one for binary mixtures containing similar components and the other for highly asymmetric binary mixtures.

The following nomenclature of symbols are used in this chapter :

- Subscript 1 and 2 represent low volatility solute and supercritical solvent respectively;
- Solid, liquid, and gas phases are designated by S, L, and G respectively.

The types of boundary curves (one degree of freedom) are:

- ——— : represents pure component equilibrium curve;
- - - - - : represents the loci of critical points produced by changing compositions;
- ····· : represents the three phase equilibrium curve, designated by LLG or SLG.

The types of points (zero degree of freedom) are:

- open circle represents the pure component critical point;
- solid circle represents the critical end points formed by the intersection of a critical line with a three phase curve, designated as Upper Critical End Point (UCEP) or Lower Critical End Point (LCEP);
- open triangle represents the pure component triple point.

2.1.1 Phase Diagrams for Binary Fluid Mixtures

One major type of binary system occurs where the critical point temperature of the light component lies well above the triple point temperature of the heavy component. The phase behavior of such systems involves only fluids. van Konynenberg and Scott [56,57] demonstrated that most observed phase diagrams can be described quantitatively by using an equation of state. Different types of phase behavior can be classified according to the shapes of the critical lines, the absence or present of three phase lines, and the way the critical lines connect with the pure component critical points and the three phase lines. Scott and van Konynenbery [56,57] classified phase diagram into six major types, designated I to VI in Figure 2.1. Type I to V are predicted using the van der Waals equation of state [58]. They recognized a sixth class (VI) that occurs in some aqueous systems which cannot be predicted by an equation of state.

Figure 2.1 a shows the type I systems which usually composes of molecules of similar size and polarity. Type I is the simplest binary system and has a continuous critical locus which connects the two pure component critical points. Above the critical line the components are completely miscible in all proportions, for example at point O. The critical locus therefore represents the upper boundary of a surface on which gas and liquid exist in equilibrium. For reprecipitation of extracted components, liquid-gas heterogeneous regions have to be entered either by isothermal

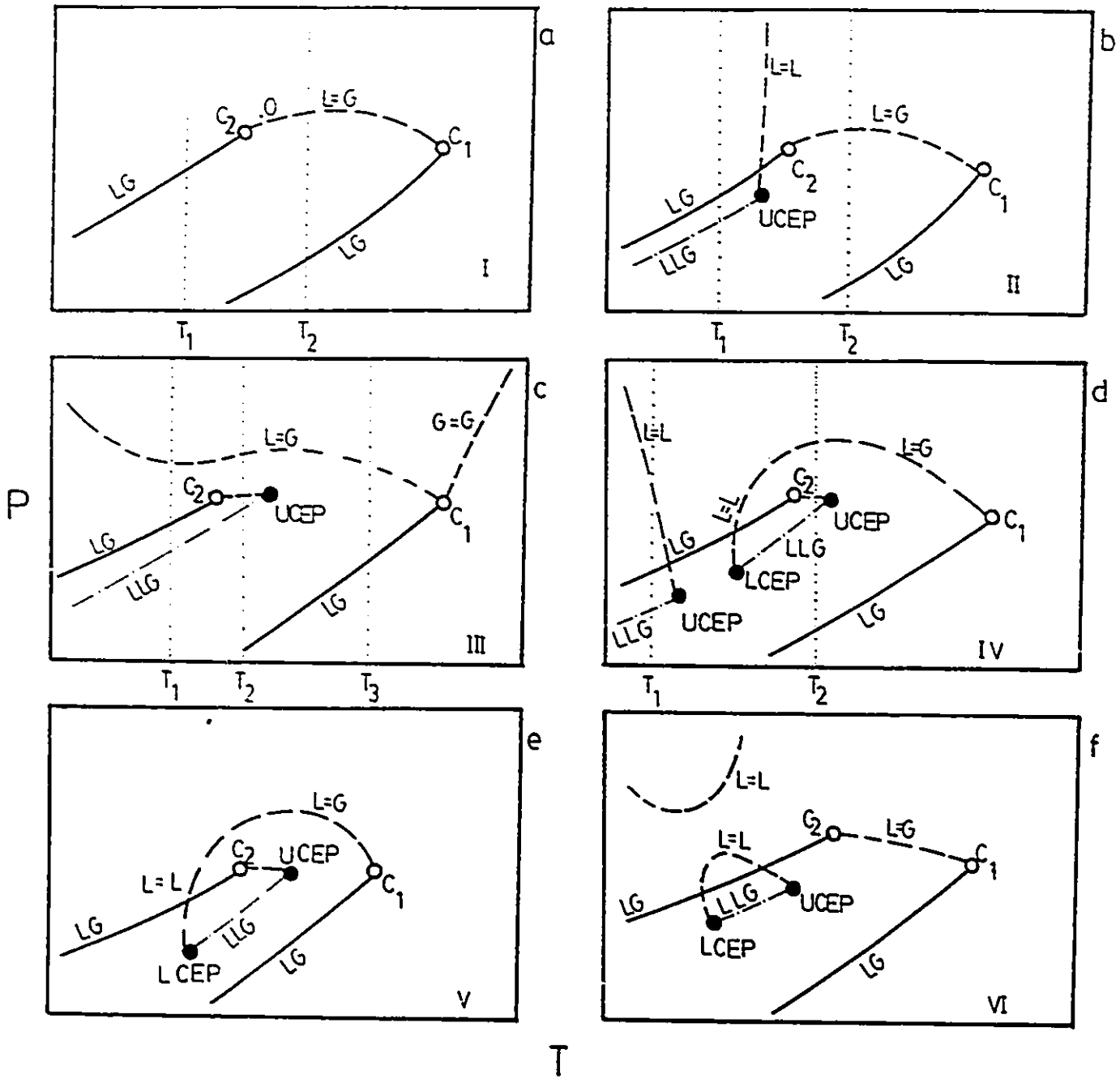

Figure 2.1 : Classification of P-T projections for binary fluid systems.
- - -:critical loci; -·-·-:three phase L-L-G coexistence curve;
——:pure component equilibrium curve;
C_1, C_2:critical points; •:critical end point.

decompression or isobaric heating. In addition, the critical line can exhibits either a pressure maximum, a pressure minimum, or neither. Examples of type I systems include methane-propane and benzene-toluene [55].

Figure 2.2 a and b show the P-x plots for two different temperatures corresponding to T_1 and T_2 of Figure 2.1 a type I systems. Saturated liquid states occur above and saturated vapor states below each isotherm. For the isotherm at T_1, it cuts the vapor pressure equilibrium line of both components and the curves therefore extend all the way across the diagram. However, for the isotherm at T_2, it passes through one mixture critical point and the curve shown in Figure 2.2 b do not extend all the way across the diagram. The saturated liquid and saturated vapor phases become identical at the critical point C.

Figure 2.1 b shows the type II systems which may occur when the size and/or polarity difference between the components increase. The critical line is still continuous except the system exhibits a region of liquid-liquid immiscibility at temperature far below the critical temperature of light component. A three phase LLG line exists below the vapor pressure curve of the light component and terminates at the upper critical end point (UCEP). A critical locus for liquid-liquid equilibrium starts at the UCEP and extends upwards in the direction of increasing temperatures and pressures. The surface bounded by the LLG line and the liquid-liquid critical line represents liquid-liquid equilibrium. Beyond the critical locus the liquid phases disappear and become miscible. Examples of type II systems include ammonia-toluene and carbon dioxide-octane [55].

Figure 2.2 c and d show the P-x plots corresponding to T_1 and T_2 of Figure 2.1 b type II systems. For the isotherm at T_1, it cuts the three phase LLG line and the vapor pressure curve of component 1. The two phase region at pressure below the three phase LLG line corresponds to liquid-gas equilibrium. At pressures above the three phase line, there is a small liquid-gas region.

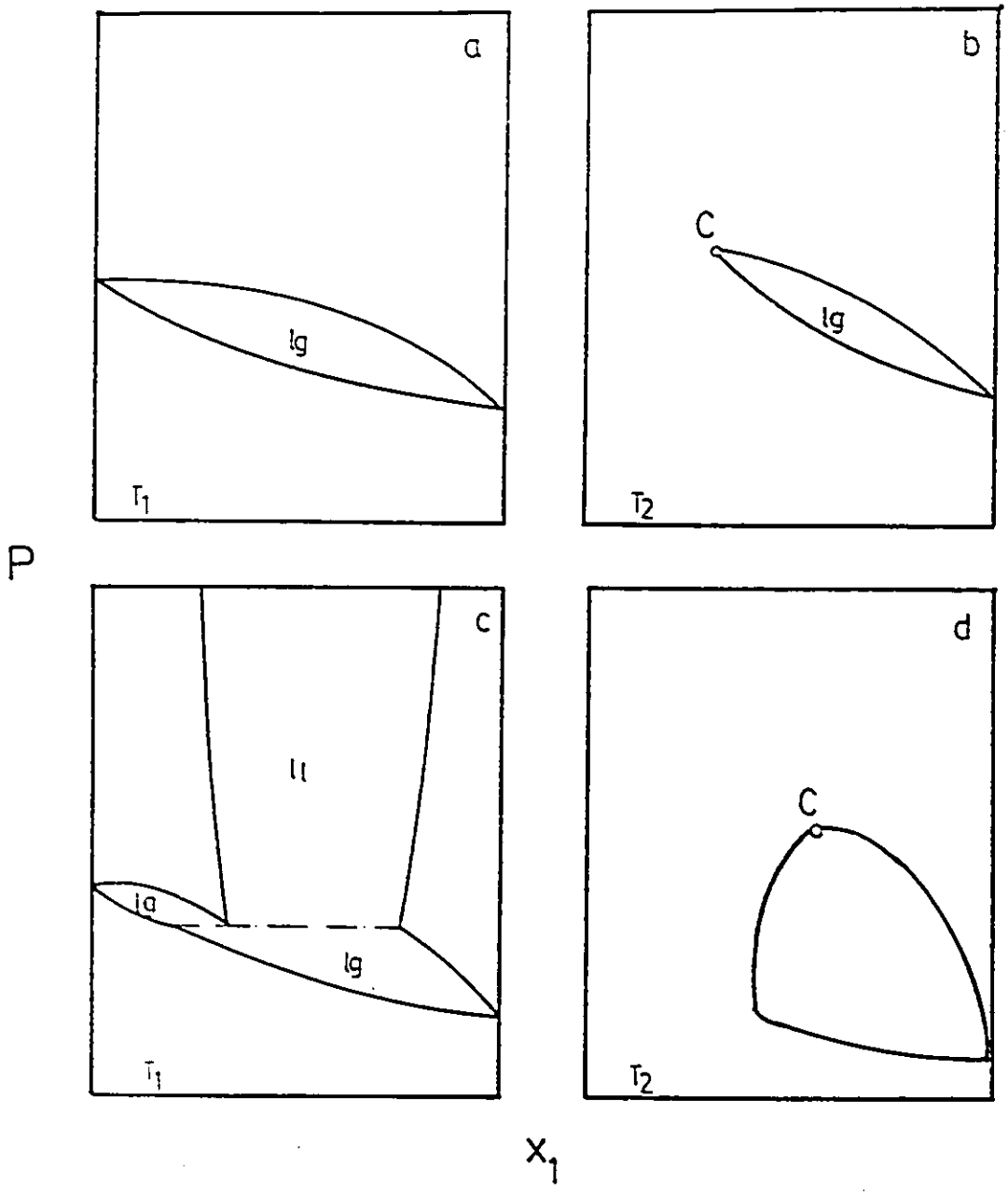

Figure 2.2: P-x diagrams for binary fluid systems of class I and II

In addition, due to the very different volatilities of the pure components, a liquid-liquid miscibility gap is found as shown in Figure 2.2 c. For isotherm at T_2, the P-x diagram is similar to that in Figure 2.2 b.

Larger size and/or polarity difference give rise to type III systems where the liquid-gas critical locus is no longer a continuous curve as shown in Figure 2.1 c. The LLG line cuts the liquid-gas critical locus into two branches. One branch connects the UCEP and the critical point of the light component. The other branch starts from the critical point of the heavy component and extends upwards into very high pressure regions, sometimes passing through maxima or minima in pressure and/or a minimum in temperature. Type III systems sometimes exhibit gas-gas equilibrium when the critical locus rises to supercritical region at high pressures. Examples of type III systems involving liquid-gas equilibrium include methane-hydrogen sulfide and carbon dioxide-hexadecane [55]. For gas-gas equilibrium, helium-hydrogen and helium-methane are the best examples [55].

Three P-x isotherms are shown in Figure 2.3 corresponding to the temperatures T_1, T_2, and T_3 of Figure 2.1 c type III systems. T_1 lies below the critical point of light component 2 and cuts the three phase LLG line, the vapor pressure curve of light component 2 and liquid-gas critical locus. The P-x diagram for T_1 isotherm is similar to that in Figure 2.2 c except the liquid-liquid miscibility gap forms a continuous locus and closes at the liquid-liquid critical point. The isotherm T_2 in Figure 2.1 c cuts the liquid-gas critical locus between C_2 and UCEP where the two phase region vanishes at this point. The liquid-liquid miscibility gap still exists but with a narrower gap. The P-x diagram for T_3 isotherm is similar to that in Figure 2.2 b.

Figure 2.1 d shows the type IV systems. Type IV systems are similar to type III systems except that the three phase LLG line is disconnected by the liquid-gas critical locus. This branch of the liquid-gas critical line starting from the critical point of heavy component has a maximum in

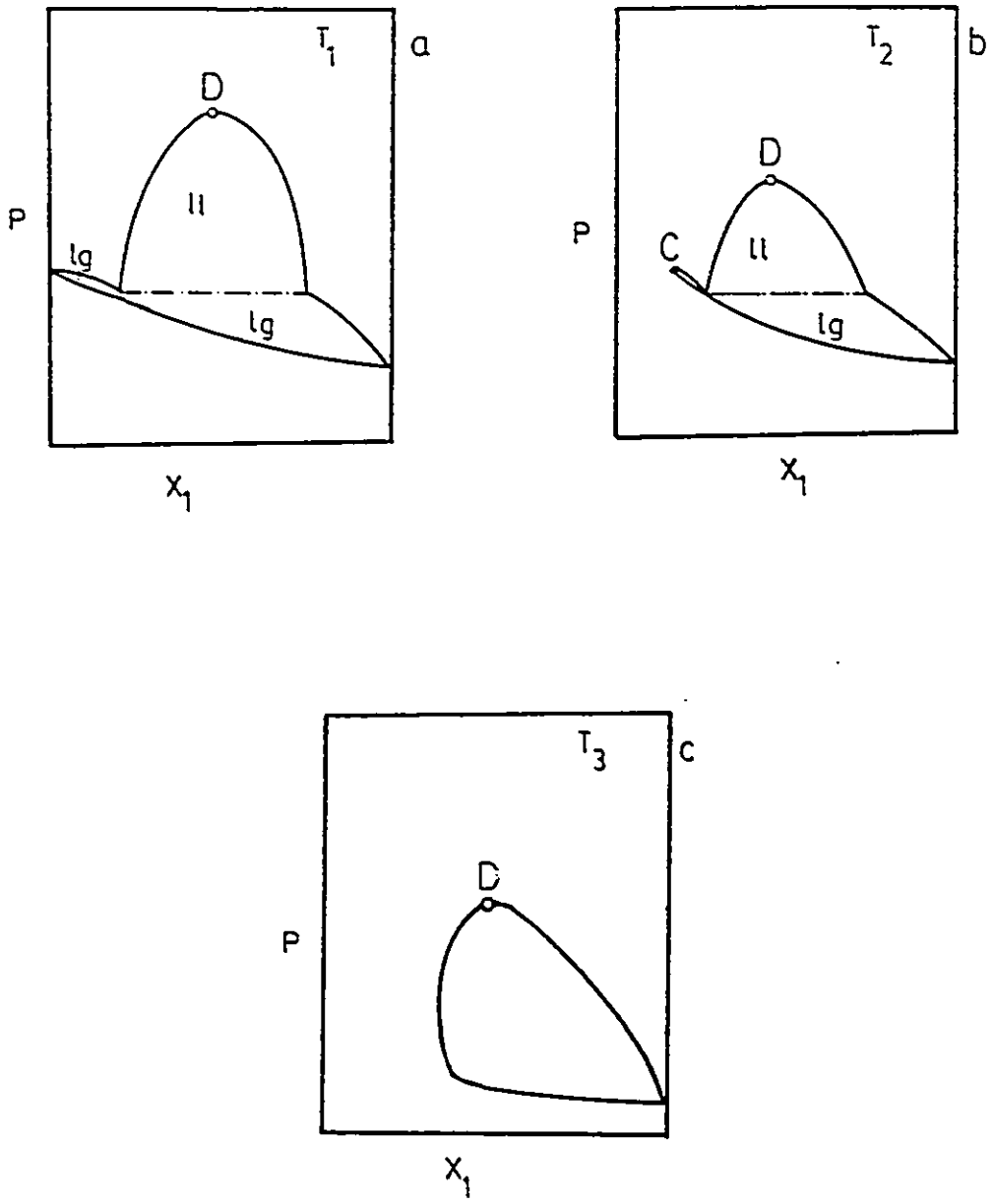

Figure 2.3: P-x diagrams for binary fluid systems of class III

pressure and passes continuously and cuts the three phase LLG line at the LCEP. A liquid-liquid critical locus starts from the other UCEP of LLG line and extends upwards into the high pressure regions. Example of type IV systems includes methane-hexane [55].

Figure 2.4 a and b show the P-x plots for temperature T_1 and T_2 of Figure 2.1 d type IV systems. Both P-x isotherms are similar to that in Figure 2.3 a and b.

Type V systems in Figure 2.1 e form if the lower branch of the LLG line of a type IV systems is absent. The liquids are completely miscible in all proportions below the LCEP. The three phase LLG line in this type is typically very short. Examples of type V systems includes ethane-ethanol [55].

Type VI systems in Figure 2.1 f occur only in aqueous mixtures such as heavy water-2 methylpyridine [55]. This type of systems have a short LLG line below the vapor pressure curve of light component with both LCEP and UCEP. The UCEP and LCEP are connected by the liquid-liquid critical locus. Also note that a second liquid-liquid critcal locus exists above the first at high pressures.

2.1.2 Phase Diagrams for Binary Mixtures Involving Solid Phase

Solid-fluid phase behavior may occur in highly asymmetric mixtures when the triple point temperature of non-volatile component is higher than the critical temperature of light component and there is no common range of temperature in which both pure components are liquids. According to the way the three phase equilibrium line connects with the critical line, the phase diagram can be classified into two groups as shown in Figure 2.5 and 2.6. Figure 2.6 can be further classified into three types according to the shape of the SLG line as shown in Figure 2.7 a, b, and c.

Figure 2.5 shows a type of phase behavior of highly symmetric binary mixtures which do not differ in molecular size, shape, and/or polarity and have a continuous liquid-gas critical line

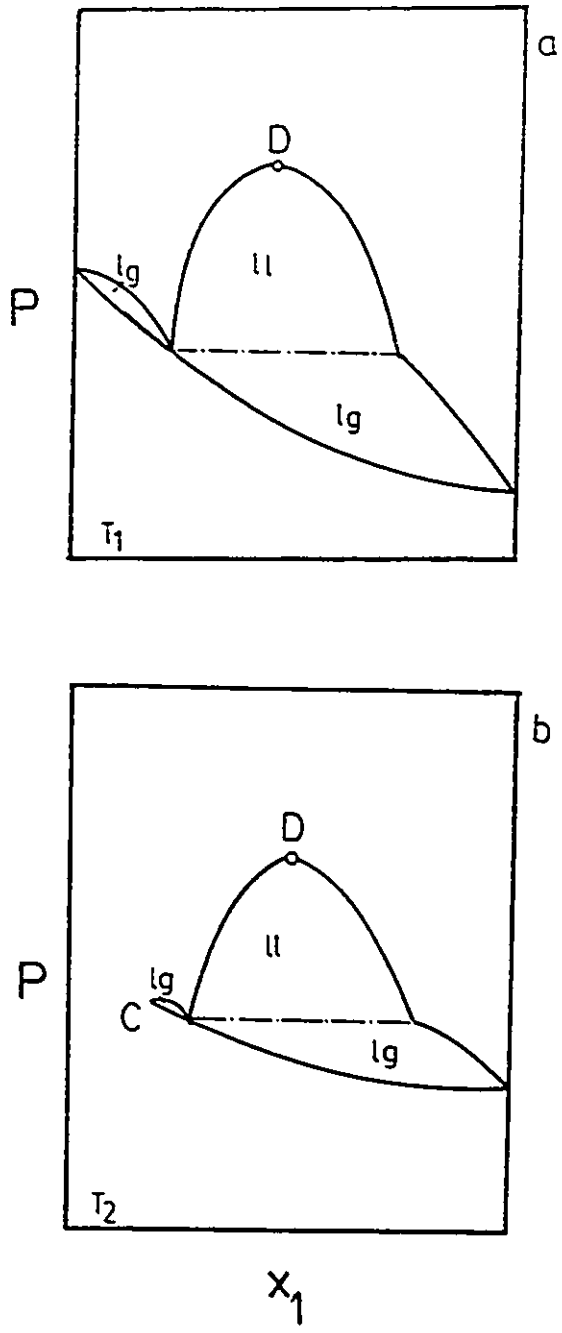

Figure 2.4: P-x diagrams for binary fluid systems of class IV

which connects the two pure components critical point. For pure substance the three phase SLG equilibrium is a point (Δ) according to the Gibbs phase rule. This nonvariant single component three phase point becomes monovariant (a line) upon addition of another component. Therefore, a three phase SLG line must orginating from the triple point of heavy component, passes through a pressure maximum and bends toward the low temperatures due to the addition of another component. This phenomenon is the so called "freezing point depression". Depends on the concentration of heavy component, different types of phase equilibrium exist above the three phase line. If the concentration of heavy component is very large, solid-gas equilibrium exists at all pressures above the three phase line. Otherwise, liquid-gas equilibrium exists until the liquid-vapor critical point is reached. Binary systems like sodium chloride-water and ethane-1,4-dichlorobenzene have this type of phase behavior [5].

Figure 2.6 illustrates another type of phase behavior of highly asymmetric mixtures which exhibit a smaller freezing point depression at high pressure. In this case, the three phase SLG line runs to pressures high enough for it to cut the liquid-gas critical line. A three phase SLG line exists below the vapor pressure curve of light component and terminates at the LCEP. For most of the binary systems reported in the literature, the LCEP usually occurs very close to the critical point of light component (C_2). The liquid-gas critical line was disconnected into two branches. One branch of liquid-gas critical line connects the LCEP and the critical point of light component. Another branch of liquid-gas critical line originates from the critical point of heavy component, (C_1), cuts the three phase SLG line which originates from the triple point of heavy component at the UCEP. Between the two branches of the SLG lines, solid-fluid equilibrium exists at all pressures. SFE process usually takes place between these regions. Liquid-gas equilibrium exists in the region bounded by the SLG line, liquid-gas critical line, and the vapor pressure curve. According to the

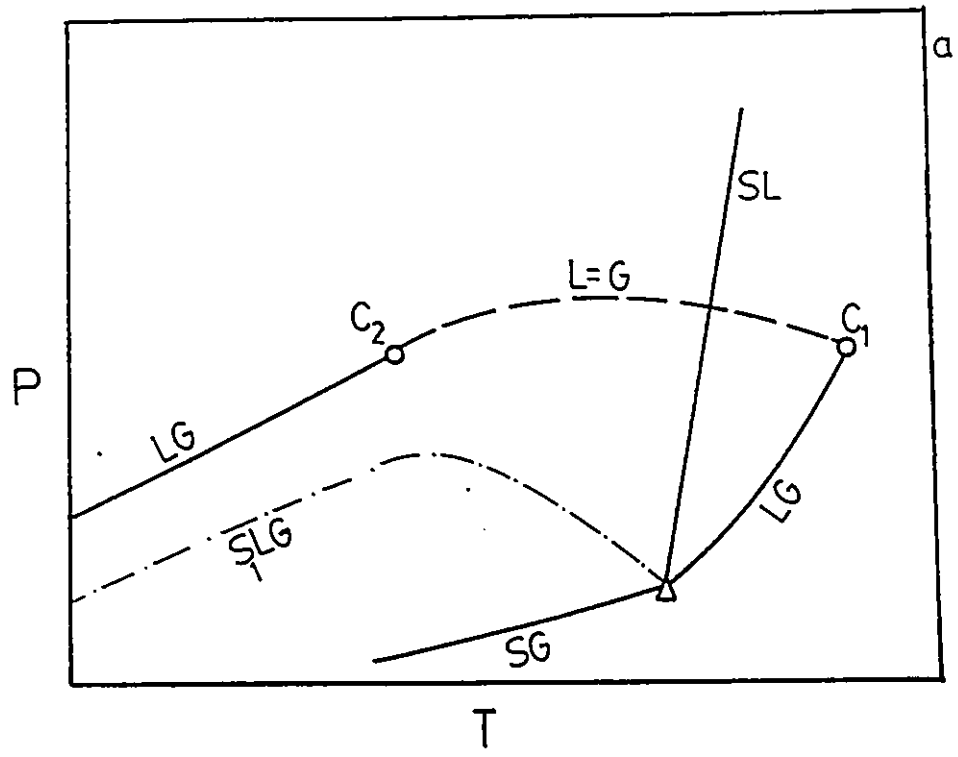

Figure 2.5 : P-T projection for binary mixtures of similar components.
- - -:L=G critical loci; -·-·-:three phase S-L-G coexistence curve;
——:pure component equilibrium curve;
C_1, C_2:critical points; Δ:triple point.

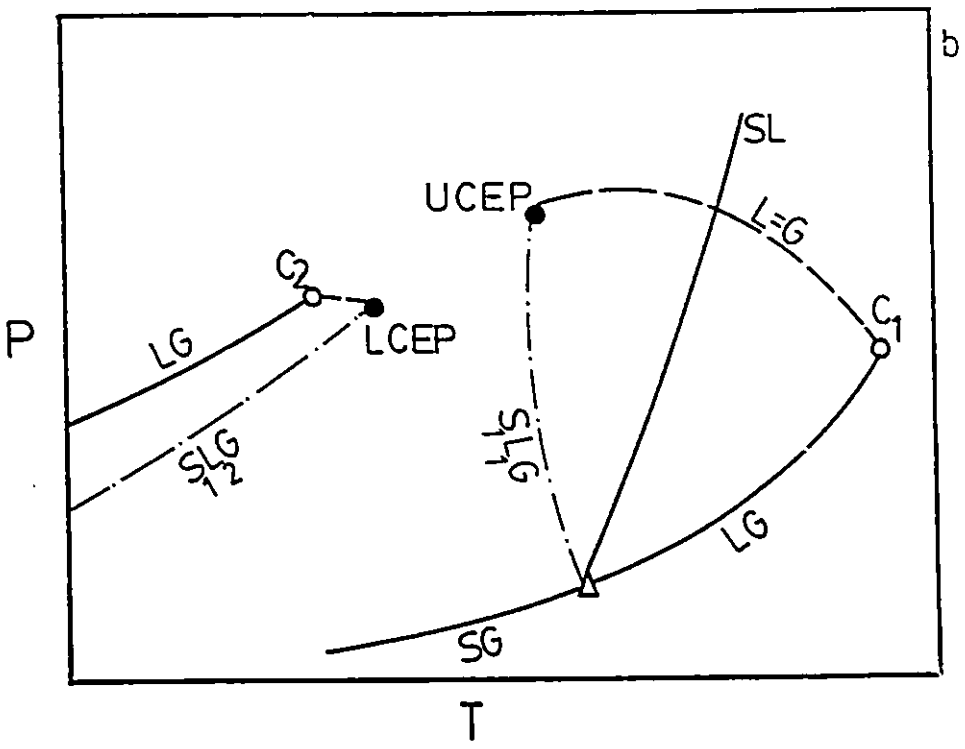

Figure 2.6 : P-T projection for highly asymmetric binary mixtures.
- - -:L=G critical loci; -·-·-:three phase S-L-G coexistence curve;
——:pure component equilibrium curve;
C_1, C_2:critical points; Δ:triple point; •:critical end point.

shape of the SLG line, the phase diagram can be further classified into three types as shown in Figure 2.7 a ,b, and c.

Figure 2.7 a shows the first type where the SLG line has a negative slope. Binary systems such as naphthalene-ethylene, biphenyl-ethylene, naphthalene-methane, and diphenylamine-carbon dioxide exhibit behavior of this type [5]. The region bounded by the vapor pressure curve of heavy component, the three phase SLG line, and the liquid-gas critical line is a region of liquid-gas equilibrium. In the temperature range between the LCEP and UCEP, no liquid phase exists and the solid phase of heavy component is in equilibrium with a light component rich gas phase.

Figure 2.8 shows the P-x diagram for four different temperatures corresponding to T_1, T_2, T_3, and T_4 of Figure 2.7 a. T_1 isotherm lies below the critical point of light component and cuts both the three phase SLG line and the vapor pressure curve. Below the three phase line, solid-gas equilibrium exists until the SLG line is reached as the light component is compressed. Above the three phase line, there is a small liquid-gas region and a solid-fluid region.

As the temperature increases from T_1 to T_2, the small liquid-gas region of Figure 2.8 a decreases in size, and vanishes at the LCEP. As temperature between the LCEP and UCEP, only solid-fluid equilibrium exists. The P-x diagram shown in Figure 2.8 b illustrates enhanced solubility of heavy component in supercritical solvent as the pressure increase.

Figure 2.8 c shown the P-x diagram for temperature between the UCEP and the melting temperature of heavy component. The isotherm passes through a solid-gas region, a liquid-gas region, and a solid-fluid region. Since the isotherm T_3 cuts the liquid-gas critical line, the liquid-gas region vanishes at point C.

Figure 2.8 d shown the P-x diagram for temperature between the melting temperature and the critical temperature of heavy component. At these temperature range, the solid-gas region

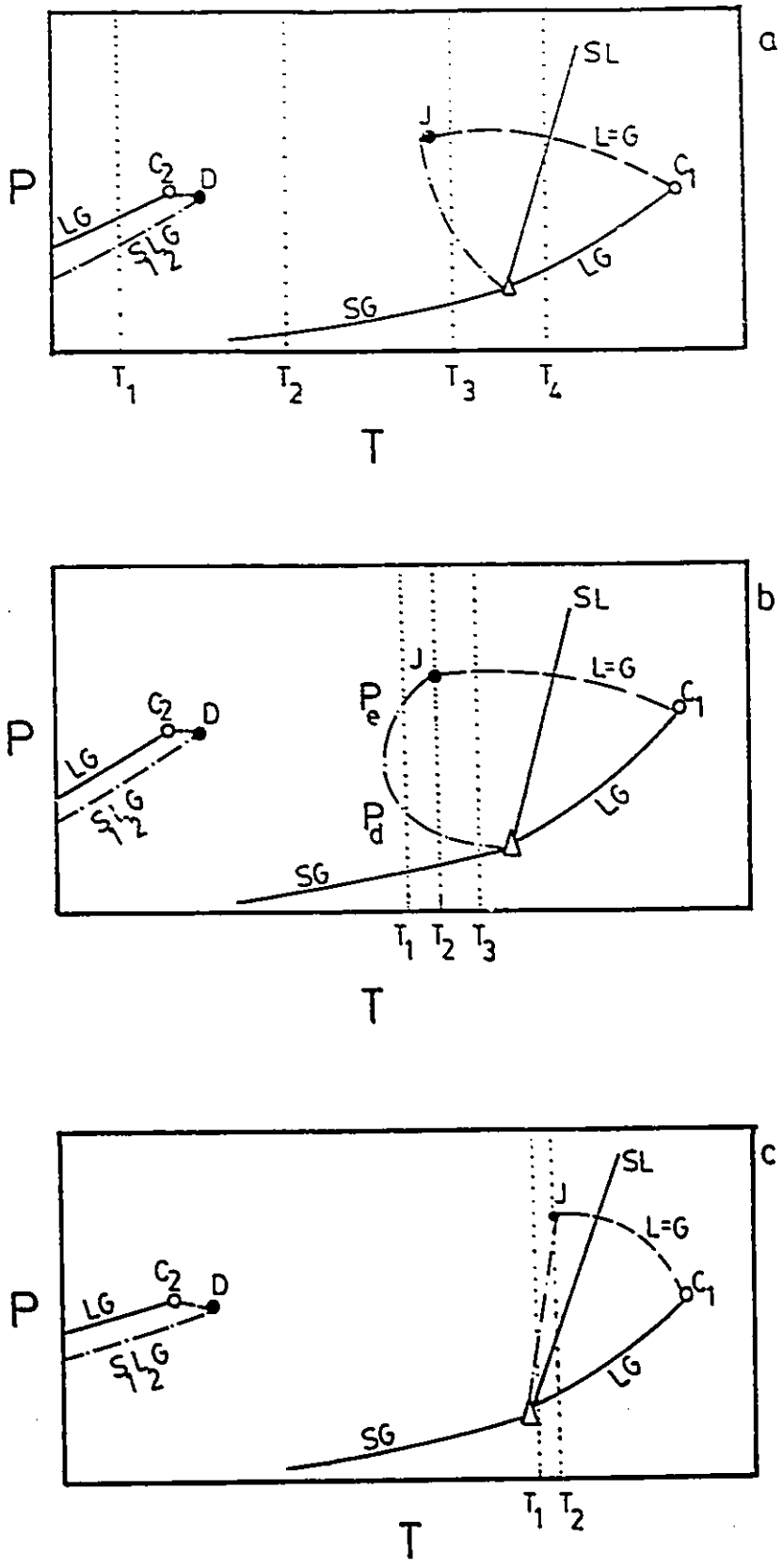

Figure 2.7 : Three types of P-T projection for highly asymmetric binary mixtures.
- - -:L=G critical loci; -·-·-:three phase S-L-G coexistence curve;
——:pure component equilibrium curve;
C_1, C_2:critical points; Δ:triple point;
J:upper critical end point; D:lower critical end point.

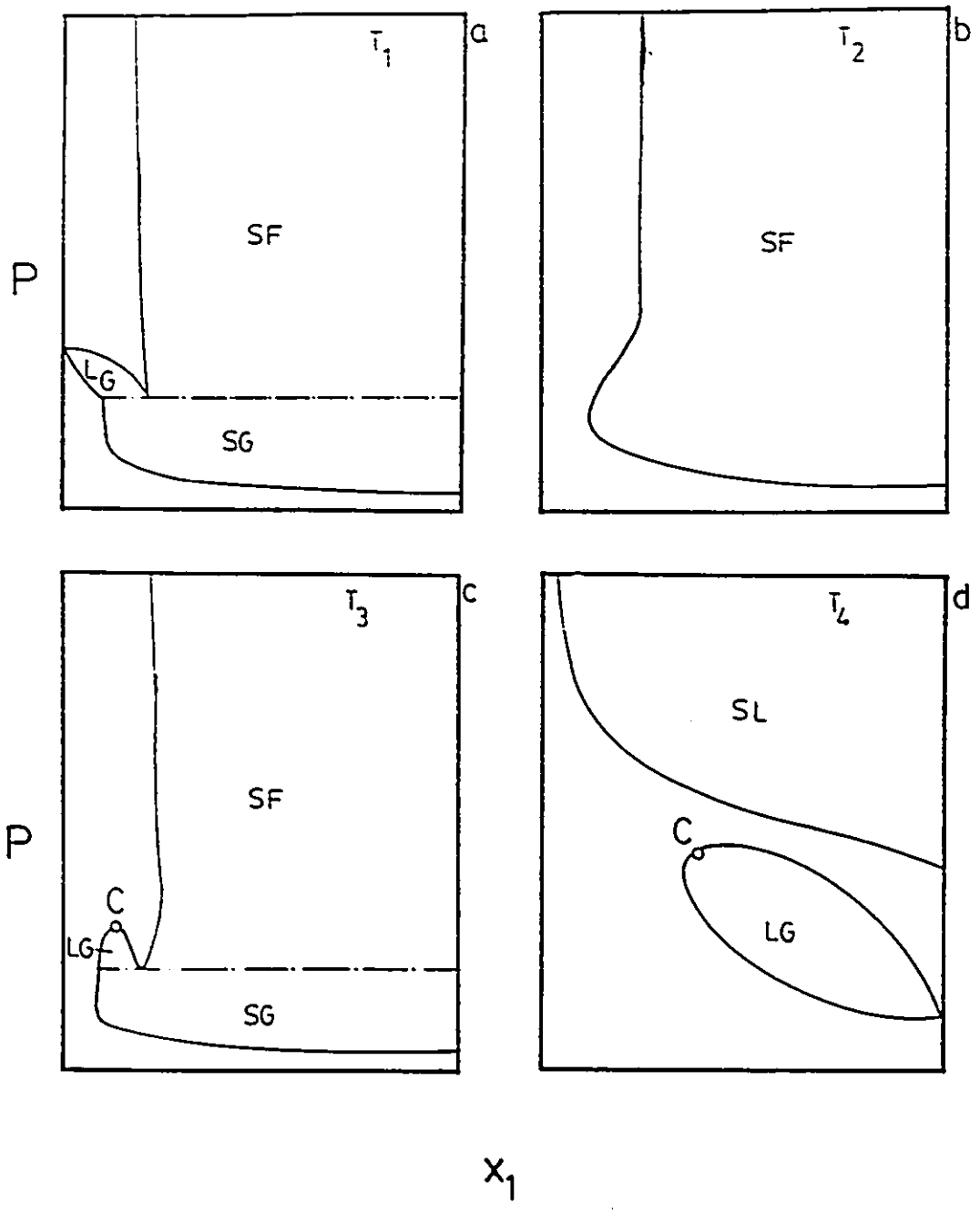

Figure 2.8 : P-x diagrams for Type I binary solid-fluid mixtures in Figure 2.7 a.

disappears and the liquid-gas region increases in size until it forms a close loop. As shown in Figure 2.8 d two completely separated phases are formed, one corresponding to liquid-gas region and the other corresponding to solid-liquid region.

Figure 2.7 b illustrates another type of phase behavior. In this case there is a temperature minimum in the SLG line. Examples of this type include naphthalene-carbon dioxide and biphenyl-carbon dioxide systems [5]. Solid-gas equilibrium exists at all pressures below the temperature minimum of the three phase line. Above the UCEP, solid-fluid equilibrium exists.

Three P-x isotherms are shown in Figure 2.9 corresponding to the temperatures T_1, T_2, and T_3 of Figure 2.7 b. T_1 isotherm lies between the UCEP and the temperature minimum of the three phase line. The P-x diagrams arouse great interest since the three phase line is intersected twice. As shown in Figure 2.9 a, solid-gas equilibrium exists at low pressures until the three phase SLG line is first interested at P_d. The three phases in equilibrium are shown by a horizontal line. Between the pressure P_d and P_e, either liquid-gas, solid-liquid, or a single liquid phase exists depending on the overall mixture concentration. The solid-liquid line bends back toward left and eventually merges with the liquid branch of the liquid-gas loop. Above the second three phase line, solid-fluid equilibrium exists at all pressures. This is the region where solubility increases dramatically as the pressure slightly increases. As pressure increases further, the solubility of heavy component in light phase quickly attains a limiting value.

Figure 2.9 b corresponding to isotherm at the UCEP temperature. From thermodynamics, a horizontal inflection must occur at this point. The solid-liquid line shifts towards left further as the pressure increases and eventually a horizontal inflection point occur at the UCEP temperature where the liquid and gas phases become identical. Near the UCEP pressure, the solubilities increase dramatically. The magnitude of the solubility enhancement depends on how close the temperature

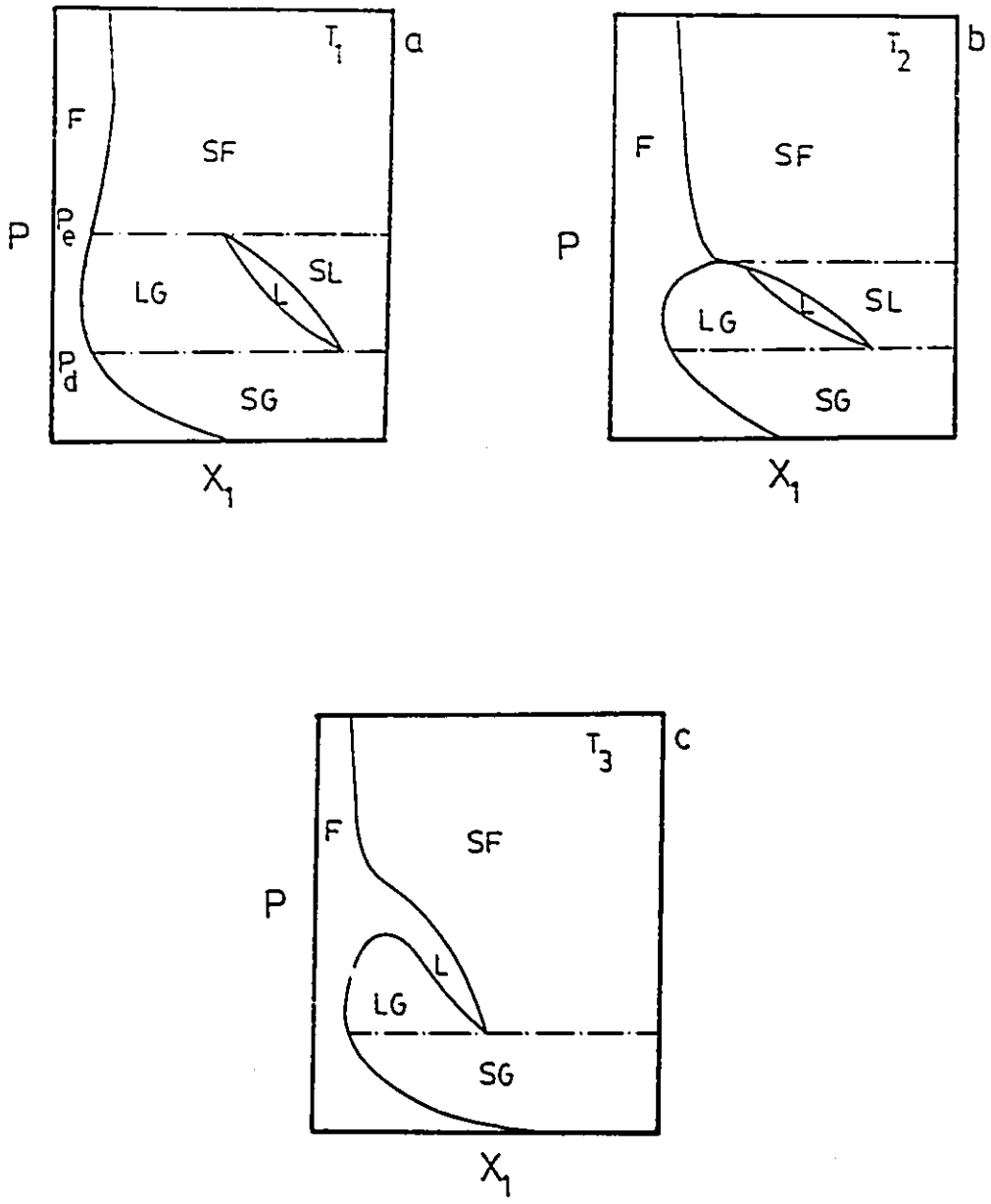

Figure 2.9 : P-x diagrams for Type II binary solid-fluid mixtures in Figure 2.7 b.

is to the UCEP temperature. As the pressure is increased above the UCEP pressure, the solubility quickly reach a limiting value.

Figure 2.9 c shows the P-x diagram corresponding to T_3 of Figure 2.7 b. This isotherm lies below the triple point temperature of heavy component and above the UCEP temperature. The P-x diagram is similar to that in Figure 2.8 c except the liquid-gas region increases in size.

Finally, Figure 2.7 c shows the last type of phase behavior in which the SLG line has a positive slope. Examples of this type include hydrogen-carbon dioxide [126] and nitrogen-argon [127]. Solid-fluid region exists at all pressure for temperature lies below the triple point temperature of heavy component and above the LCEP temperature.

Two P-x isotherms are depicted in Figure 2.10 corresponding to temperature T_1 and T_2 of Figure 2.7 c. Between the vapor pressure curve of heavy component and the three phase line, either liquid-gas, solid-liquid, and single liquid phase exists depending on the overall mixture composition. Above the three phase line, solid-fluid equilibrium exists. Figure 2.10 b shows the phase behavior at the UCEP temperature. At this temperature, the single liquid region increases in size and the liquid-gas mixture becomes critical and a horizontal inflection point must occurs.

2.2 Thermodynamics Modelling of Phase Equilibria at Supercritical Conditions

Although experimental data for a few simple mixtures are available in the literature, they are far from satisfactory. Experimental data for highly asymmetric mixtures are scarce. Accurate prediction and correlation of the phase behavior of highly compressed gases is difficult or even impossible because of the limitation of scientific knowledge and experimental data at high pressure conditions. Therefore, more reliable data are required in practical and theoretical terms. Direct experimen-

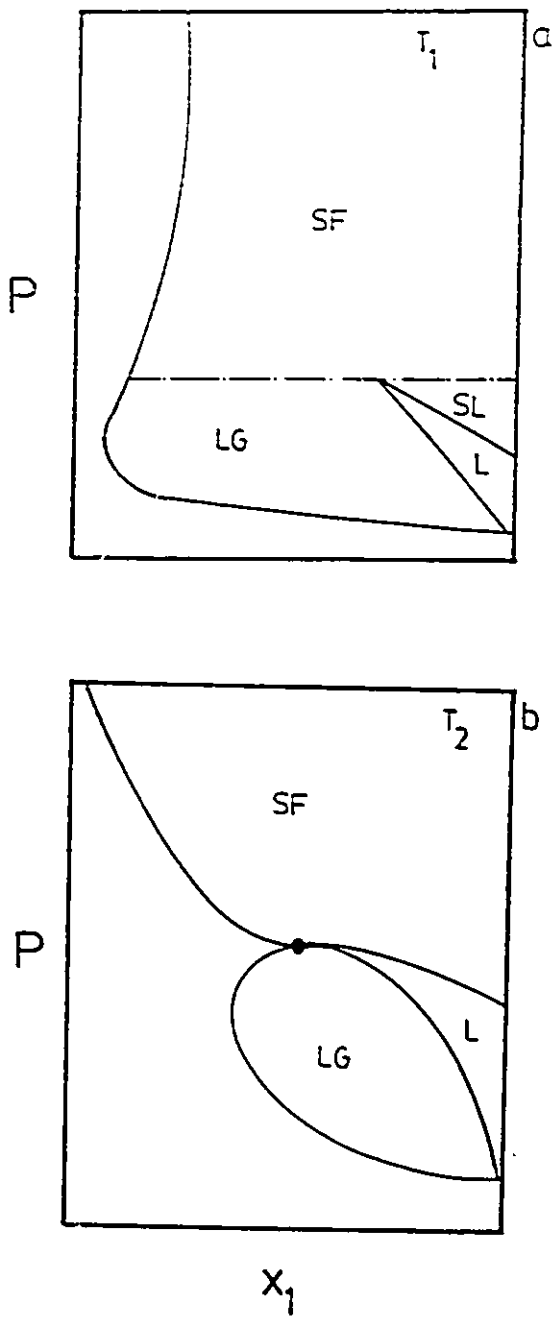

Figure 2.10 : P-x diagrams for Type III binary solid-fluid mixtures in Figure 2.7 c.

tal investigation of phase behavior at high pressures is time consuming and costly. For process design, it is highly desirable to limit the experimental effort by using appropriate thermodynamic models to predict and correlate the phase behavior at supercritical conditions. In this section, various thermodynamic methods for prediction and correlation of high pressure phase behavior are discussed.

2.2.1 Classical Thermodynamics of Phase Equilibria

The fundamental treatment of phase equilibria is first proposed by Gibbs [59] in terms of chemical potentials. For m phases, i components system, the following conditions must be satisified at equilibrium :

$$T^{\alpha} = T^{\beta} = \cdots = T^{m} \tag{2.1}$$

$$p^{\alpha} = p^{\beta} = \cdots = p^{m} \tag{2.2}$$

$$\mu_i^{\alpha} = \mu_i^{\beta} = \cdots = \mu_i^{m} \tag{2.3}$$

where the superscript denoted difference phases, either solid (s), liquid (l), or gas (g), and subscript i denoted the components. μ_i is the chemical potential of component i in mixture. However, the fugacity obtained by a simple transformation from chemical potential is more useful for practical engineering purpose. Using the definition of μ_i, i.e. $\mu_i = \mu_i^{\circ} + RT\ln \hat{f}_i$, equation (2.3) is further transformed into :

$$\hat{f}_i^{\alpha} = \hat{f}_i^{\beta} = \cdots = \hat{f}_i^{m} \tag{2.4}$$

where $\hat{f}_i$ is the fugacity of components i in mixture. Like other thermodynamic properties, the fugacity is a function of temperatures, pressures, and compositions.

2.2.2 Correlation of Solid - Gas Equilibria

The condition of phase equilibrium between a solid component (1) and a supercritical gas (2) is formulated on the basis of equal fugacity criterion :

$$\hat{f}_i^s = \hat{f}_i^g \tag{2.5}$$

where $i = 1, 2$ and superscripts s and g stand for solid and gas, respectively. The theory of solid-gas equilibria is easily formulated if the solid phase is assumed to be pure and incompressible. An expression for y_1, the solubility of the solid in supercritical gas, have been obtained by Prausnitz [60] :

$$\phi_1^{sat} \; P_1^{sat} exp\left[\frac{(P - P_1^{sat})\bar{V}_1^s}{RT}\right] = \hat{\phi}_1^g y_1 P \tag{2.6}$$

Rearranging this equation yields

$$y_1 = \frac{P_1^{sat}}{P} E \tag{2.7}$$

where E is the enhancement factor and is defined as :

$$E = \frac{\phi_1^{sat} exp\left[\frac{(P - P_1^{sat})\bar{V}_1^s}{RT}\right]}{\hat{\phi}_1^g} \tag{2.8}$$

In equation (2.7) and (2.8),

P_1^{sat} = saturated vapor pressure of pure solid;

P = total pressure;

T = system temperature;

ϕ_1^{sat} = fugacity coefficient evaluated at P_1^{sat};

$\hat{\phi}_1^g$ = gas phase fugacity coefficient of solute in the mixture at system T and P;

$\bar{V}_1^s$ = pure solute component molar volume.

The enhancement factor contains three terms : ϕ_1^{sat}, $\hat{\phi}_1^g$, and the exponential term called the poynting correction. Due to the low vapor pressure of solid, ϕ_1^{sat} is always near unity. Also, the poynting correction seldom gives high enhancement factor value. The increase in the value of the enhancement factor observed experimentally is mainly due to a sharp decrease in the solid fugacity coefficient, $\hat{\phi}_1^g$, in the gas phase.

A simplified expression for the enhancement factor has been derived by Rowlinson and Richardson [61] using the virial equation truncated after the second term. The expression illustrated the effect of pressure and temperature on the solubiltiy and is as follows :

$$E = exp\left[\frac{\bar{V}_1^g - 2B_{12}}{\bar{V}^g}\right] \tag{2.9}$$

The cross second virial coefficient (B_{12}) is often large and negative [60], thus giving a large enhancement factor. At low to moderate pressure, $\bar{V}^g$ is very large and hence E is near unity. Therefore the solubility of solid in supercritical gas is described by the ideal solubility term. When the pressure approaches the gas critical value, the gas phase becomes highly compressibile and $\bar{V}^g$ decrease dramatically giving rise to a dramatic increase in solid solubility. The effect of temperature on the solid solubility depends on the system pressure. Near the system critical pressure, the system volume is very sensitive to temperature change. A moderate increase in temperature lead to a large increase in gas volume and make B_{12} more positive, hence the solubility decrease. On the other hand, well above the system critical pressure, the system volume is insenitive to temperature change. At high pressure, increasing the system temperature will increase P_1^{sat} and make B_{12} more positive. These two opposing factors become important and the solubility of solute will have a maximum value at an optimum temperature representing a compromise between the effects of solid vapor pressure and E [5].

The major disadvantage of virial equation is that higher order virial coefficients are unavailable and the equation is suitable only for pressure less than $0.5P_c$ [5]. Other quantitative correlation and prediction of y_1 is obtained from using an empirical equation of state [62,63,64]. The application of equation of state is complicated and requires the introduction of more complex mixing rules as proposed by Vidal [65].

A completely different approach has made use of the density or the solubility parameter of the liquid phase as the variables.

There are several simple expressions proposed in the literature. One of the expressions was proposed by Robin and Vodal in 1953 [66] for representing their solubility data of phenanthrene in compressed gas and takes the form :

$$\log m = A + B \cdot d \tag{2.10}$$

where m is the mass of the solute in gram per cm^3 of the compressed gas, d is the density of the gas. A and B are constants which are independent of density.

Czubryt et al. [67], using regular-solution theory, proposed the following equation in terms of the solubility parameter :

$$\log y = a\delta^2 + b\delta + c \tag{2.11}$$

where y is the solute mole fraction in the compressed gas, and δ is the solubility parameter of the solute. The constant a, b, and c were considered to be density dependent.

In 1978, Stahl et al. [68] proposed a simple relationship in the form :

$$\ln c = m \ln d + constant \tag{2.12}$$

which related the gas density d and the concentration of the solute in a compressed gas c. The solubility factor m in equation (2.12) was considered as a function of density only.

Recently, Chrastil [46] proposed the following equation which related solubility and density as follow :

$$c = d^k \exp\left(\frac{a}{T} + b\right) \tag{2.13}$$

rearranging equation (2.13) yields

$$\ln c = k \ln d + \left(\frac{a}{T} + b\right) \tag{2.14}$$

which is similar to equation (2.12). One characteristic of Chrastil equation is that this expression includes the dependence of solubility upon temperature.

Later, Adachi and Lu [69] modified Chrastil equation by considering the constant k to be density dependent and they found that the modified Chrastil equation gives better representation of the solubility data than other expressions and simple equations of state.

2.2.3 Correlation of Liquid - Gas Equilibria

Unlike the equilibrium between a solid and a gas, in which the solid is assumed to be pure, the thermodynamic analysis for liquid-gas equilibria is more complicated and difficult because the compositions in both phases are unknown. In addition, the gas dissolves in the liquid phase and affects the liquid properties. In liquid-gas equilibria, the equal fugacity criterion is :

$$\hat{f}_i^l = \hat{f}_i^g \tag{2.15}$$

where i refers to components.

For gas phase, the fugacity coefficient, $\hat{\phi}_i^g$, is defined as :

$$\hat{\phi}_i^g = \frac{\hat{f}_i^g}{y_i P} \tag{2.16}$$

The activity coefficient, γ_i, which relates the liquid phase fugacity to mole fraction and

standard state fugacity is defined as :

$$\gamma_i = \frac{\hat{f}_i^l}{x_i f_i^{\circ l}} \tag{2.17}$$

substitute equation (2.16) and (2.17) into (2.15), the following key equation is obtained :

$$\hat{\phi}_i^g y_i P = x_i \gamma_i f_i^{\circ l} \tag{2.18}$$

The liquid phase activity coefficient can be obtained either by an excess function or by solution models such as van Laar, Margules, non random two liquid (NRTL) or UNIQUAC [60].

Another way to describe liquid-gas equilibria is to use the fugacity coefficients for both phases, i.e.

$$\hat{\phi}_i^g y_i = \hat{\phi}_i^l x_i \tag{2.19}$$

The thermodynamic relation for obtaining fugacity coefficient of component i in both phases is given by the following expression [60] :

$$RT\ln\hat{\phi}_i = \int_v^\infty \left[\left(\frac{\partial P}{\partial n_i} \right)_{T,V,n_j} - \frac{RT}{V} \right] dV - RT\ln Z \tag{2.20}$$

Thermodynamics models which utilize equation of state for the gas phase and liquid solution models for the liquid phase are proposed and have been an active area of research in recent years [70,71]. This models, however, have a major problem when describing mixtures with supercritical components as it is difficult to define a reference liquid state [72]. Therefore, fugacity coefficient with the use of cubic equations of state to predict liquid-gas phase behavior is widely used.

Correlation and prediction of liquid-gas equilibrium for binary and ternary systems using cubic equations of state (EOS) have been analyzed extensively in the literature. Hsu and Lu [73] have presented a thermodynamic analysis where the Redlich - Kwong (RK) equation of state is used to describe both the gas and the liquid phases. Tsonopoulos and Heidman [74] examined three cubic EOS in the prediction of liquid-gas equilibrium for mixtures containing H_2, CO_2, or water.

The most commonly used cubic equation of state of the van der Waals form are Redlick - Kwong (RK) [75] and Soave's modification [76] and Peng - Robinson (PR) [77].

The prediction of liquid-gas equilibrium is largely determined by two factors : reproduction of vapor pressure and the form of mixing rules. Most cubic EOS used Soave [76] approach for fitting the vapor pressure, and therefore the form of mixing rules is the most important factor in accurate equilibrium prediction.

Peng - Robinson [77,78] modified the attractive term and retained the repulsive term of the Redlick - Kwong EOS to improve liquid density predictions and take the form :

$$P = \frac{RT}{v-b} - \frac{a}{v(v+b)+b(v-b)} \tag{2.21}$$

where

$$a = 0.45724\,\frac{R^2T_c^2}{P_c}\cdot\alpha(T) \tag{2.22}$$

$$b = 0.07780\,\frac{RT_c}{P_c} \tag{2.23}$$

The temperature dependence of α retains the form proposed by Soave :

$$\alpha = \left[1 + m(1 - T_r^{\frac{1}{2}})\right]^2 \tag{2.24}$$

but with

$$m = 0.37464 + 1.54226\omega - 0.26992\omega^2, \omega < 0.5 \tag{2.25}$$

$$m = 0.37964 + 1.48503\omega - 0.16442\omega^2 + 0.01667\omega^3 \tag{2.26}$$

where ω is the acentric factor defined by Pitzer [60]. Equation (2.26) was used for $0.2 \leq \omega \leq 2.0$.

For pure component, a and b are directly obtained using the above equations . For mixtures, most EOS use the "conventional" one-parameter random mixing rules, that is

$$a_{mix} = \sum_i \sum_j x_i x_j \cdot a_{ij} \tag{2.27}$$

$$a_{ij} = (a_i a_j)^{\frac{1}{2}} (1 - k_{ij}) \tag{2.28}$$

$$b_{mix} = \sum_i x_i b_i \tag{2.29}$$

The binary interaction parameter, k_{ij}, corrects for the deviation of a_{ij} from the geometric mean. For most hydrocarbon-hydrocarbon systems, k_{ij} is closed to zero. However, non-zero k_{ij}'s are required when the components are very different in molecular size [79,80].

The optimal values of k_{ij} are determined from available experimental data by minimizing the difference between the calculated and experimental values of a selected equilibrium property. Several criteria have been used for the evaluation of k_{ij} and are as follows :

- Minimization of deviation in predicted K values [81,82];
- Minimization of deviation in predicted bubble point pressures [83,84,85,86];
- Minimization of deviation in predicted bubble point vapor composition [83,84];
- Minimization of the flash volume variance [85];
- Minimization of the sum of variance of system properties, e.g. the flash vapor and liquid compositions [87].

An improvement to the "conventional" one-parameter random mixing rules is to replace equation (2.29) with

$$b_{mix} = \sum_i \sum_j x_i x_j \cdot b_{ij} \tag{2.30}$$

$$b_{ij} = \left(\frac{b_i + b_j}{2}\right) (1 - l_{ij}) \tag{2.31}$$

where l_{ij} corrects for the deviation of b_{ij} from the arithmetic mean. Setting $l_{ij} = 0$ gives the original mixing rule.

The advantage of "conventional" one or two-parameter mixing rules is that these mixing rules are easy to use with short computation time. However, these mixing rules only suitable for non-polar or slightly polar compounds. For polar systems, other mixing rules to calculate a_{ij} have been proposed [88,89,90,91,92]. For example, the local composition (LC) mixing rules, or the density-dependent (DD) mixing rules [93,94,95,96]. Other example include the modified conventional mixing rules by Adachi et al. [88].

Huron and Vidal [91] form of the LC mixing rules recognize that components in mixture do not distribute randomly because of intermolecular interactions. Two disadvantages of the LC mixing rules are that they do not readily reduce to the "conventional" mixing rules and increase computation time. A more serious limitation is that in low-density limit, all LC mixing rules do not reduce to the theoretically correct quadratic mole fraction dependence for the mixture's second virial coefficient. Therefore, LC mixing rules are recommended for polar systems only [74].

The Density-dependent (DD) mixing rules are proposed to solve the problems by introducing an arbitrary interpolation between the theoretical correct quadratic mixing rules at zero density and some high order mixing rules at high density. These models are solved iteratively and required excessive computation time. However, the improvement over the conventional mixing rules is limited and is similar to LC mixing rule.

In this study, the PR EOS with one or two-parameter random mixing rules is used to correlate the experimental data obtained in the work.

2.2.4 Correlation of Solid - Liquid - Gas Equilibria

The condition of phase equilibrium of binary system between a solid, a liquid, and a supercritical gas phase is formulated again on the basis of equal fugacity between these three phases :

$$\hat{f}_i^s = \hat{f}_i^l = \hat{f}_i^g \tag{2.32}$$

where superscript s, l, and g stand for solid, liquid, and gas respectively and subscript $i = 1, 2$.

The solid phase is normally considered to be pure and incompressible, the equal fugacity criterion becomes

$$f_1^s = \hat{f}_1^g \tag{2.33}$$

$$\hat{f}_i^l = \hat{f}_i^g \tag{2.34}$$

where $i = 1, 2$. Equation (2.33) reduced to equation (2.6) and rearranging this equation yields

$$y_1 = \frac{P_1^{sat}}{P} \frac{\phi_1^{sat} exp\left[\frac{(P - P_1^{sat})V_1^s}{RT}\right]}{\hat{\phi}_1^g} \tag{2.35}$$

Using the definition of fugacity coefficient $\hat{\phi}_i$, equation (2.34) reduces to equation (2.19),

$$\hat{\phi}_i^g y_i = \hat{\phi}_i^l x_i \tag{2.19}$$

Therefore, the solid-liquid-gas equilibrium values can be determined by solving (2.35) and (2.19) simultaneously. A computer program used to fit the equilibrium values along the S-L-G curve using PR EOS with conventional one or two-parameters mixing rules is given in Appendix G.

2.2.5 Correlation of T-x Values along the Three Phase SLG Curve

Following the approach of Prausnitz [60], the following expression is obtained for $x_1\gamma_1$:

$$\ln x_1 \gamma_1 = -\left(\frac{\Delta \tilde{H}_f^\circ}{R}\right)\left(\frac{1}{T} - \frac{1}{T_m}\right) \tag{2.36}$$

where x_1 and γ_1 are the mole fraction and the activity coefficient of heavy component in the liquid phase respectively. $\Delta \bar{H}_f^\circ$ and T_m are the heat of fusion and the melting temperature of heavy component. In the derivation of equation (2.36), the difference between the specific heat capacities of the liquid and solid phase are neglected. In addition to the above assumption, $\Delta \bar{G}_f^\circ$ is assumed to be independent of pressure. The first assumption is made because both ΔC_p of the heavy component and the temperature range of this study are small. As the pressure effect on the $\Delta \bar{G}_f^\circ$ is unknown due to the lack of information about partial molar volume of heavy component of the liquid and solid phases, the second assumption is made.

In this study, the van Laar equation is used to estimate the activity coefficient, γ_1. Together with the values of $\Delta \bar{H}_f^\circ$ and T_m available in the literature, the correlation of T-x data along the three phase line is possible.

The van Laar equation is expressed as follows :

$$\ln\gamma_1 = \frac{A_{12}}{\left(1 + \frac{A_{12}x_1}{A_{21}x_2}\right)^2} \tag{2.37}$$

A_{12} and A_{21} are binary constants and are temperature independent.

The calculation procedures are as follows :

- using experimental T & x, calculate γ_1 from equation (2.36),
- using equation (2.37) to find the best fitted A_{12} and A_{21} values by optimize $\sum(\gamma_{exp} - \gamma_{cal})^2$.

Chapter 3

Experimental

Studies of high pressure phase equilibria have increased recently not only because of the practical importance in petroleum, natural gas, and related industries, but also serve as a test for the theoretical concepts involved such as pair potentials, liquid theories, and equations of state, etc. Although correlation and prediction methods have been developed, the accuracy of those methods largely depend on the available of phase equilibria data. Therefore, more and more experimental data at high pressure and/or high temperature are required to extend the use of those available methods. In this chapter, details experimental aspects of this research are given. Review of experimental methods at high pressure condition is given first. The experimental equipment, material, and procedures are then discussed

3.1 Review of Experimental Techniques at High Pressure

Experimental equilibria data are essential in the design and development of many industrial separation processes. Since experimental work is time consuming and costly, correlation and prediction methods based on existing data are more attractive than carrying out new experiments to extent

the experimental information to systems not experimentally measured. However, up to date, no predicting method can afford to neglect using experimental data to extent its use and to improve its accurancy. Therefore, new and more accurate data are required for both theoretical and practical purposes. In the literature, experimental techniques have been developed for more than fifty years which can be divided into three types, namely : static, flow and force-recirculation method. The brief description of experimental methods below just serve to explain the underlying principles of modern techniques. For more details in any practical high pressure experimental methods, reviews by Vodar [97], Schneider [98], and Young [99] are excellent references.

3.1.1 Static Method

This method have been developed for many years and is probably one of the oldest methods still used today in investigating phase equilibria. This methods can be further classified into synthetic and analytic modes depending on the way to determine the phase compositions. The idea of synthetic mode, such as Dew Point and Bubble Point (DPBP) Method, consists of introducing a mixture of known composition and to observe its behavior by adjusting either temperature and/or pressure. Sampling and analysis of separate phases are eliminated. In contrast to the synthetic mode, analytic mode requires sampling and analysis of coexisting phases. Static and Total Pressure (STP) Method belongs to this mode.

The principle procedure of DPBP method consists of introducing a gas and/or liquid mixtures of known compositions into an equilibrium cell. The system is then brought to the desired experimental temperature. During the experiment the pressure is varied until the formation or disappearance of a phase is observed. The pressure at which the formation of first micro-drops of liquid when gas mixture is compressed is called the "Dew Point" pressure. The "Bubble Point" pressure is defined when an infinitesimal amount of vapor appears in the form of small bubbles

when liquid is decompressed at constant temperature. The dew point and bubble point pressures can be determined by a series of phase transition or determined separately. The way to control the volume of the cell depends on the type of cell. For constant volume cell, the pressure is adjusted by addition of measured amount of material into the cell [100,101]. If the volume of the cell is variable, the pressure is adjusted either by a mercury-filled compressor [102,103], by the motions of piston [104,105,106], or bellow [107]. In order to reach equilibrium inside the cell, efficient mixing is achieved either by magnetic stirring, by rocking the cell, or by a magnetic pump.

The dew point and bubble point pressures are determined by direct observed the phase transition or by graphical methods such as the appearance of discontinuities in the pressure-volume curve. The graphical method was recently employed by Robinson et al. for carbon dioxide-heavy hydrocarbon systems [108,109,110]. The results of synthetic experiments are sets of phase boundaries at constant composition (isopleths). The equilibrium conditions are then determined by cross plotting, i.e. the intersection of the dew point curve of one composition with the bubble point curve of the other composition.

The main advantage of DPBP method is that the phase compositions need not be analyzed. Therefore it does not require complicated analytical devices and it is relatively inexpensive. However, the DPBP method cannot be applied to study multicomponent system.

In the STP methods a mixture is placed into the equilibrium cell at a controlled temperature. The mixture is then agitated thoroughly. After equilibrium is reached, the equilibrium conditions are then recorded or measured. The results of this method usually consist of either a series of complete measurements (P-T-x-y) or a series of total pressure measurements (P-T-x). In complete measurement, samples of the gas and liquid are withdrawn and analyzed by appropriate methods. In total pressure measurement, the gas phase compositions are calculated directly from the

thermodynamic relationship based on the measured liquid composition and total pressure data.

Most analytic methods require that the sample taken is in a well defined state. Therefore the problem of analysis is mainly the preparation of the sample. Two types of sampling technique are discussed below. The following discussion is not limited to the static method but is also applicable to the flow and recirculation methods when phase compositions need to be analyzed.

For components with high vapor pressures at ambient temperature, no components of the samples are lost through condensation in the sampling assembly. Therefore one can assume that the compositions of the phases within the cell is the same as the input compositions of the analytical devices. Wisotzki and Schneider [111] used this type of sampling method to measure the phase compositions for nitrogen-ethane and nitrogen-pentane system.

If one of the components is a high-boiling substance, for example, mixtures of supercritical gas with a low-volatile compound, precipitation of the low-volatile component cannot be avoided when the pressure is reduced during sampling through flushing. Therefore, the samples are not introduced into the analytical device immediately. Instead, the samples are analyzed in two steps : firstly, the samples are expanded into evacuated glass vessels. The pressure is reduced and the supercritical component is in a gaseous state and its amount is calculated volumetrically based on PVT data. Secondly, the low-volatile component precipitated and flushed out with an organic solvent and the solution is then analyzed by gas chromatography [112].

The static methods are the only experimental methods which can reach the true equilibrium state. Analytic methods are slower and more expensive. Since long residence time is required to obtain the equilibrium state, the STP method has a disadvantage for heat labile components where thermal decomposition may occur. Furthermore, a drop in the pressure during sampling will disturbs the equilibrium state and therefore cannot be applied in the vicinity of critical points. On

the other hand, the synthetic method does nothing to disturb the equilibrium so that it is reliable and especially useful in the vicinity of critical points.

3.1.2 Flow Method

For liquid-gas systems, the apparatus of the flow method usually composed of four main parts : a degassing and mixture injection assembly, a preheater and mixing assembly, an equilibrium cell or phase separator, and sampling systems. A degassed liquid stream was compressed and mixed with a gas stream. The two mixed stream was heated to the desired temperature in the preheater chamber. Before entering the equilibrium cell, the mixture was allowed to flow into a static mixer to ensure the attainment of equilibrium in a short time. The saturated phases were separated in an equilibrium cell. Samples of gas and liquid are withdraw and analyzed. A continuous analysis of the sample is also possible. Using the flow method, equilibrium can be reached quickly by intimate contact between the gas and the liquid during condensation. In addition, large quantities of samples can be obtained continuously. The major difficulties of flow method are that it is very difficult to control the pressure and temperature well in the cell while rapid condensation occurs and this method is not suitable near the critical region because the separation of phases becomes very difficult near the critical region.

The apparatus used for solid-gas systems usually composed of four main parts : a solvent injection assembly, a solvent preheater, an equilibrium column, and sampling systems. A high pressure pump is used to deliver compressed gas continuously at a flow rates slow enough to insure that equilibrium between the solid and the gas is obtained. The compressed gas then flows through the preheater to insure that it reaches the system temperature before it contacts the solid. After reaching thermal equilibrium, the heated gas is fed to the high pressure equilibrium column. The equilibrium column is packed with the solid. Glass wool was inserted at the exit of the packed

column to prevent entrainment of the solid in the gas-rich phase. The saturated gas-rich phase leaving the column is then expanded across a heated metering valve and the heavy component falls out of the mixture and is collected using a cold trap. The amount of heavy component dissolved is determined gravimetrically. The amount of gas is measured with a wet-test meter.

This method was employed by Grayson and Streed [113] to measure liquid-gas equilibrium data of hydrogen-gas oil at temperature up to $750°C$ for pressure up to $20\,MPa$. Sebastian et al. [114] and Lin et al. [115] used a flow apparatus to measure equilibrium data of carbon dioxide-toluene at elevated temperatures and pressures. Other apparatus which are capable of determining high pressure equilibrium data have been reported by Inomata et al. [116,117] for carbon dioxide-heavy compounds systems. Solubility of solid mixtures in supercritical fluid using a flow type apparatus was also reported by many researchers [24,25,118,119].

3.1.3 Force - Recirculation Method

In this technique, the experimental procedure is similar to the static method except gas and/or liquid are withdrawn from the equilibrium cell and was recirculated back through the liquid by means of a pumping device. Equilibrium was achieved by continuously bringing the recirculated stream into contact with the liquid. According to the number of recirculated streams, the force-recirculation methods can be classified into three groups : (1) vapor recirculation ;(2) condensate recirculation ; (3) or liquid phase and vapor condensate recirculation method.

In this section, only the vapor recirculation method is discussed. The principle of other methods is similar and is discussed in detailed by Malanowski [128].

The vapor recirculation method was first proposed by Inglis [129]. Using this method, vapor was continuously withdrawn from the cell by a magnetic pump and recirculated back at the bottom of the cell where it bubbled up through the liquid until equilibrium is attained. Then the pressures,

temperatures, and the compositions of the coexisting phases are measured. The limitations of this methods include the possibility of liquid entrainment in the vapor stream, the pressure fluctuation caused by pumping of the vapor stream, the change of vapor phase composition due to the pressure fluctuation, and condensation of vapor during recirculation. Owing to the above limitations, exact equilibrium conditions cannot be achieved. However, when the cell is operated at pressure above $0.5\,MPa$, the influence of pressure fluctuation caused by the pump on composition can be neglected. Therefore this methods are considered to be most accurate for obtaining equilibrium data when the operating pressures are in the range $1 - 50\,MPa$. This method was employed by Kobayashi et al. [120,121] to measure equilibrium data of hydrogen-tetralin and carbon dioxide-n-hexadecane systems up to $27.33\,MPa$ and $26\,MPa$ respectively.

3.2 Experimental Measurements of the S-L-G Three Phase Coexistence Curve

Various experimental techniques for determining the equilibrium values of the S-L-G coexistence curve for binary systems consisting of one solid and one supercritical fluid are described in the literature [40]. In general, it can be divided into the following three techniques.

In the first experimental technique, known as the "Static Solubility Measurement", the P-T projection of the S-L-G curve is deduced from the intersection of the liquid-gas equilibrium isopleths and the solid-gas or solid-fluid equilibrium isopleths at constant composition [122,123]. By introducing a known amounts of solid and gas into a high pressure view cell, the isopleths are determined at various conditions. The isopleths of L-G boundary curve are determined by slowly increasing the pressure at constant temperature until one of the phase disappears depending on the overall mixture composition. If the prepared composition is greater than the composition of the

mixture at the UCEP, the pressure is increased slowly at constant temperature until the gas phase disappears into the liquid phase. Otherwise, the pressure is slowly increased until the liquid phase disappears into the gas phase. The S-F or S-G curve is determined by slowly heating a solid-fluid or solid-gas mixture at constant pressure until the solid phase has disappeared. The advantage of this method is that the equilibrium composition values along the S-L-G curve are readily determined. Sampling and analysis of separate phases are avioded. However, these method is time consuming and a lot of experimental time is required for all isopleths determination.

The second technique, the so called "First Melting Point" method, is used by McHugh et al. [3,38] and van Gunst et al. [48]. Using this method, only the P-T values are determined along the S-L-G coexistence curve. Starting from a solid-fluid condition, the mixture is heated slowly until the solid begins to melt. At this condition, the temperature and pressure are taken as the three phase coexistence equilibrium values. The advantages of this method are the P-T projection of the three phase curve is determined quickly and the technique is simple. The main drawbacks are that the composition of the equilibrium phases along the three phase curve is not determined and the results may not be very reliable.

The final technique, known as the "First Freezing Point" method, provides the P-T-x characteristics of the three phase curve [40,124]. Starting with the solid-fluid mixture, the temperature was increased until the solid was completely melted. The mixture was mixed thoroughly by stirring the mixture or by a pumping device. The temperature was then decreased slowly until the first crystal was observed in the equilibrium cell. The conditions under which when the first crystal appeared were taken as the three phase coexistence point and the liquid phase was then sampled and the composition measured. These method eliminated the disadvantages of both static solubility method and the first melting point method. This method provided a fast and reliable determination

of the P-T projection as well as the liquid composition along the three phase S-L-G curve.

In this study, the "First Freezing Point" technique was used to determined the P-T-x equilibrium values of the three phase coexistence curve.

3.3 Experimental Apparatus

The schematic diagram of experimental apparatus used to measure the equilibrium values (P-T-x) along the three phase (S-L-G) coexistence curve is shown in Figure 3.1. The apparatus consisted of four major sections : a pressurizing system, a temperature controlled air bath, a high pressure through-window cell equipped with a magnetic pump, and a liquid phase sampling system.

In the pressurizing system, an air-operated automatic pressure intensifier E (Futurecraft Corporation, part no. 90793, max. 68.9 MPa) was used to pressurize the ethylene from a supply cylinder. A hand loader type pressure regulator (Futurecraft Corporation, part no. 40590) was adjusted to a desired outlet pressure and the pressure intensifier operated automatically until reaching the adjusted setting. The system pressure was measured using a calibrated pressure transducer D (Data Instrument Inc., series no. A06342, max. 68.9 MPa). Pressure readings were indicated by a pressure digital recorder (InterTechnology, model no. RB-201-10000) which was not shown in Figure 3.1. The pressure transducer was calibrated with a dead weight pressure tester (Testing Instrument Co. Inc.). The calibration curve for the transducer is shown in Appendix A. The accuracy of the pressure transducer was estimated to be ± 0.05 MPa. The transducer was located very close to the high pressure view cell. Pressure gauge H was used to obtain a rough indication of pressure.

The temperature controlled air bath (Ruska Instrument Corporation, model no. 2320-801-16800, range ambient to 450 K) consists of the following components : the temperature bath, the

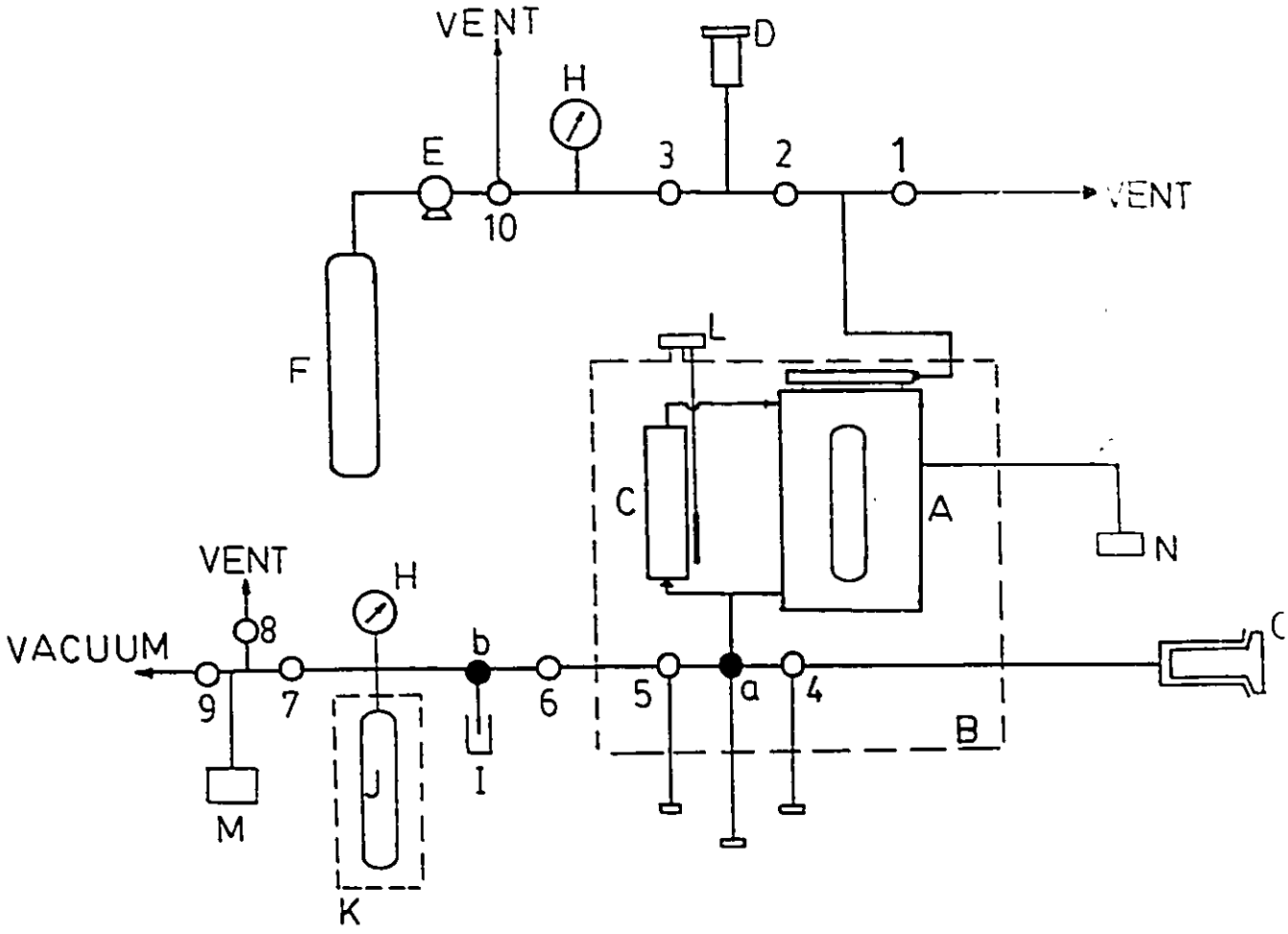

Figure 3.1 : Schematic diagram of experimental apparatus.
A : high pressure view cell; B : air both; C:magnetic pump;
D : pressure transducer; E : pressure intensifier;
F : gas cylinder; G : syringe; H : pressure gauge;
I : solid sampler; J : sample cylinder; K : water bath;
L : variable speed motor; M : vacuum gauge;
N : temperature indicator;
a,b : three way valve, 1 to 10 : valves.

fan and motor, the heating unit, and electronic control components. The heating was established through the application of variable heating speeds. Various combinations of main heater may have to be used in order to reach desired temperatures. The main heater was installed inside the air bath. A direct drive fan was used to create the circulating rate inside the temperature bath and to ensure the temperature uniformity of the air bath. The air bath temperature is controlled using a LFE electronic temperature controller. The air bath temperature could be maintained within ± 0.03 K.

The high pressure through-window cell A (Ruska Instrument Corporation, model no. 2329-801-60900, max. 68.9 MPa) with an internal volume of approximately 40 cm^3 was used as an equilibrium cell. To hasten establishment of equilibrium, recirculation and mixing of liquid phase through the vapor phase was especially helpful. A high pressure magnetic pump C (Ruska Instrument Corporation, model no. 2330-802, max. 82.7 MPa) was used to circulate the liquid phase through the vapor phase in the equilibrium cell. The magnetic pump was mounted inside the air bath, while the motor was mounted outside the temperature bath. Recirculation of liquid phase was achieved by the doughnut-shaped magnet which was moved vertically up and down by a motor. A cathetometer was used to observed the appearance of crystal formed inside the equilibrium cell. The system temperature was measured using a thermocouple which was installed on the outside surface of the cell. The thermocouple was calibrated at the triple point of pure water and other temperatures with a calibrated Hewlett-Packard quartz thermometer (model no. 2801A, sensor no. 1126-44). The calibration of the thermocouple is shown in Appendix B. The accuracy of the temperature measurements was estimated to be 0.01 K.

For liquid phase sampling system, a three-way valve a (Autoclave Engineers, SW-2075, max. 75.8 MPa at room temperature) was connected to the circulation loop. Valve a was located very

closed to the high pressure view cell to ensure that a saturated liquid phase could be sampled. Three long handles which extended out of the air bath were used to control the three valves a, 4, and 5 in Figure 3.1. The line between valves 4 and 5 was used as the sampling loop. Another three-way valve b (Whitey, SS-41X32, max. 17.2 MPa at 293.15 K) was used to analyze the solid or gas phase. The two three-way valves had different function. Valve a had the feature that only the way connected to the cell was opened or closed while the other two ways connected to valves 4 and 5 were always on. The function of valve b was to connect the sampling loop either to a solid sampler I (glass beaker, 200 cm^3) or to a sample cylinder J (Whitey, internal volume 300 cm^3). The sample cylinder J was immersed in a water bath K and a Bourdon-tube Heise gauge H was used to measure the gas pressure released from liquid phase during the expansion process. The water bath temperature was measured using a Hewlett-Packard quartz thermometer (model no. 2801A, sensor no. 1126-44). The liquid solidified on the sample loop was dissolved using acetone. Acetone was injected through the sample loop and line using the syringe G in Figure 3.1. The sample loop and the line were heated using a heating tape to prevent clogging. The liquid sample was collected using the solid sampler I. After drying, the solid collected was weighed using a micro-balance (Fisher Scientific, Mettler H20). The accuracy of the weighing is about ± 0.0001 g. Gas residuals remained on the sample loop and line was removed using the vacuum system which was not shown in Figure 3.1. The main components of the vacuum system consisted of a vacuum pump and a glass cold trap immersed in iced water. The function of the glass cold trap is to trap condensable materials and to aviod corrosion and damage to the vacuum pump.

3.4 Experimental Procedures

After the system was thoroughly cleaned to remove all possible contaminating solid using acetone as a solvent, the whole system was pressure/vacuum tested for leaks. To accomplish the pressure test, valves a,1,3,4 and 8 were closed. The system is pressurized to about 13.79 MPa with ethylene gas and a leak test is performed at room temperature using a leak detector. All the elements of the system are included in the test. After the pressure had stabilized, the system was left for about 12 to 24 hours to observe any pressure drop in the system. If there was a pressure drop, it indicated a leakage in the system When no pressure drop, the system was then considered leak proof up to the test pressure.

After the system had been tested for pressure/vacuum leakage, a known amount of solid was loaded into the equilibrium cell. At this moment, the sample loop and line between valves 4 and 9 was evacuated using the vacuum system. The high pressure view cell was purged of air with ethylene at approximately 1 MPa through valve 1. After three to four purgings, valve 1 was closed. The temperature was then increased until the solid completely melted. The system was then brought to a desired pressure. The magnetic pump was then turned on to circulate the liquid phase through the vapor phase in the equilibrium cell. The system was maintained there for about 8 to 10 hours to ensure liquid phase was saturated with ethylene. Thereafter, the system temperature was decreased slowly until the first appearance of the solid crystal was observed using a cathetometer. At this condition, the pressure and temperature were taken to be the equilibrium values and as the three-phase coexistence conditions. The solid may then melted and frozen again to obtain the second measurement to ensure a consistent and accurate measurement. In most cases, the difference between the first and second temperature measurement was within ± 0.1 K.

When the first crystal was observed, the composition of the liquid phase at the three-phase

conditions was sampled rapidly using the spacing between valves 4 and 5 as the sample loop. The three-way valve a was opened, saturated liquid flowed into the sample loop and valve a was then closed immediately. Valve 5 was then opened. The saturated liquid phase expanded into the loop and solidified very quickly between valves 5 and 6. Valve 6 was opened slowly so that ethylene was expanded into the sample cylinder through the three-way ball valve b. The rise of pressure at the water bath temperature was then recorded and corrected to the condition at 298.15 K using an ideal gas equation. The calibration equation related the rise of pressure and the number of moles of gas is presented in Appendix C. The amount of ethylene dissolved in liquid phase was calculated using the calibration equation C.1. After the expansion process, valve 4 was then opened and solid was dissolved and collected by forcing acetone to the solid sampler through the three-way ball valve b.

3.5 Specifications and Properties of Materials

The 99.9+ % purity naphthalene with melting temperature of 353.15 K was supplied by the Fisher Scientific Company. The 99+ % purity biphenyl with melting temperature of 342.4 K was supplied by the Aldrich Chemical Company Inc.. Compressed ethylene with C.P. Grade 99.5+ % was supplied by Air Products and Chemicals Inc.. Acetone with minimum purity of 99.5+ % was supplied by BDH Chemicals Canada Limited. All these Chemicals were used without further purification.

The critical properties of the three components, naphthalene, biphenyl, and ethylene are listed in Table 3.1. The pure solid properties of naphthalene, and biphenyl are listed in Table 3.2.

Table 3.1: Critical properties of naphthalene, biphenyl and ethylene.

Substance	$P_c(atm)$	$T_c(K)$	$\tilde{V}_c(\frac{cm^3}{mole})$	ω
Naphthalene	40.0	748.4	410.0	0.302
Biphenyl	38.0	789.0	502.0	0.364
Ethylene	49.7	282.4	129.0	0.085

Table 3.2: Physical properties of naphthalene and biphenyl.

Properties	Naphthalene	Biphenyl
molecular structure	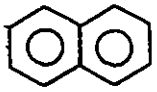	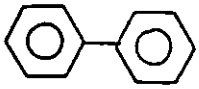
molecular formula	$C_{10}H_8$	$C_{12}H_{10}$
molecular weight	128.174	154.212
$T_m(K)$	353.15	342.4
$\tilde{V}^s(\frac{cm^3}{mole})$	128.6	131.0
$\Delta\tilde{H}_f^\circ(\frac{J}{mole})$	18814.56	19627.90
Antoine coefficient		
A	7.2144	9.4068
B	2926.6	4262.0
C	-35.8	0.0

Antoine equation: $\log P^{sat} = A - \frac{B}{T+C}$

where T in K and P^{sat} in 10^{-1} MPa

Chapter 4

Results and Discussions

The equilibrium values along the three-phase (S-L-G) coexistence curve of naphthalene-ethylene and biphenyl-ethylene systems were obtained using the "first freezing point" method. This chapter contains a presentation for the experimental data obtained. The results are correlated using the van Laar equation for the T-x values and the Peng-Robinson equation of state with one or two-parameter random mixing rules for the P-T-x values.

4.1 Naphthalene(1) - Ethylene(2) System

The results of experimental measurements for ethylene binary involving naphthalene was obtained in this study and are listed in Table 4.1. The raw experimental data are presented in Appendix D, Table D.1 and D.2. Sample calculation of liquid-phase compositions are shown in Appendix E. The measurements cover a temperature range of 325 to 346 K and pressure to approximately 17.58 MPa.

A typical graphical representation of the P-T projection of S-L-G curve is given in Figure 4.1. The P-T projection obtained in this study is compared to those of other workers. Figure 4.2

Table 4.1 : Pressure-temperature-x_1 values of the three phase (S-L-G) coexistence curve for naphthalene(1)-ethylene(2) system.

P/MPa	T/K	x_1
2.420	345.35	0.839
2.726	344.45	0.822
3.048	343.43	0.803
3.465	342.52	0.779
4.001	341.52	0.750
4.460	340.45	0.731
5.404	338.51	0.680
6.330	335.60	0.631
7.346	333.69	0.586
8.359	331.85	0.546
9.628	330.16	0.527
10.64	329.05	0.493
12.16	327.73	0.477
13.78	326.62	0.421
15.35	325.95	0.409
16.32	325.60	0.381
16.80	325.40	0.372
17.57	325.30	0.359
17.58	325.30	0.354

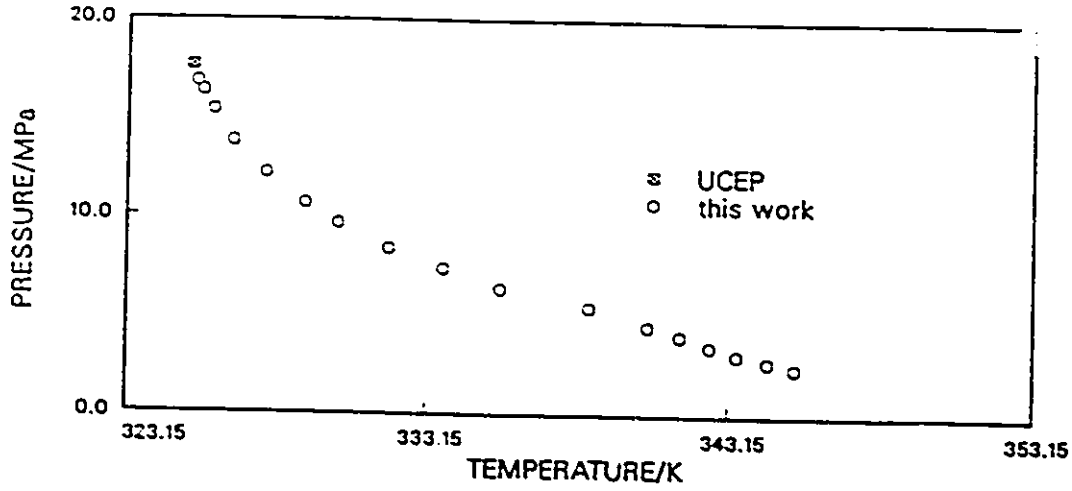

Figure 4.1 : P-T projection of naphthalene-ethylene S-L-G curve obtained in this study.

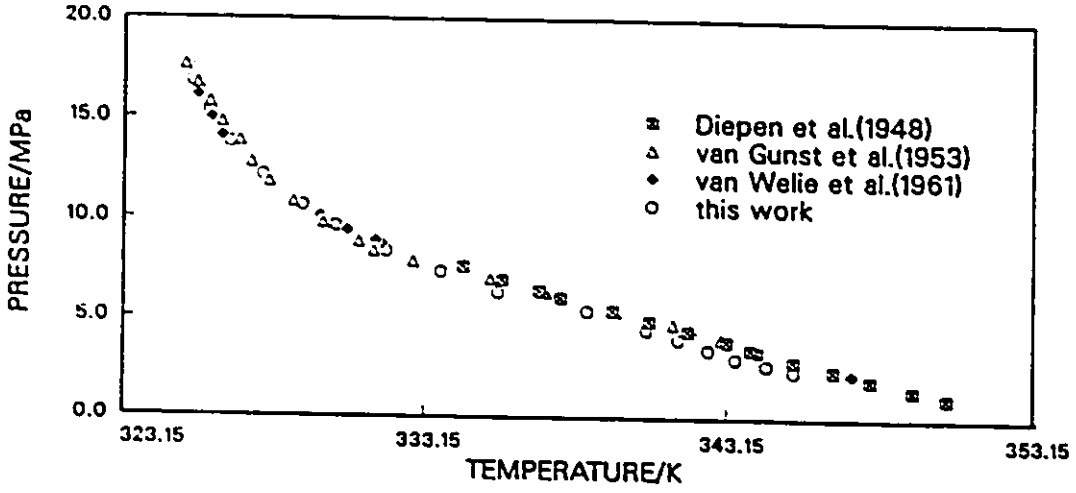

Figure 4.2 : Comparison of the P-T projection of the naphthalene-ethylene S-L-G curve obtained in this study to that of van Gunst et al.[48], van Welie et al.[123], and Diepen et al.[36].

shown the comparison of the P-T projection to that of van Gunst et al.[48], van Welie et al.[123], and Diepen et al.[36]. The values obtained in this study using the "first freezing point" method are compared with those values determined by the "first melting point" method reported by van Gunst et al.[48], and Diepen et al.[36]. In their study, the temperature is increased slowly until the solid just begins to melt. At these conditions, the pressure and temperature are taken as the three-phase equilibrium values. From Figure 4.2, some discrepancy exist between the results obtained in this work and those reported in the literature. In the "first melting point" method, uniformity of the liquid phase composition and saturation of liquid phase when the solid just begins to melt cannot be ensured due to the difficulities in stirring the mixture. Besides, it is very difficult to observe and judge when the solid starts begin to melt. The above problems were avoided using the "first freezing point" method. Starting with liquid-gas mixture, saturation of liquid phase was ensured by circulating the liquid phase through the gas phase by the used of a pumping device. In addition, the conditions under which when the first crystal appeared in the liquid phase can be easily observed. The other advantage is that experimental measurements can be reproduced independently to within ± 0.1 K. Thus the "first freezing point" method was shown to be more consistent and reliable than the "first melting point" method. van Welie et al.[123] used the "static solubility measurement" method. The P-T values of the three-phase curve were determined from every intersection of the liquid-gas isopleths and the solid-gas or solid-fluid isopleths at constant compositions. The "static solubility measurement" method is considered to be the most reliable technique although van Welie did not report the error in his data. This works agree well with the work of van Welie. Hence the "first freezing point" method used in this study is considered to be reliable.

The P-x projection of the three phase line obtained in this study are compared to the work

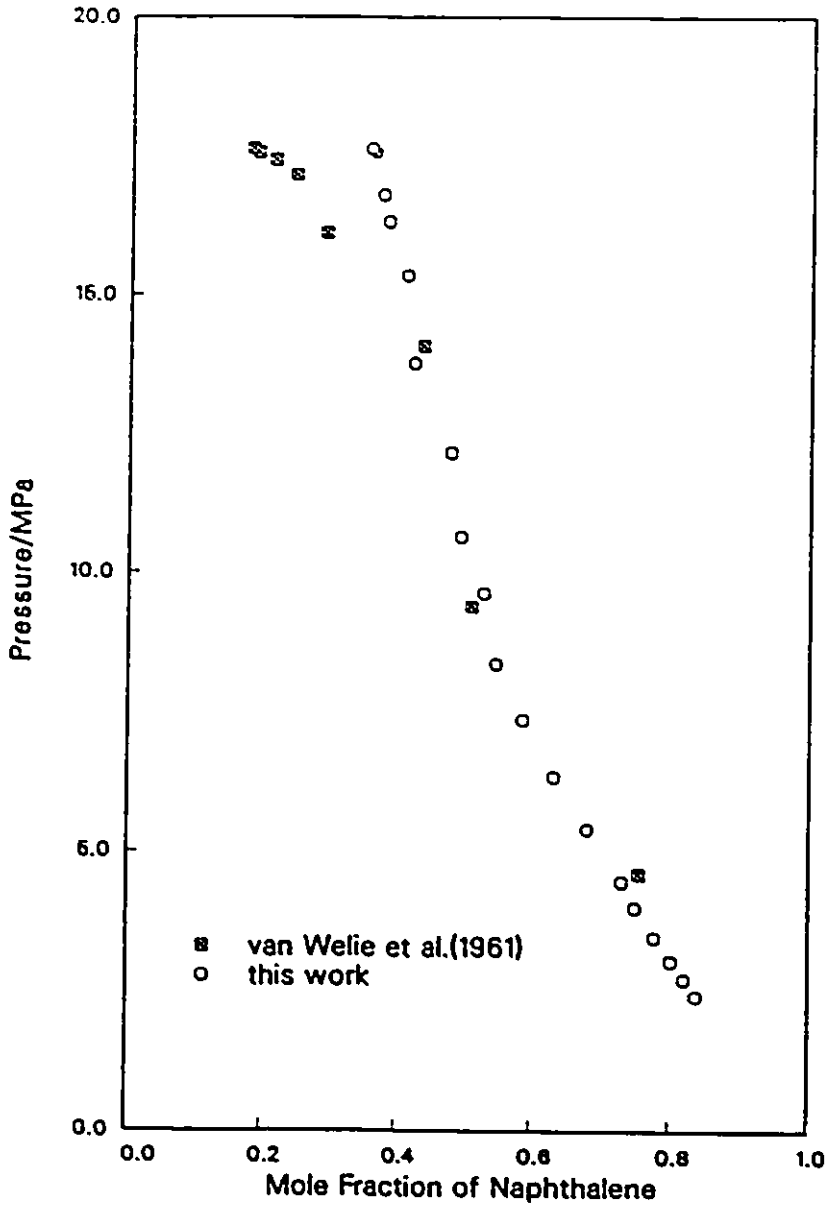

Figure 4.3 : Comparison of the P-x projection of the naphthalene-ethylene S-L-G curve obtained in this study to that of van Welie et al.[123].

of van Welie et al.[123]. and the comparison is shown in Figure 4.3. Equally excellent agreement exists between van Welie's data and the present work data at high temperatures. In contrast, fair agreement is obtained at low temperatures. In the figure, scattering of composition data obtained in this study are observed, especially at the low temperature region. The reason for this is mainly due to the sampling process. During the sampling process, the system pressure was disturbed and the saturated liquid phase solidified very quickly. Sampling was extremely difficult and it was impossible to obtain smooth composition data.

The T-x data obtained in this study were correlated using equation (2.36) and (2.37). Using the experimental T and x_1 data, the γ_1 values were calculated from equation (2.36). The van Laar equation, i.e. equation (2.37), was used to estimate the γ_1 values. The calculations were made with the use of a non-linear regression techniuqe. The A_{12} and A_{21} values in equation (2.37) were found by minimizing the sum of squares of the difference between the experimental and calculated γ_1 values. Correlation of T-x projection is shown in Figure 4.4. The best fitted values of A_{12} and A_{21} for naphthalene-ethylene system were 1.9524 and 1.0492 respectively (%AAD in γ_1 is 1.3303). From Figure 4.4, the T-x projection of the three-phase curve is well correlated using equation (2.36) and (2.37).

Proper evaluation of the experimental three-phase data is an essential element in the overall experimental effort. Up to date, no particular models have been reported which can correlate the equilibrium values of the three-phase coexistence curve successfully. In this work, the Peng-Robinson equation of state together with one or two-parameter random mixing rules are used in the prediction of equilibrium data.

Correlations using the PR equation of state and two-parameter random mixing rules are shown in Figure 4.5. The optimized k_{12} and l_{12} values were 0.28127 and 0.15832 respectively.

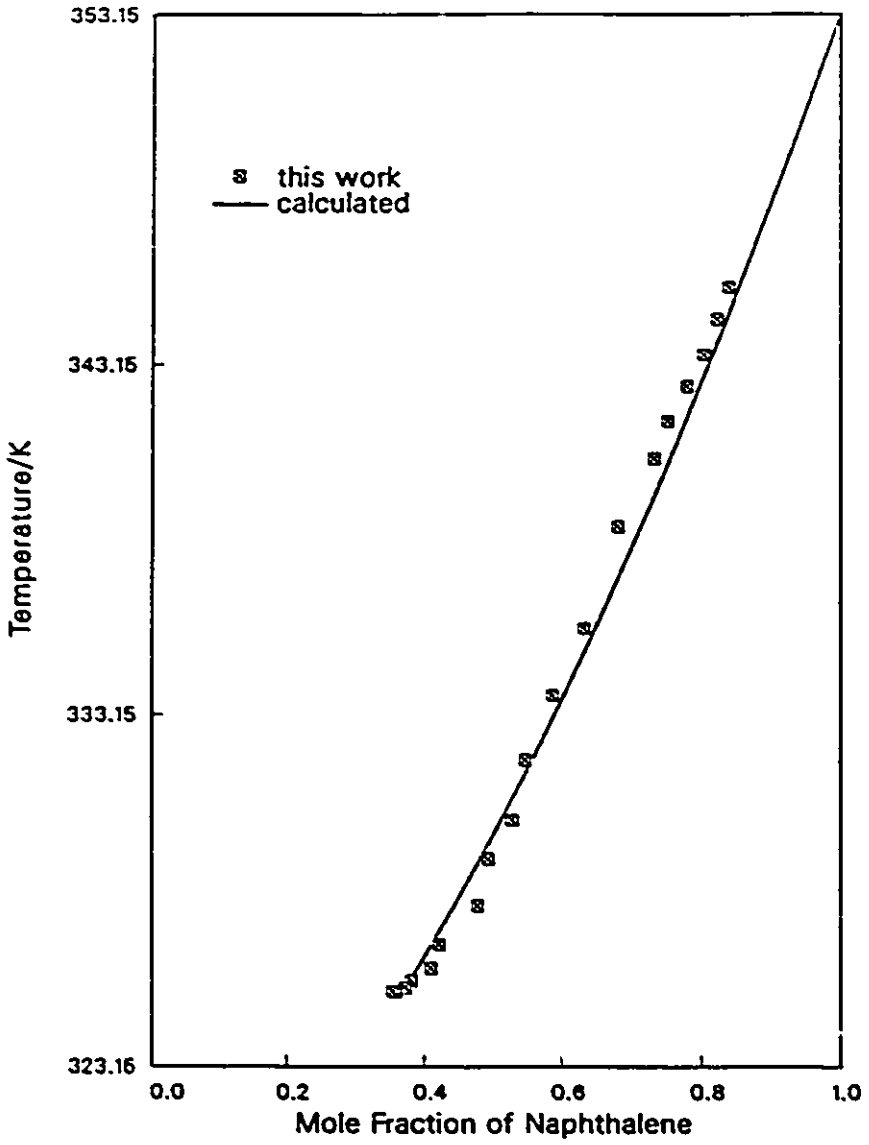

Figure 4.4 : Comparison of the experimental and correlated T-x values along the S-L-G curve for naphthalene-ethylene system.
($A_{12} = 1.9524, A_{21} = 1.0492$)

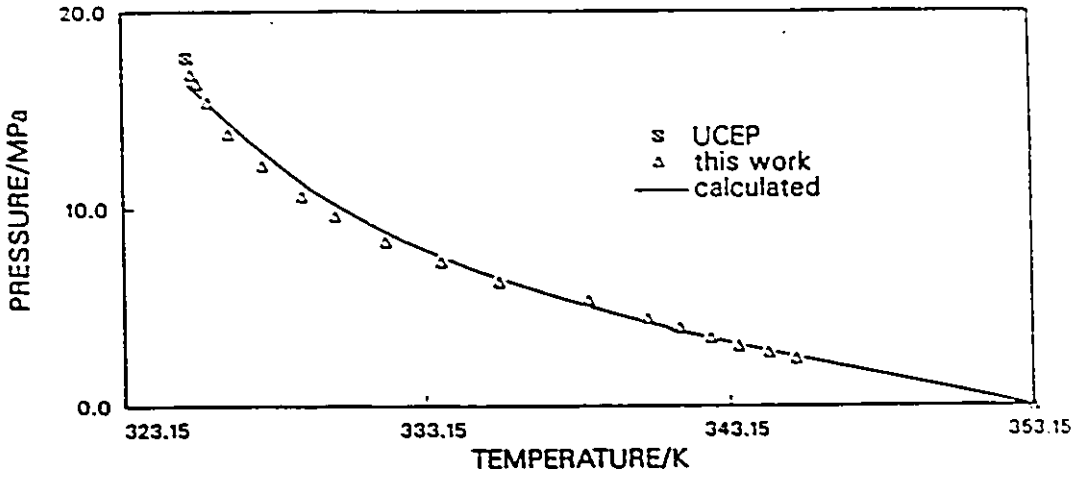

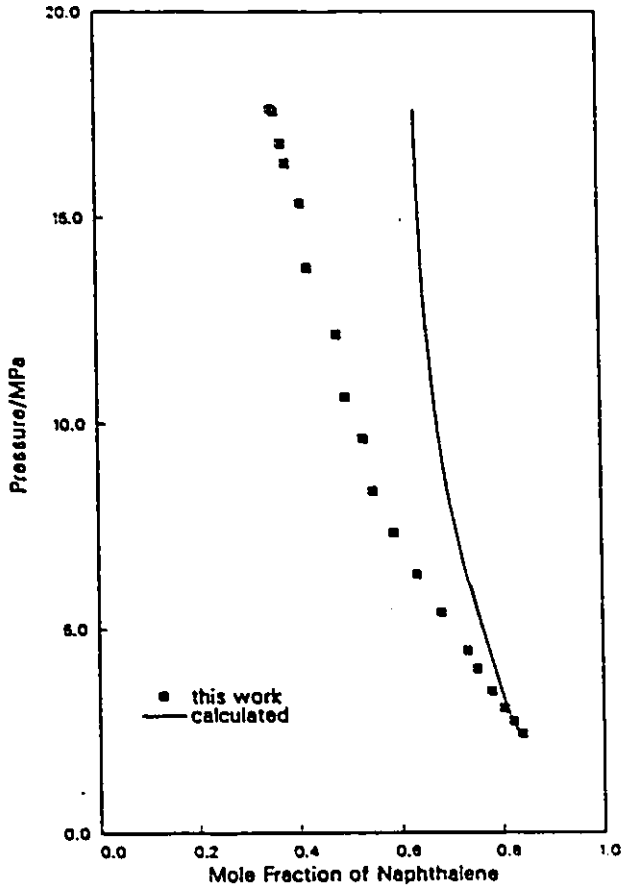

Figure 4.5 : Comparison of the experimental and correlated P-T and P-x values of the naphthalene-ethylene S-L-G curve.
(k_{12}=0.28127, l_{12}=0.15832)

These two parameters are considered to be temperature independent. From Figure 4.5, the P-T projection of the three-phase curve is well correlated using the above model. However, correlation of P-x projection is very poor. In order to improve the prediction, k_{ij} values were evaluated at each isotherm to see the effect of k_{ij} on the representation of data. The inclusion of k_{ij} in equation (2.28) was found to have a profound effect on the representation of equilibrium data. The differences between experimental and calculated pressure and liquid phase composition values can be impoved by properly selected k_{ij} values alone. By minimizing the deviations in the pressure values from the dew-point calculations, all k_{ij} values were evaluated at isothermal conditions. Attempts were then made to correlate these values by means of the following temperature function,

$$k_{ij} = a_0 + a_1 T + a_2 T^2 + a_3 T^3 \tag{4.1}$$

Correlation of k_{ij} values at isothermal conditions using equation (4.1) is shown in Figure 4.6. From Figure 4.6, the k_{ij} values are well correlated using equation (4.1). The coefficients a_0, a_1, a_2, and a_3 of equation (4.1) for naphthalene-ethylene were 0.7056×10^3, -0.6377×10^1, 0.1922×10^{-1}, and -0.1931×10^{-4} respectively.

The result of calculations of equilibrium values of three-phase curve using equation (4.1) for k_{ij} values is shown in Figure 4.7. The fit for the P-T projection is very good. The fit for both P-x and T-x are much improved although the fit is clearly inadequate. One reason for this is that the Antoine equation coefficients used to predict the solid vapor pressure do not apply to the temperatures studied and hence affected the calculation of vapor mole fractions in equation (2.35). The other reason may be the PR equation of state with the random mixing rules is inadequate in describing high pressure phase behavior.

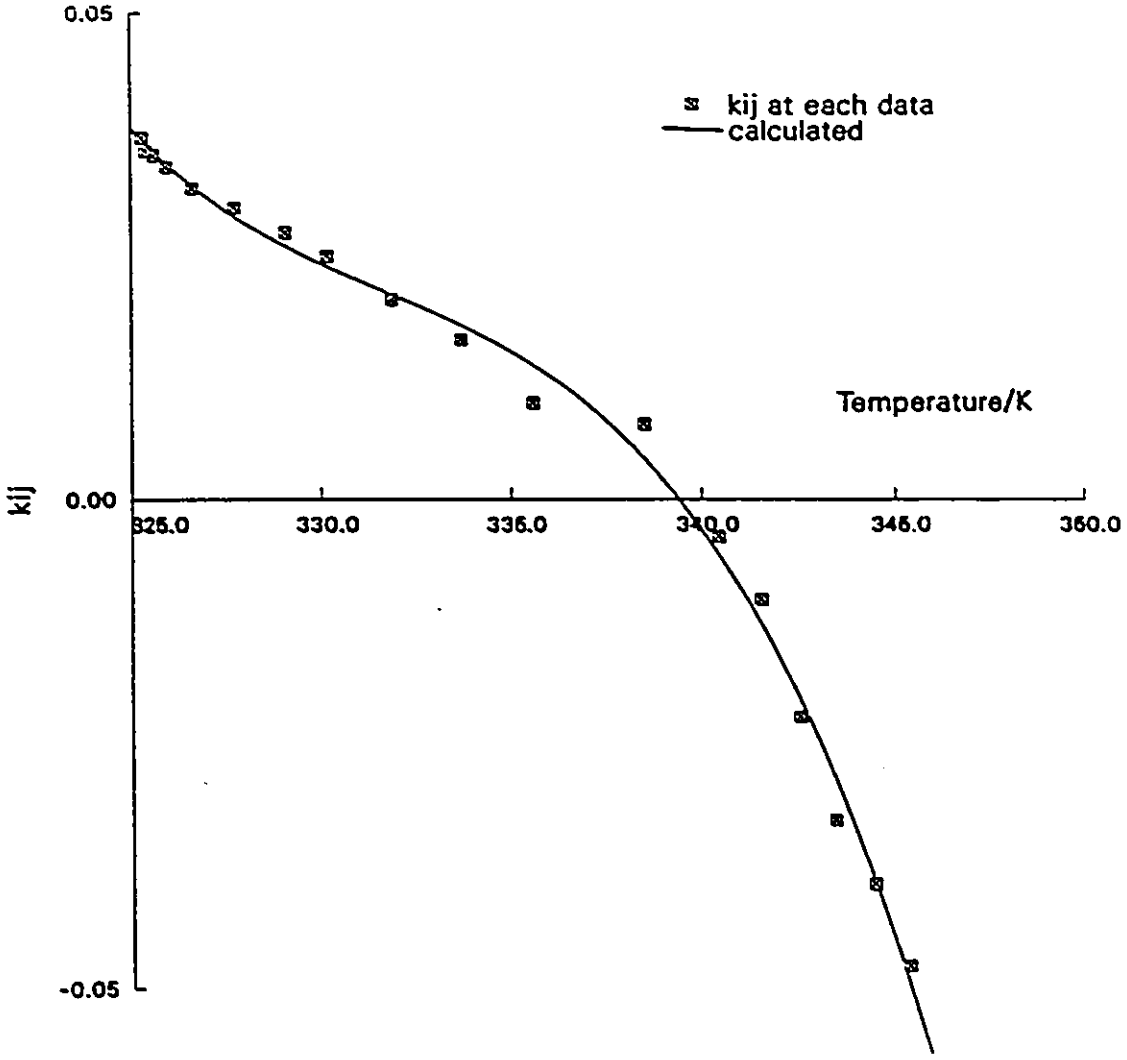

Figure 4.6 : Correlation of k_{ij} values at isothermal conditions as a function of temperature for naphthalene-ethylene system.

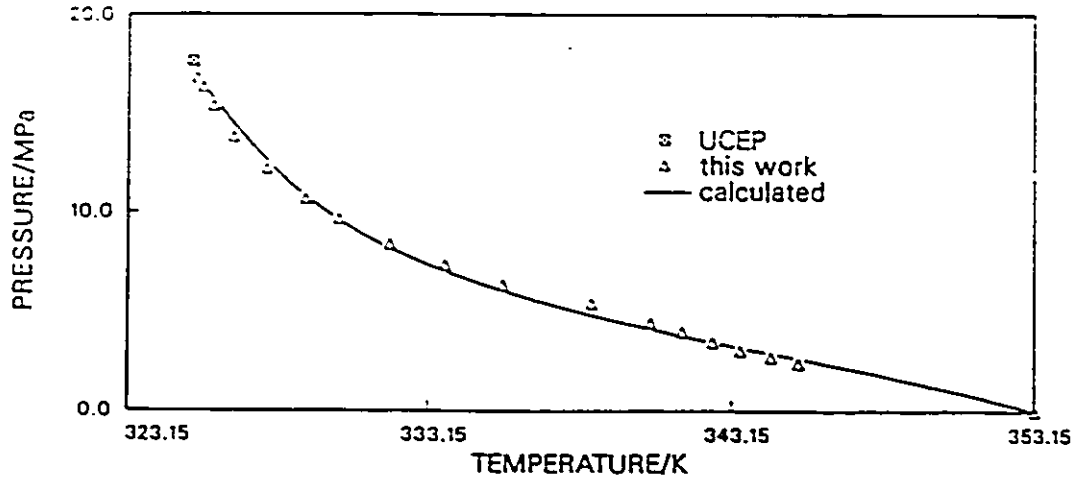

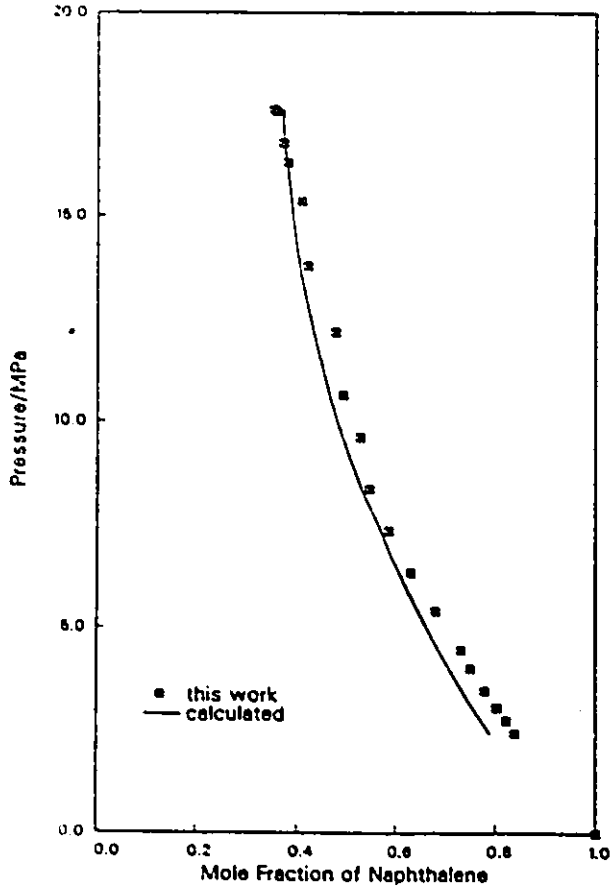

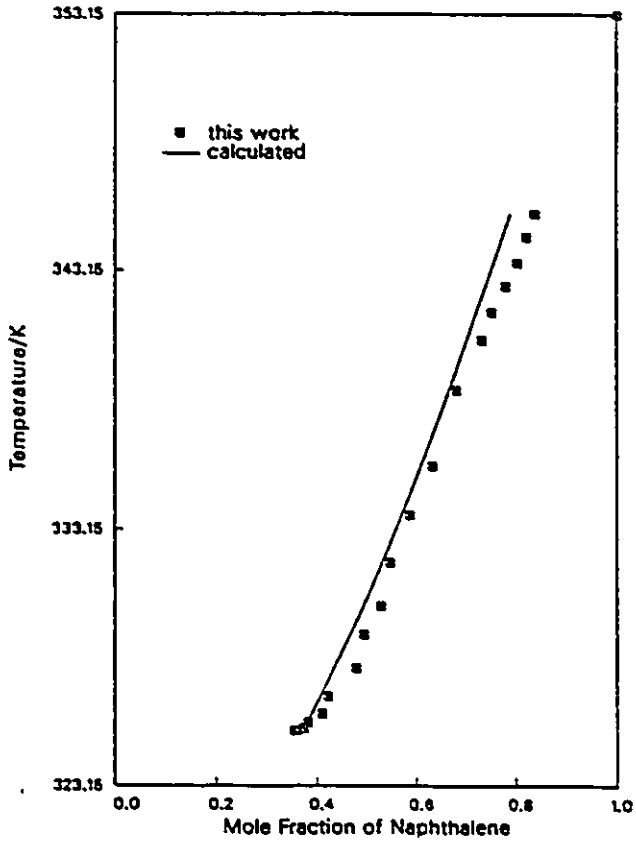

Figure 4.7 : Comparison of the experimental and correlated P-T, P-x, and T-x values of the naphthalene-ethylene S-L-G curve.
$k_{12} = f(T)$ (equation 4.1)

4.2 Biphenyl(1) - Ethylene(2) System

The results of experimental measurements for biphenyl-ethylene system obtained in this study are listed in Table 4.2. The raw experimental data are presented in Appendix D, Table D.3 and D.4. The measurements cover a temperature range of 314 to 338 K and pressure to approximately 22.18 MPa.

Figure 4.8 shown the P-T projection of S-L-G curve obtained in this study. In Figure 4.9 a comparison of P-T data obtained in this study with those acquired by Diepen et al.[36] and McHuge et al.[38] is shown indicating a good agreement. Diepen et al. and McHuge et al. determined the P-T values by the "first melting point" method. In McHugh's study, the P-T data of the three-phase curve were determined by alternatively frozen and melted the solid several time so that the temperature interval of solid-fluid and liquid-fluid was decreased to within ± 0.1 K. From Figure 4.9, discrepancy between McHugh's work, Diepen's work, and this work exist. The reasons for this are discussed in Section 4.1. The discrepancy between McHugh's data and Diepen's data confirm that the experimental data cannot be reproduced by the "first melting point" method and indicating that the "first freezing point" method has its merit.

The method of T-x correlation is essentially the same as that reported in the previous section for naphthalene-ethylene system. Correlation of T-x projection is shown in Figure 4.10. The T-x projection of the three-phase curve is again well correlated using equation (2.37) and (2.38). The best fitted values of A_{12} and A_{21} for biphenyl-ethylene system were 3.0647 and 1.0481 respectively (%AAD in γ_1 is 0.6732).

The parameter k_{ij} is considered to be a function of temperature similar in the previous section. Figure 4.11 shown the correlation of k_{ij} values using equation (4.1). All k_{ij} values used in the correlation were again evaluated at isothermal conditions. From Figure 4.11, the k_{ij} values

Table 4.2 : Pressure-temperature-x_1 values of the three phase (S-L-G) coexistence curve for biphenyl(1)-ethylene(2) system.

P/MPa	T/K	x_1
1.313	337.41	0.905
2.368	334.50	0.818
3.372	331.78	0.769
4.063	329.95	0.735
4.659	328.65	0.704
5.259	326.31	0.650
6.076	324.49	0.630
6.865	323.28	0.590
7.334	322.27	0.574
7.761	321.38	0.550
8.415	320.18	0.534
9.061	319.39	0.530
9.726	319.09	0.492
10.54	318.19	0.462
11.35	317.70	0.459
12.47	317.10	0.419
13.26	316.20	0.390
15.71	315.61	0.350
16.62	315.41	0.320
17.74	315.31	0.305
18.65	315.11	0.300
19.95	315.01	0.270
21.17	314.81	0.262
22.18	314.81	0.245

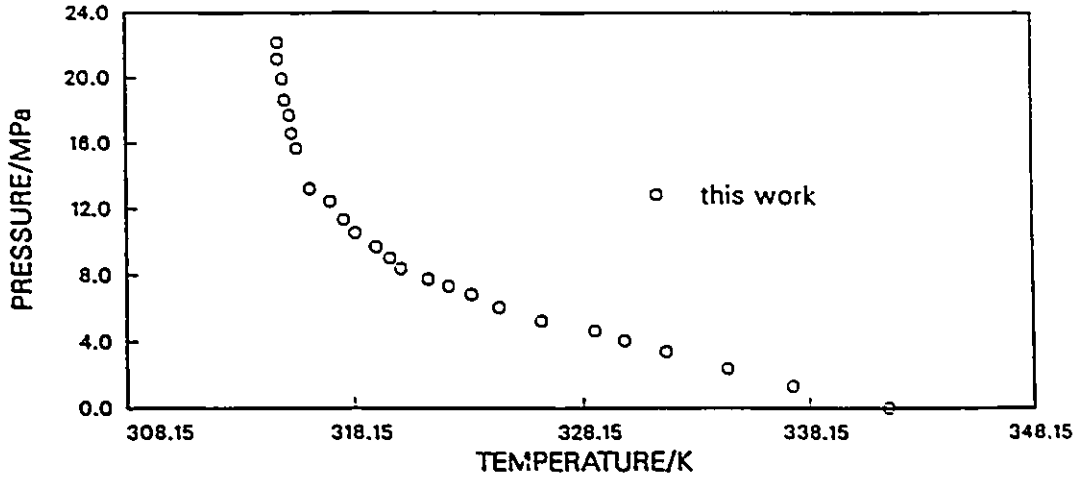

Figure 4.8 : P-T projection of biphenyl-ethylene S-L-G curve obtained in this study.

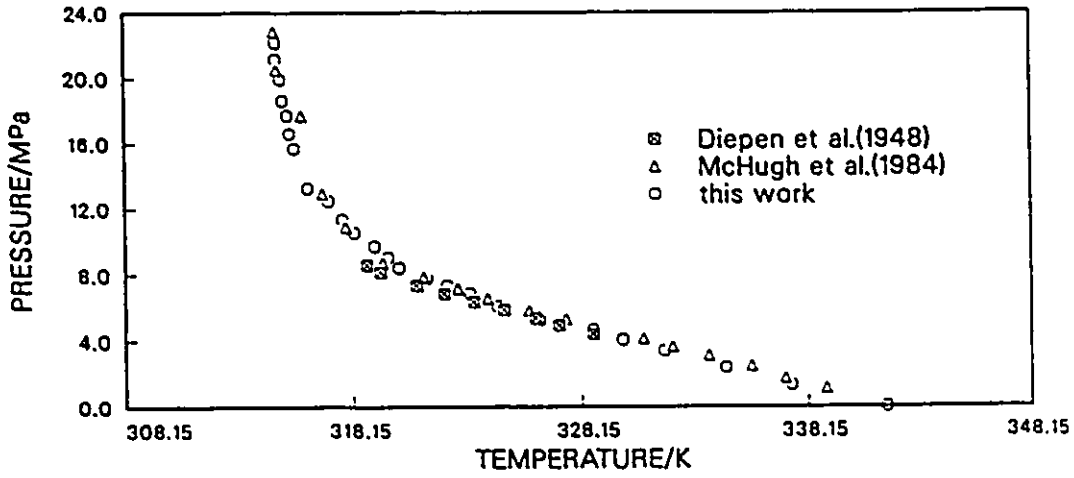

Figure 4.9 : Comparison of the P-T projection of the biphenyl-ethylene S-L-G curve obtained in this study to that of McHugh et at.[38], and Diepen et al.[36].

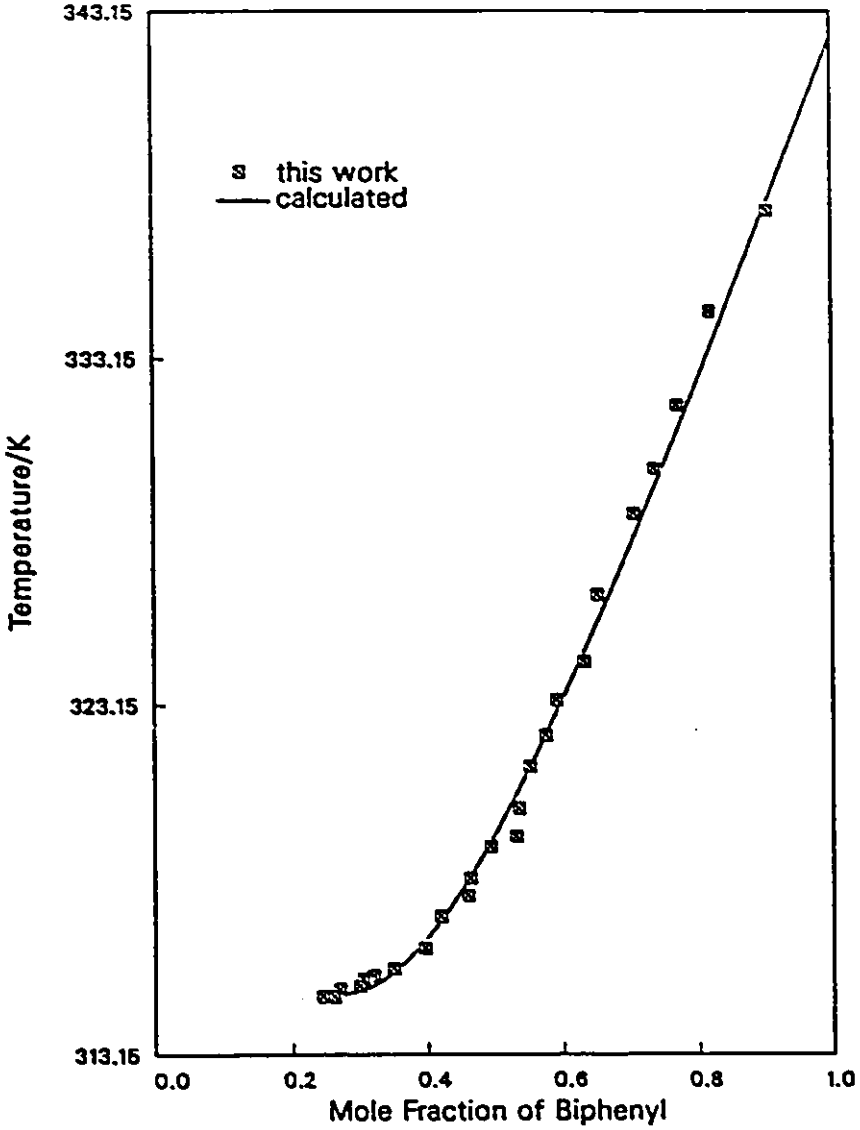

Figure 4.10 : Comparison of the experimental and correlated T-x values along the S-L-G curve for biphenyl-ethylene system.
($A_{12} = 3.0647, A_{21} = 1.0481$)

are well correlated using equation (4.1) and the coefficients a_0, a_1, a_2, and a_3 were 0.9086×10^3, -0.8494×10^1, 0.2648×10^{-1}, and -0.2753×10^{-4} respectively.

Using the temperature dependent k_{ij} function, correlation of equilibrium values along the three-phase coexistence curve is shown in Figure 4.12. Again, the P-T, P-x, T-x projections could be correlated using the above mentioned thermodynamic model.

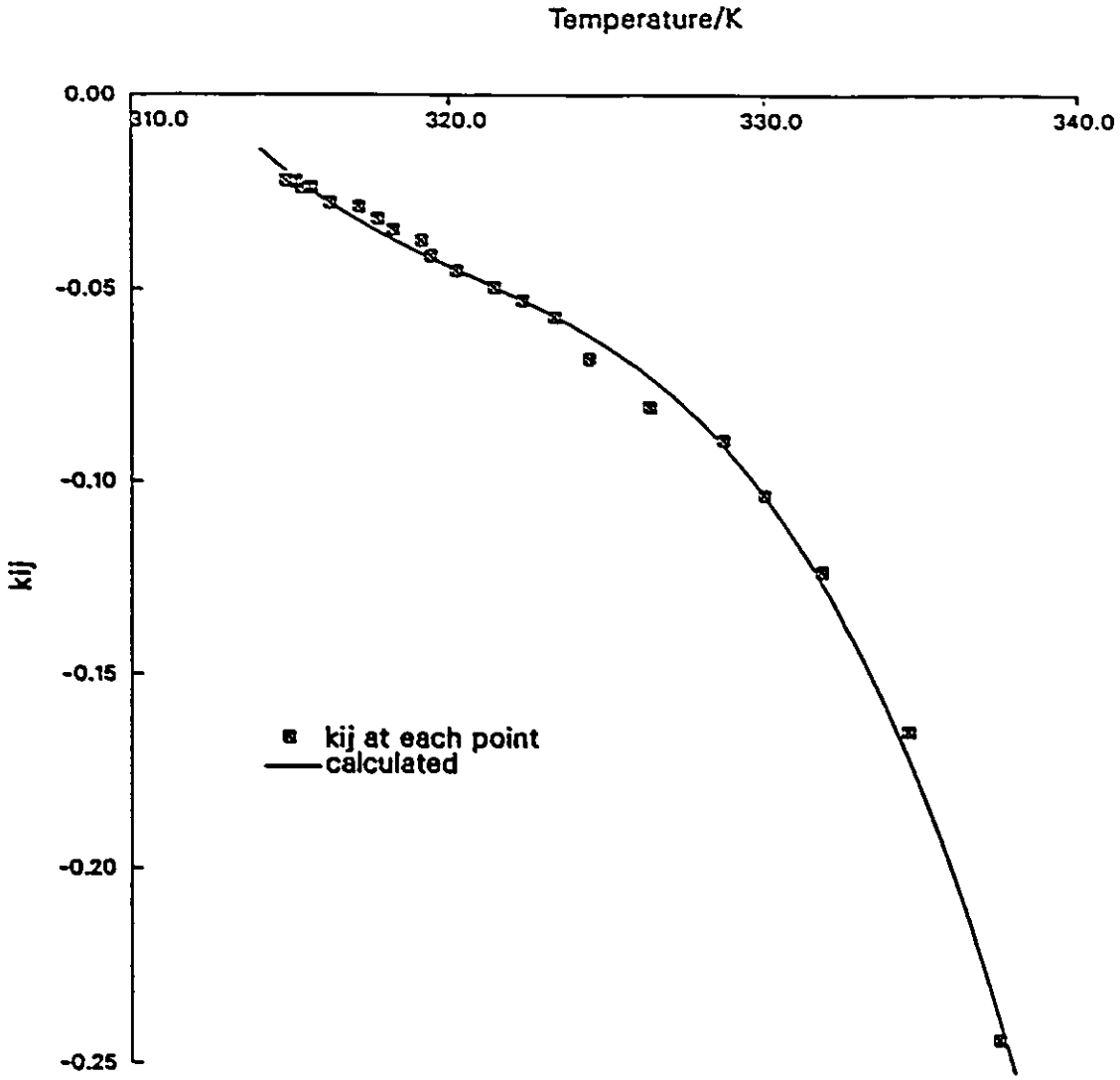

Figure 4.11 : Correlation of k_{ij} values at isothermal conditions as a function of temperature for biphenyl-ethylene system.

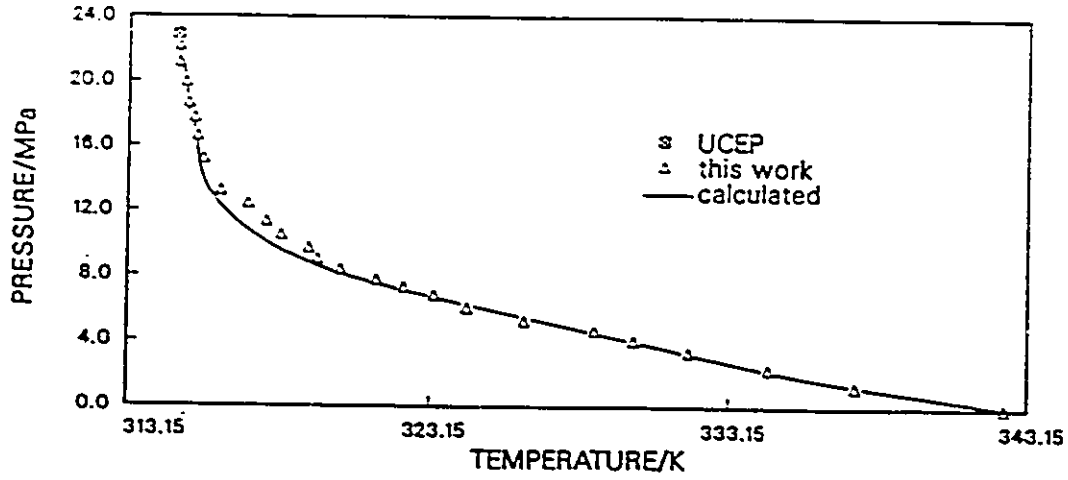

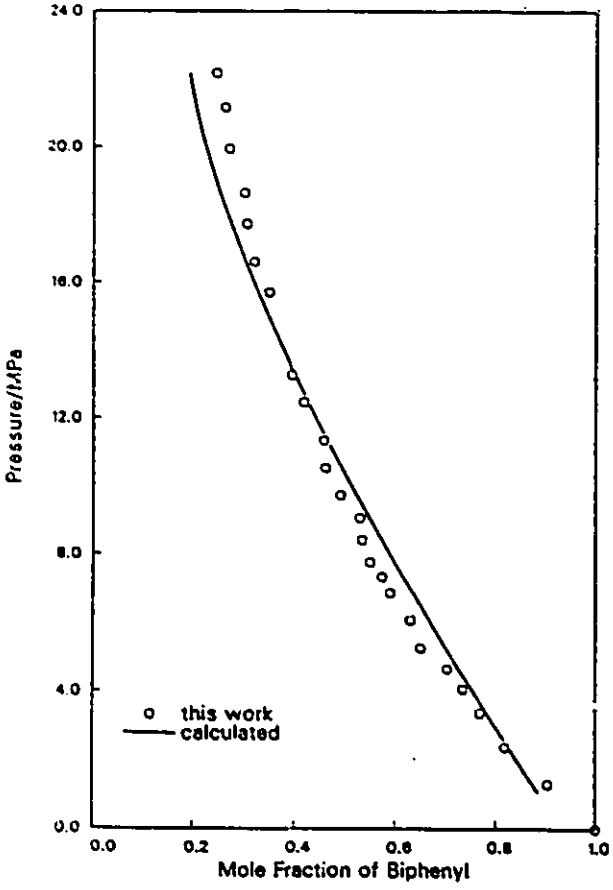

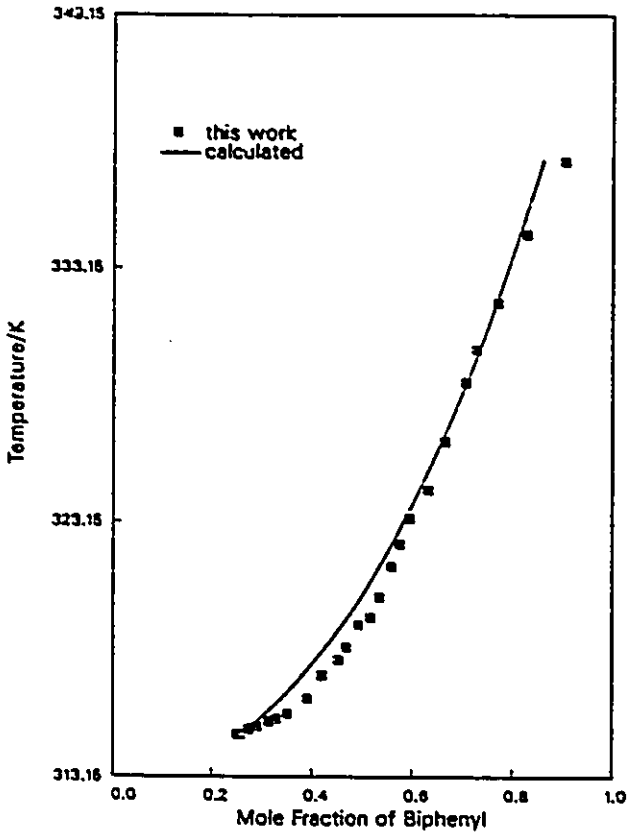

Figure 4.12 : Comparison of the experimental and correlated P-T, P-x, and T-x values of the biphenyl-ethylene S-L-G curve.
$k_{12} = f(T)$ (equation 4.1)

Chapter 5

Conclusions and Recommendations

The "first freezing point" method used in this study provide a fast and reliable measurements of the P-T-x section of the three-phase (S-L-G) coexistence curve. The two systems investigated, naphthalene-ethylene and biphenyl-ethylene, exhibited phase behavior which differed from the naphthalene-carbon dioxide and biphenyl-carbon dioxide systems. The major difference between these systems is the shape of the three-phase coexistence curve, i.e. the binary systems containing ethylene did not exhibited a temperature minimum in the P-T projection of the three-phase coexistence curve. As point out by McHugh [3], the solubility behavior of this system can be significantly different from a system with a temperature minimum. Since the different types of possible phase behavior are not distinguishable from the solubility data alone, one therefore needs to determine the P-T projection of the three-phase coexistence curve to correctly interpret the solubility data either as solid-fluid equilibrium or as liquid-gas equilibrium.

The composition data obtained in this study together with the solution model provide useful information in correlating the T-x data. This correlation give fast and reliable estimate of the liquid phase compostion.

Correlation of equilibrium data (P-T-x) using the PR equation of state showed that the one-

parameter temperature dependent random mixing rules yield better representation of data than the two-parameter temperature independent random mixing rules. Although the prediction of composition is not good enough, the temperature function of k_{ij} was found to give better overall representation, especially in the prediction of liquid phase composition.

The applications of supercritical fluid extraction technology depend on our ability to understand the phase behavior in the vicinity of the critical point and in the supercritical region. It is therefore recommended that more reliable experimental data for pure solvent and highly asymmetric mixtures be obtained at near critical and high pressure regions. This information is especially important in generalizing and testing thermodynamics models. It is also suggested that other new solvent or co-solvents be studied in an effort to find a solvent(s) with high loading power and to find different type of phase behavior. Besides, thermodynamic modelling of the phase behavior at near critical or supercritical conditions should be investigated to extend the experimental information to systems not experimentally measured. This is not an easy task due to the problems of characterizing the dense gas state as well as formulating appropriate mixing rules for highly asymmetric mixtures.

Bibliography

[1] Hannary, J.B. and Hogarth, J., **Proc. R. Soc.**, London, 29:324 (1879).

[2] Smith, J.M. and Van Ness, H.C., " **Introduction to Chemical Engineering Thermodynamics** ", 4th edition, McGraw-Hill (1987).

[3] McHugh, M.A., **Doctoral Dissertation**, University of Delaware, (1981).

[4] Irani, C.A. and Funck, E.W., " **Separations Using Supercritical Gases, Recent Development in Separation Science** ", CPC Press, Vol. 3, Part A:171 (1977).

[5] Williams, D.F., **Chem. Eng. Sci.**, 36:1769 (1981).

[6] Paulaitis, M.E., Krukonis, V.J., Kurnik, R.T. and Reid, R.C., " **Supercritical Fluid Extraction** ", **Review in Chem. Eng.**, 1:179 (1983).

[7] Ely, J.F. and Baker, J.K., " **A Review of Supercritical Fluid Extraction** ", U.S. Department of Commerce, National Bereau of Standards, December (1983).

[8] Giddings, J.C., Myers, M.N., McLaren, L. and Keller, R.A., **Science**, 162:67 (1968).

[9] DeFillipi, R.P. and Moses, J.M., " **Extraction of Organics from Aqueous Solutions Using Critical Fluid Carbon Dioxide** ", C.D. Scott, ed., John Wiley & Sons, New York, 206 (1982).

[10] Vitzthum, O.G. and Hubert, P., **Angew. Chem. Int. Ed. Engl.**, 17:710 (1978).

[11] Schneider, G.M., Stahl, E. and Wilke, G., eds., " **Extraction with Supercritical Gases** ", Verlag Chemie, Deerfield Beach, Floride, (1980).

[12] Gearhart, J.A. and Garwin, L., " **A New Economical Approach to Residuum Processing** ", presented at the 1976 National Petroleum Refiners Association, San Antonio, Texas, March 30 (1976).

[13] Gearhart, J.A. and Garwin, L., **Hydrocarbon Process**, 55:125 (1976).

[14] Knebel, A.H. and Rhodes, D.E., **Chem. Eng. Prog.**, 75:44 (1979).

[15] Baldwin, R.A., Davis, R.E. and Wing, H.F., " **Critical Solvent De-Ashing – A New Solids Separation Method for Coal Liquefaction Processes** ", present at the 4th International Conference on Coal Gasification, Liquefaction, and Conversion to Electricity, Pgh., Pa, August (1977).

[16] Whitehead, J.C. and Williams, D.F., **J. Inst. Fuel**, 182 (1975).

[17] Moddocks, R.R., Gibson, J.G. and Williams, D.F., " **Supercritical Extraction of Coal - Update** ", presented at 71st Annual Meeting AIChE, Miami, Florida, November (1978).

[18] Metcalfe, R.S. and Yarborough, L., **Soc. Pet. Eng. J.**, 242 (1979).

[19] Martin, T.G. and Williams, D.F., " **Gaseous Solvent Extraction of Oil Shales & Tar Sands** ", U.S. Patent 4,108,760 (1978).

[20] Vitzthum, D. and Hubert, P., " **Process for Decaffeination of Coffee** ", German Patent, 2.357.590 (1975).

[21] Zosel, K., Angew. Chem. Int. Ed. Engl., 17: 702 (1978).

[22] Kohn, P.M., Savage, P.R. and McQueen, S., Chem. Eng. News, PP. 41, March 12 (1979).

[23] Friedrich, J.P., List, G.R. and Heakin, A.J., " Petroleum Free Extraction of Oil from Soybeans with Supercritical CO_2 ", presented at 72nd Annual Am. Oil Chem. Soc. Meeting, New Orleans, May (1981).

[24] O'Neill, A.J., M.A.Sc. Thesis, University of Ottawa, (1987).

[25] Anon, Food Eng. Intl., 45 (1981).

[26] Vitzthum, O.G., Hubert, P. and Sirtl, W., " Production of Hop Extracts ", U.S. Patent 4,104,409 (1970).

[27] Stahl, E., Rev. Latinoam. Quim., 11:1 (1980).

[28] Calame, J.P. and Steiner, R., Chem. Ind., 399 (1982).

[29] DeFillipi, R.P., Kyukonis, V.J. and Modell, M., Environment Protection Agency Report No. EPA-600/2-80-054, (1980).

[30] Chang, H. and Marrell, D.G., J. Chem. Eng. Data, 30:74 (1985).

[31] Krukonis, V.S. and Kurnik, R.T., J. Chem. Eng. Data, 30:247 (1985).

[32] DeFillipi, R.P., Chem. Ind., 390 (1982).

[33] Elgin, J.C. and Weinstock, J.J., J. Chem. Eng. Data, 4:3 (1959).

[34] Klesper, E., Corwin, A.H. and Turner, D.A., J. Org. Chem., 27:700 (1962).

[35] Klesper, E., Angew. Chem. Int. Ed. Engl., 17: 738 (1978).

[36] Diepen, G.A.M. and Scheffer, F.E.C., J. Phys. Chem., 57:575 (1953).

[37] Tsekhanskaya, Y.V., Iomtev, M.B. and Muskina, E.V., Russ. J. Phys. Chem., 38:1173 (1964).

[38] McHugh, M.A. and Yogan, T.J., J. Chem. Eng. Data, 29:112 (1984).

[39] Krukonis, V.J., McHugh, M.A. and Secker, A.J., J. Phys. Chem., 88:2687 (1984).

[40] Cheong, P.L., M.A.Sc. Thesis, University of Ottawa, (1985).

[41] McHugh, M.A., Secker, A.J. and Yogan, T.J., Ind. Eng. Chem. Fundam., 23:493 (1984).

[42] Van Leer, R.A. and Paulaitis, M.E., J. Chem. Eng. Data, 25:257 (1980).

[43] Johnston, K.P. and Eckert, C.A., AIChE J., 27:773 (1981).

[44] McHugh, M.A. and Paulaitis, M.E., J. Chem. Eng. Data, 25:326 (1980).

[45] Johnston, K.P., Zlger, D.H. and Eckert, C.A., Ind. Eng. Chem. Fundam., 21:191 (1982).

[46] Chrastil, J., J. Phys. Chem., 86:3016 (1982).

[47] Kurnik, R.T., Holla, S.J. and Reid, R.C., J. Chem. Eng. Data, 26:47 (1981).

[48] van Gunst, C.A., Scheffer, F.E.C. and Diepen, G.A.M., J. Phys, Chem., 57:578 (1953).

[49] Ciklis, D.S., Russ. J. Phys. Chem., 50:825 (1976).

[50] Franck, E.U., Henderson, D., Jost, W. and Eyring, H., Phys. Chem., 73:135 (1969).

[51] Schneider, G.M., Fortschr. Chem. Forch., 13:559 1970).

[52] Schneider, G.M., Adv. Chem. Phys., 17:1 (1970).

[53] Schneider, G.M., " Chemical Thermodynamics, Vol. 2, A Specialist Periodical Reports ", Chapter 4, London, (1978).

[54] Schneider, G.M., Angew. Chem. Int. Ed. Engl., 17:716 (1978).

[55] Rowlinson, J.S., " Liquid and Liquid Mixtures ", Butterworths, London, (1982).

[56] Scott, R.L. and van Konynenburg, P.H., Discuss. Faraday Soc., 49:87 (1970).

[57] van Konynenburg, P.H. and Scott, R.L., Philos. trans. R. Soc., London, A298:495 (1980).

[58] van der Waals, J.D., Doctoral Dissertation, Leiden, Holland (1873).

[59] Gibbs, J.W., " The Scientific Papers of J.Willard Gibbs ", Dover Publication Inc., New York, I:55 (1961).

[60] Prausnitz, J.M., " Molecular Thermodynamics of Fluid-Phase Equilibria ", 2nd ed., Prentice-Hall, Englewood Cliffs, N.J. (1986).

[61] Rowlinson, J.S. and Richardson, M.J., Advan. Chem. Phys., 2:85 (1959).

[62] Deiters, U. and Schneider, G.M., Ber. Bunsenges. Phys. Chem., 80:1316 (1976).

[63] Peter, S. and Wenzel, H., " Phase Equilibrium from Equation of State, Application to Supercritical Extraction ", proceeding of the 2nd International Conference on Phase Equilibrium and Fluid Properties in the Chemical Industry, DECHEMA, Frankfurt/Main, 355 (1980).

[64] Kurnik, R.T. and Reid, R.C., AIChE J., 27:861 (1981).

[65] Vidal, J., Ber. Bunsenges. Phys. Chem., 88:784 (1984).

[66] Robin, S. and Vodar, B., **Discuss. Faraday Soc.**, 36:233 (1953).

[67] Czubryt, J.J., Myers, M.N. and Gidding, J.C., **J. Phys. Chem.**, 74:4260 (1970).

[68] Stahl, E., Schilz, W., Schültz, E. and Willing, E., **Angew. Chem. Int. Ed. Engl.**, 17:731 (1978).

[69] Adachi, Y. and Lu, B.C.-Y., **Fluid Phase Equilibria**, 14:147 (1983).

[70] Huron, M.J. and Vidal, J., **Fluid Phase Equilibria**, 3:255 (1979).

[71] Chueh, P.L. and Prausnitz, J.M., **" Computer Calculations for High Pressure Vapor-Liquid Equilibria "**, Prentice-Hall, Englewood Cliffs, N.J. (1968).

[72] Prausnitz, J.M., **Chem. Eng. Sci.**, 18:613 (1963).

[73] Hsi, C. and Lu, B.C.-Y., **Can. J. Chem. Eng.**, 19:134 (1971).

[74] Tsonopoulos, C. and Heidman, J.L., **Fluid Phase Equilibria**, 29:391 (1986).

[75] Redlich, O. and Kwong, J.N.S., **Chem. Rev.**, 44:233 (1949).

[76] Soave, G., **Chem. Eng. Sci.**, 27:1197 (1972).

[77] Peng, D.-Y. and Robinson, D.B., **Ind. Eng. Chem. Fundam.**, 15:59 (1976).

[78] Robinson, D.B. and Peng, D.-Y., **GPA Research Report**, 28 (1978).

[79] Kato, K., Nagahama, K. and Hirata, M., **Fluid Phase Equilibria**, 7:219 (1981).

[80] Lin, H.M., **Fluid Phase Equilibria**, 16:151 (1984).

[81] Orye, R.V., **Ind. Eng. Chem. Process Des. Dev.**, 8:579 (1969).

[82] Zudkevitch, D. and Joffe, J., AIChE J., 16:112 (1970).

[83] Lu, B.C.-Y., Kato, M. and Chung, W.K., Chem. Eng. Sci., 31:733 (1976).

[84] Huron, M.J., Dutour, G.N. and Vidal, J., Fluid Phase Equilibria, 1:247 (1977/78).

[85] Graboski, M.S. and Daubert, T.E., Ind. Eng. Chem. Process Des. Dev., 17:448 (1978).

[86] Plöckner, U., Knapp, H. and Prausnitz, J., Ind. Eng. Chem. Process Des. Dev., 17:324 (1978).

[87] Evelein, K.A. and Moore, R.G., Ind. Eng. Chem. Process Des. Dev., 18:618 (1979).

[88] Adachi, Y. and Sugie, H., Fluid Phase Equilibria, 28:103 (1986).

[89] Radosz, M., Lin, H.M. and Chao, K.C., Ind. Eng. Chem. Process Des. Dev., 21:653 (1982).

[90] Vidal, J., Chem. Eng. Sci., 33:787 (1978).

[91] Huron, M.J. and Vidal, J., Fluid Phase Equilibria, 3:255 (1979).

[92] Reid, R.C. and Panagiotopolos, A.Z., " Equation of State - Theories & Applications ", ACS Symposuium, Series no. 300 (1986).

[93] Mathias, P.M. and Crepman, T.W., Fluid Phase Equilibria, 13:91 (1983).

[94] Mollerup, J., Fluid Phase Equilibria, 7:121 (1981).

[95] Whiting, W.B. and Prausnitz, J.M., Fluid Phase Equilibria, 9:119 (1982).

[96] Luedecke, D. and Prausnitz, J.M., Fluid Phase Equilibria, 22:1 (1985).

[97] Le Neindre, B. and Vodar, B., eds., " Experimental Thermodynamics, Vol. II, Experimental Thermodynamics of Non-Reacting Fluid ", Butterworths, London, (1975).

[98] Schneider, G.M., " Phase Equilibria of Liquid and Gaseous Mixtures at High Pressure, Part 2 ", Chapter 16, ibid.

[99] Young, C.L., " Chemical Thermodynamics, Vol. 2 " , The Chemical Society, London, Chapter 3 (1978).

[100] Sage, B.H. and Lacey, W.N., Ind. Eng. Chem., 26:103 (1934).

[101] Sage, B.H. and Lacey, W.N., Ind. Eng. Chem., 26:1218 (1934).

[102] Kay, W.B., Ind. Eng. Chem., 28:1014 (1936).

[103] Feller, M. and McDonald, H.J., Anal. Chem., 22:338 (1950).

[104] Selleck, F.T., Garmichael, L.T. and Sage, B.H., Ind. Eng. Chem., 44:2219 (1952).

[105] Matzik, I. and Schneider, G.M., Phys. Chem., 89:551 (1985).

[106] Lesavre, M.M., Richnon, D. and Renon, H., Ind. Eng. Chem. Fundam., 20:284 (1981).

[107] Rousseaux, P., Richon, D. and Renon, H., Fluid Phase Equilibria, 11:153 (1983).

[108] Gasem, K.A.M. and Robinson, Jr. R.L., J. Chem. Eng. Data, 30:53 (1985).

[109] Anderson, J.M., Barrick, M.W. and Robinson, Jr. R.L., J. Chem. Eng. Data, 31:172 (1986).

[110] Barrick, M.W., Anderson, J.M. and Robinson, Jr. R.L., J. Chem. Eng. Data, 32:372 (1987).

[111] Wisotzki, K.D. and Schneider, G.M., Phys. Chem., 89:21 (1985).

[112] Konrad, R.K., Swaid, I. and Schneider, G.M., Fluid Phase Equilibria,10:307 (1983).

[113] Grayson, H.G. and Streed, C.W., present at 6th World Petroleum Congress, Frankfurt/main. Section VII, Paper 20, June 19-26 (1963).

[114] Sebastian, H.M., Simnick, J.J., Lin, H.M. and Chao, K.C., **J. Chem. Eng. Data**, 25:246 (1980).

[115] Lin, H.M., Kim, H., Leet, W.A. and Chao, K.C., **Ind. Eng. Chem. Fundam.**, 24:260 (1985).

[116] Inomata, H., Arai, K. and Saito, S., **Fluid Phase Equilibria**, 29:225 (1986).

[117] Inomata, H., Arai, K. and Saito, S., **Fluid Phase Equilibria**, 36:107 (1987).

[118] Mohamed, R.S. and Holder, G.D., **Fluid Phase Equilibria**, 32:295 (1987).

[119] Kurnik, R.T. and Reid, R.C., **Fluid Phase Equilibria**,8:93 (1982).

[120] Nasir, P., Martin, R.J. and Kobayashi, R., **Fluid Phase Equilibria**, 5:279 (1980/81).

[121] Charoensombut-Amon,T., Martin, R.J. and Kobayashi, R., **Fluid Phase Equilibria**, 31:81 (1986).

[122] Prins, A., **Acad. Sci. Arnsterdam**, 17:1095 (1915).

[123] van Welie, G.S.A. and Diepen, G.A.M., **Rec. Trav. Chem.**, 80:659 (1961).

[124] Cheong, P.L., Zhang, D., Ohgaki, K. and Lu. B.C.-Y., **Fluid Phase Equilibria**, 29:555 (1986).

[125] Diepen, G.A.M. and Scheffer, F.E.C., **J. Phys. Chem.**, 70:4085 (1948).

[126] Tsang, C.Y. and Streett, W.B., **Chem. Eng. Sci.**, 36:993 (1981).

[127] Streett, W.B. and Hill, J.L.E., **J. Chem. Phys.**, 54:5088 (1971).

[128] Malanowski, S., **Fluid Phase Equilibria**, 8:197 (1982).

[129] Inglis, J.K.H., **Philos. Mag.**, 11:640 (1906).

[130] Dobbs, J.M., **Doctoral Dissertation**, University of Texas at Austin, (1986).

Appendix A

Calibration of the Pressure Measurement

A dead weight pressure tester (Testing Instrument Co. Inc.) was used to calibrate the pressure transducer (B1 : model RB-201-10000, series number 99429, Data Instruments Inc., Lexington, mass. 02173, maximum 34.46 MPa or 50000 psi) of Figure (3.1) . The calibration curve for the transducer is shown in Figure A.1.

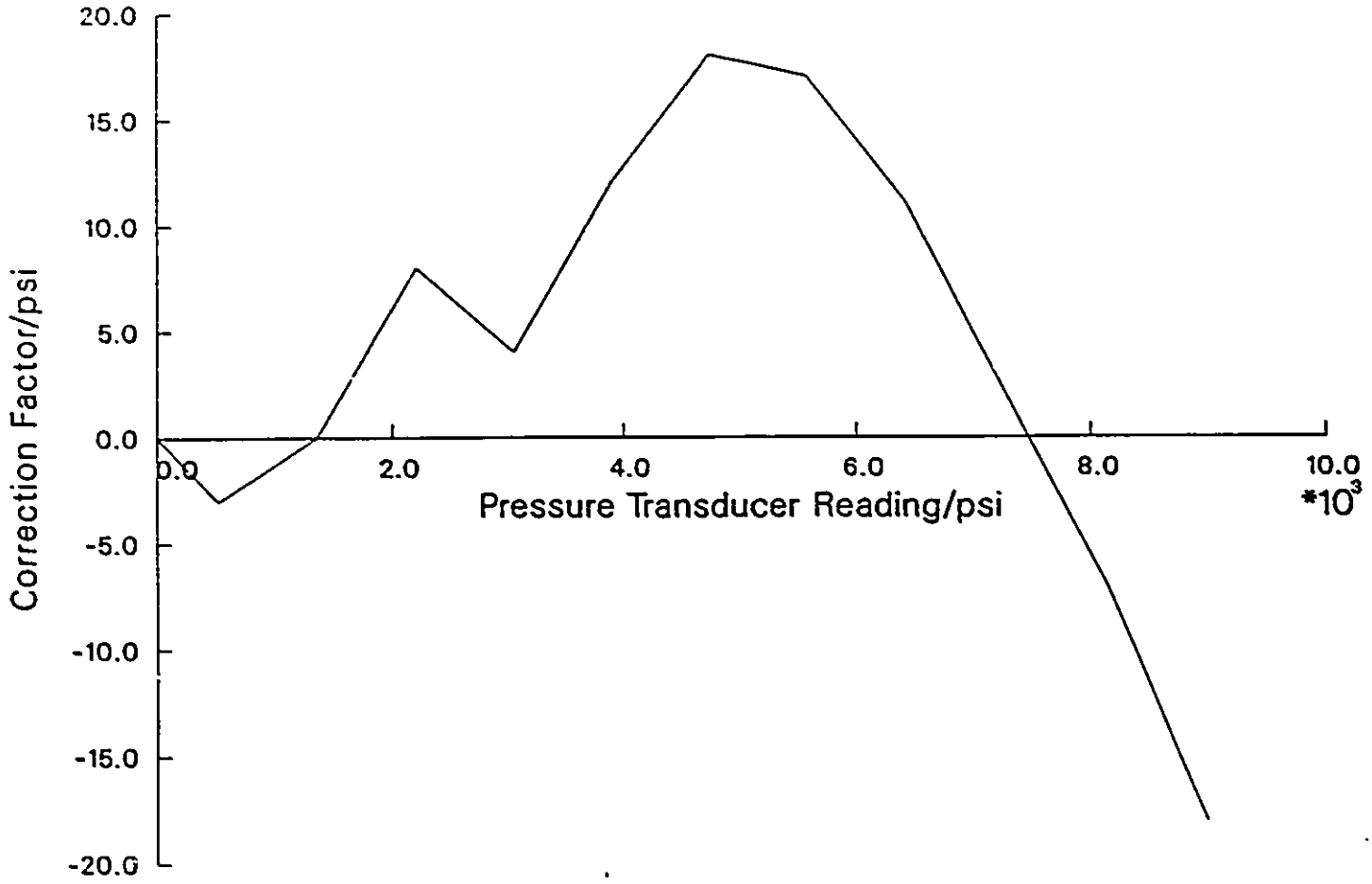

Figure A.1 : Calibration curve for the pressure transducer.

Appendix B

Calibration of the Temperature Measurement

The thermocouples with indicator (model Doric Trendicator 410A, Doric Scientific Division, Emerson Electric Co.) used to measure the temperatures at the upper pump, the lower pump, and the equilibrium cell were calibrated at the triple point (273.16 K) of pure water as well as calibration with a calibrated Hewlett Packard quartz thermometer (model 2801A) with sensor (series number 1126-44). The calibrated results at triple point as well as other temperatures are listed in Table B.1. The calibration curve is shown in Figure B.1.

Table B.1 : Calibration of the thermocouples.

Quartz Thermometer Reading	Thermocouples Reading (T_c)			Correction factor
$T_Q / \circ C$	index 8	index 9	index 10	($\circ C$)
* 0.01	0.0	0.0	0.0	0.0
30.44	31.20	31.20	31.20	-0.76
40.17	40.80	40.80	40.80	-0.63
50.02	50.70	50.70	50.70	-0.68
60.04	60.60	60.60	60.60	-0.56
70.07	70.60	70.60	70.60	-0.53
80.14	80.60	80.60	80.60	-0.46

* Triple point of water

Correction factor = T_Q - T_c

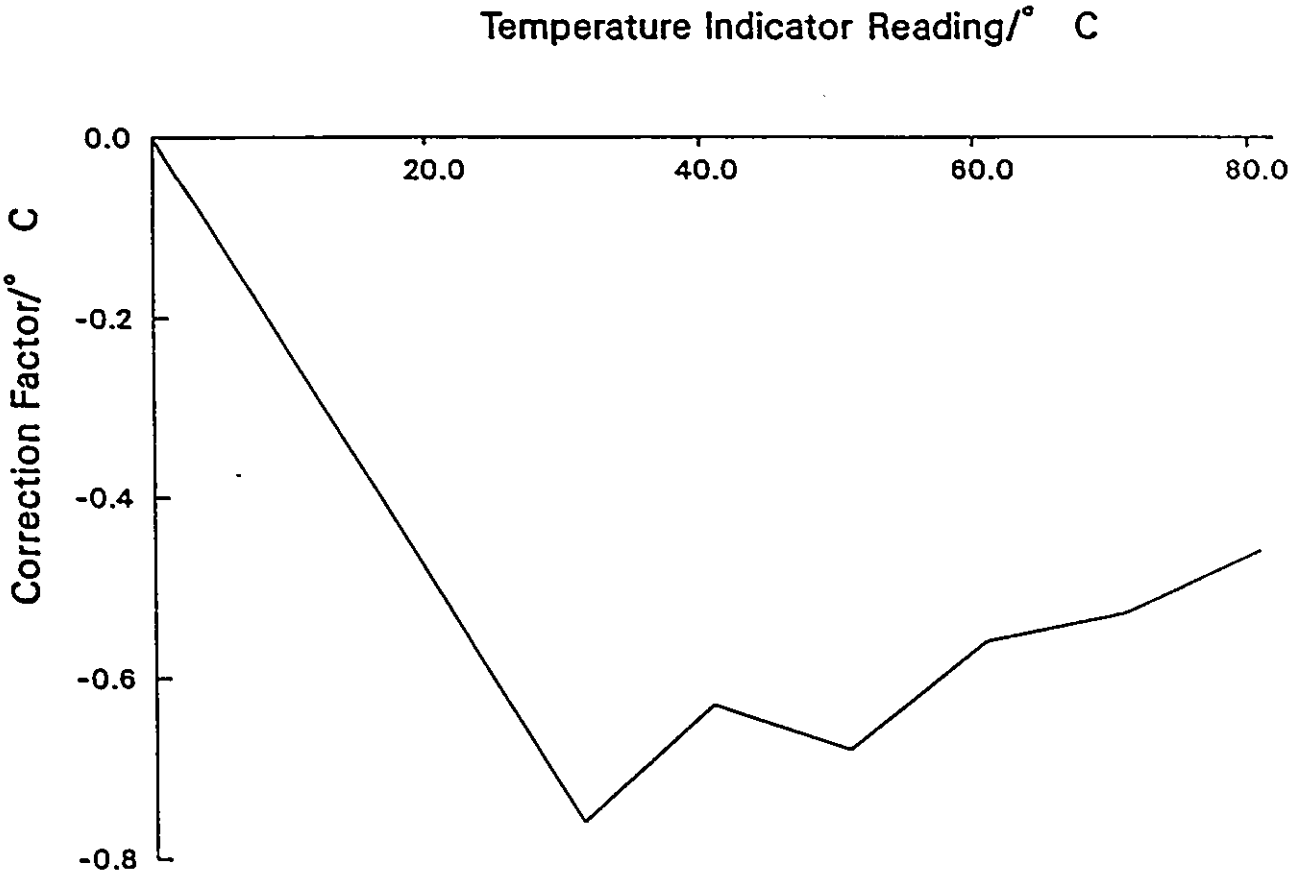

Figure B.1 : Calibration curve for the thermocouples.

Appendix C

Calibration of the Sampler Volume for the P-T-x Measurement

The calibration of the sampler volume in Figure (3.1) was performed in the following procedure. A known amount of gas was expanded into the sample cylinder of Figure (3.1), an increase in pressure of the high accuracy pressure gauge was then recorded. By expanding different amount of gas into the sample cylinder, the calibration of the sampler volume could be obtained.

The calibration factor obtained is $1.275 * 10^{-3}$ at bath temperature 298.15 K. At other bath temperature, the equation obtained is

$$n = (1.275 * 10^{-3})(298.15)\frac{\Delta P}{T_{bath}} \qquad \text{(C.1)}$$

Appendix D

Raw Data

The raw data of P-T-x_1 measurement of the three-phase coexistence curve for naphthalene(1)-ethylene(2) and biphenyl(1)-ethylene(2) systems are listed in Table D.1 through Table D.4. The sample calculation of the liquid-phase composition is presented in Appendix E.

Table D.1 : Raw data of the P-T measurements for the naphthalene-ethylene system.

Run #	T/K	P/MPa
1	345.35	2.420
2	344.45	2.726
3	343.43	3.048
4	342.52	3.465
5	341.52	4.001
6	340.45	4.460
7	338.51	5.404
8	335.60	6.330
9	333.69	7.350
10	331.85	8.359
11	330.16	9.628
12	329.05	10.64
13	327.73	12.16
14	326.62	13.78
15	325.95	15.35
16	325.60	16.32
17	325.40	16.80
18	325.30	17.57
19	325.30	17.58

Table D.2 : Raw data of the liquid-phase naphthalene composition for the naphthalene(1)-ethylene(2) system.

run #	$\Delta P/psia$	T_{bath}/K	W_1/g	$n_2 \cdot 10^4$	$n_1 \cdot 10^3$	x_1
1	0.305	298.71	0.25935	3.880	2.023	0.839
2	0.360	298.84	0.27053	4.580	2.111	0.822
3	0.400	297.60	0.26673	5.109	2.081	0.803
4	0.470	297.68	0.27119	6.000	2.116	0.779
5	0.520	299.52	0.25428	6.599	1.984	0.750
6	0.550	298.00	0.24440	7.016	1.907	0.731
7	0.725	298.18	0.25189	9.240	1.965	0.680
8	0.915	299.92	0.25464	1.160	1.987	0.631
9	0.305	298.71	0.25935	3.880	2.023	0.839
10	1.270	298.17	0.25031	16.19	1.953	0.546
11	1.400	298.73	0.25462	17.80	1.986	0.527
12	1.480	299.13	0.23402	18.80	1.826	0.493
13	1.560	298.91	0.23152	19.84	1.806	0.477
14	1.860	299.23	0.32041	23.63	2.499	0.421
15	1.950	298.96	0.22023	24.80	1.718	0.409
16	2.100	298.78	0.21100	26.72	1.646	0.381
17	2.180	298.19	0.21135	27.79	1.649	0.372
18	2.330	298.15	0.21251	29.60	1.658	0.359
19	2.350	298.95	0.20990	29.88	1.638	0.354

Table D.3 : Raw data of the P-T measurements for the biphenyl-ethylene system.

Run #	T/K	P/MPa
1	337.41	1.313
2	334.50	2.368
3	331.78	3.372
4	329.95	4.063
5	328.65	4.659
6	326.31	5.259
7	324.49	6.076
8	323.28	6.865
9	322.27	7.334
10	321.38	7.761
11	320.18	8.415
12	319.39	9.061
13	319.09	9.726
14	318.19	10.54
15	317.70	11.35
16	317.10	12.47
17	316.20	13.26
18	315.61	15.71
19	315.41	16.62
20	315.31	17.74
21	315.11	18.65
22	315.01	19.95
23	314.81	21.17
24	314.81	22.18

Table D.4 : Raw data of the liquid-phase biphenyl composition for the biphenyl(1)-ethylene(2) system.

run #	$\Delta P/psia$	T_{bath}/K	W_1/g	$n_2 \cdot 10^4$	$n_1 \cdot 10^3$	x_1
1	0.170	297.16	0.32023	2.175	2.077	0.905
2	0.365	298.36	0.32144	4.650	2.084	0.818
3	0.495	300.16	0.32168	6.294	2.086	0.769
4	0.590	297.96	0.32165	7.527	2.086	0.735
5	0.690	297.97	0.32225	8.803	2.090	0.704
6	0.850	298.21	0.31005	10.84	2.011	0.650
7	0.940	298.75	0.31365	11.96	2.034	0.630
8	1.140	298.65	0.32188	14.51	2.087	0.590
9	1.210	297.76	0.32102	15.45	2.082	0.574
10	1.350	298.74	0.32424	17.18	2.103	0.550
11	1.440	299.12	0.32325	18.30	2.096	0.534
12	1.500	298.75	0.33202	19.09	2.153	0.530
13	1.690	298.90	0.32114	21.49	2.082	0.492
14	1.910	298.78	0.32130	24.30	2.083	0.462
15	1.960	298.57	0.32699	24.95	2.120	0.459
16	2.320	298.78	0.32986	29.52	2.139	0.419
17	2.490	299.05	0.31864	31.65	2.066	0.390
18	3.040	298.27	0.32166	38.74	2.086	0.350
19	3.380	298.54	0.31258	43.04	2.027	0.320
20	3.600	298.78	0.31025	45.80	2.012	0.305
21	3.890	298.24	0.32845	49.58	2.130	0.300
22	4.290	299.24	0.31036	54.50	2.013	0.270
23	4.550	298.14	0.31797	58.01	2.062	0.262
24	4.880	297.99	0.32115	62.25	2.083	0.245

Appendix E

Sample Calculation of Equilibrium Liquid Composition

In this Appendix, the sample calculation of the liquid-phase composition (x_1) is illustrated in the following example for naphthalene(1)-ethylene(2) system.

For run # 10, the increase in pressure (ΔP) was found to be 1.270 psi at the bath temperature 298.12 K (T_{bath}). From Appendix C, the number of moles of ethylene was determined using the calibration result, i.e. equation C.1,

$$n_2 = (1.275 * 10^{-3})(298.15)\frac{\Delta P}{T_{bath}}$$

$$n_2 = 0.001619$$

Weight of naphthalene (W_1) collected was found to be 0.25031 g. Thus the number of moles of naphthalene was calculated as follows :

$$n_1 = \frac{w_1}{naphthalene\ molecular\ weight}$$

$$n_1 = \frac{0.25031}{128.174}$$

$$n_1 = 0.001953$$

Since n_1 and n_2 were known, the liquid phase naphthalene composition was then easily determined,

$$x_1 = \frac{n_1}{n_1 + n_2}$$

$$x_1 = 0.5460$$

Appendix F

Computer Program for T-x Correlation

The binary constants of the van Laar equation, i.e. A_{12} and A_{21}, are evaluated by data reduction of the experimental T-x data. The activity coefficient γ_1 is calculated and the binary constants are optimized by minimizing the sum of square of difference between the calculated and experimental activity coefficient.

The program used to evaluate the binary constants is presented in this Appendix.

computer program for T-x correlation (page 1 of 4)

```
C
C---- SPECIFICATIONS.
      IMPLICIT DOUBLE PRECISION (A-Z)
      INTEGER I,IER,NDATA,NPARM,IOPT
      CHARACTER LABEL*40,TUNIT*1,PUNIT*4,REF*80,COMP(2)*15
      EXTERNAL BINFIT
      DIMENSION PARM(2),G(2),H(3),WORK(6),PROP(20)
      DIMENSION XCAL(200)
      COMMON /DATA/ T(200),P(200),X(200)/NDATA/NDATA
      COMMON /RESULT/ GACAL(200),GAEXP(200)
C
C---- READ IN DATA. PERFORM UNIT CONVERSIONS TO T IN K AND P IN MPA.
      READ (5,*) COMP,LABEL
      READ (5,*) R,DELTAH,TM
      READ (5,*) REF
      READ (5,*) NDATA
      READ (5,*) TUNIT,PUNIT
      READ (5,*) (T(I),P(I),X(I),I=1,NDATA)
      DO 1011 I=1,NDATA
         CALL PCONV(P(I),PUNIT,' MPA')
         CALL TCONV(T(I),TUNIT,'K')
         GAEXP(I)=(DEXP(-(DELTAH/R)*((1/T(I))-(1/TM))))/X(I)
 1011 CONTINUE
C
C---- INITIAL PARAMETER GUESSES. SCALE BY 100 TO AVOID CONFUSING ZXMIN.
      NPARM=2
      DO 1000 I=1,NPARM
         IF (I .EQ. 1) THEN
            WRITE (8,*) 'INITIAL PARAMETER GUESSES (A12):'
         ELSE
            WRITE (8,*) 'INITIAL PARAMETER GUESSES (A21):'
         END IF
         READ (7,*) PARM(I)
         PARM(I)=PARM(I)*1D2
 1000 CONTINUE
C
C---- PERFORM CALCULATIONS.
      WRITE (8,*) 'SINGLE POINT (1) OR OPTIMIZATION (2):'
      READ (7,*) IOPT
      IF (IOPT.EQ.2) THEN
         CALL ZXMIN(BINFIT,NPARM,4,100,3,PARM,H,G,F,WORK,IER)
      ELSE
         CALL BINFIT(NPARM,PARM,F)
      END IF
      AADG=0D0
      DO 1040 I=1,NDATA
         AADG=AADG+DABS(GAEXP(I)-GACAL(I))/GAEXP(I)/DFLOAT(NDATA)
 1040 CONTINUE
C
C---- OUTPUT RESULTS.
      WRITE (6,'(130(1H=))')
      WRITE (6,*)
      WRITE (6,*) '*** T-X CORRELATION *** '
      WRITE (6,*)
      WRITE (6,*) COMP,LABEL
```

```
      WRITE (6,*) REF
      WRITE (6,*) 'TEMPS IN K, PRESSURES IN MPA'
      WRITE (6,*)
      WRITE (6,'(A20,G15.5)') 'A12 = ',PARM(1)/1D2
      IF (NPARM.EQ.2) WRITE (6,'(A20,G15.5)') 'A21 = ',PARM(2)/1D2
      WRITE (6,'(A20,G15.5)') 'RMSD IN GAMMA = ',DSQRT(F/DFLOAT(NDATA))
      WRITE (6,'(A20,G15.5)') '%AAD IN GAMMA = ',AADG*1D2
      WRITE (6,*)
      WRITE (6,'(69(1H-))')
      WRITE (6,'(3X,A1,20X,A5,22X,A1,6X,A1)')
     1    'T','GAMMA','X','P'
      WRITE (6,'(10X,31(1H-),4X,20(1H-))')
      WRITE (6,'(13X,A3,8X,A4,8X,A3,11X,A3,4X,A3)') 'EXP','PRED','DEV',
     1    'EXP','EXP'
      WRITE (6,'(69(1H-))')
      WRITE (6,'(F6.2,2F12.4,F12.4,F12.4,F9.3)')
     1 (T(I),GAEXP(I),GACAL(I),GAEXP(I)-GACAL(I),X(I),P(I),I=1,NDATA)
      WRITE (6,'(69(1H-))')
      WRITE (6,*)
      IF (IOPT.EQ.2) THEN
         WRITE (6,*) 'STATISTICAL SUMMARY:'
         WRITE (6,*)
         WRITE (6,*) 'METHOD IS LEAST SQUARES FIT OF GAMMA'
         WRITE (6,*) 'WITH',NDATA,'POINTS AND',NPARM,'PARAMETERS.'
         WRITE (6,*) 'CONVERGED TO',IDINT(WORK(3)),'DIGITS IN',
     1               IDINT(WORK(2)),'ITERATIONS.'
         WRITE (6,*)
         WRITE (6,'(A30,2G15.5)') 'PARAMETER VALUES: ',
     1        (PARM(I),I=1,NPARM)
         WRITE (6,'(A30,G15.5)') 'SUM OF SQUARED RESIDUALS: ',F
         WRITE (6,'(A30,2G15.5)') 'GRADIENT: ',(G(I),I=1,NPARM)
         WRITE (6,'(A30,3G15.5)') 'HESSIAN (SYMMETRIC MODE): ',
     1        (H(I),I=1,NPARM*(NPARM+1)/2)
         WRITE (6,*)
      END IF
      WRITE (6,*)
      WRITE (6,*) 'T-X EXPERIMENTAL DATA'
      WRITE (6,*)
      WRITE (6,*) NDATA
      WRITE (6,'(20(1H-))')
      WRITE (6,'(3X,A2,11X,A1)') 'X1','T'
      WRITE (6,'(20(1H-))')
      WRITE (6,*)
      DO 910 I=1,NDATA
         WRITE (6,'(F13.6,F12.4)') X(I),T(I)
  910 CONTINUE
      WRITE (6,*)
      WRITE (6,'(20(1H-))')
      WRITE (6,*)
      WRITE (6,*) 'T-X CORRELATION DATA'
      WRITE (6,*)
      A12=PARM(1)/1D2
      A21=PARM(2)/1D2
      WRITE (6,'(20(1H-))')
      WRITE (6,'(3X,A2,11X,A1)') 'X1','T'
```

```
      WRITE (6,'(20(1H-))')
      X1=0.005
 500  IF (X1 .LE. 1.0) THEN
         GAM=DEXP(A12/((1+((A12*X1)/(A21*(1-X1))))**2))
         TEMP=((-(DLOG(GAM*X1)*(R/DELTAH)))+(TM)**(-1))**(-1)
         WRITE (6,'(F13.6,F12.4)') X1,TEMP
         X1=X1+0.005
         GOTO 500
      ELSE
         GOTO 550
      END IF
 550  WRITE (6,'(20(1H-))')
      STOP
      END
C
C
C*********************************************************************
*
*                  BINFIT(NPARM,PARM,RESID)
*
* USED BY IMSL ROUTINE ZXMIN TO OBTAIN OBJECTIVE FUNCTION.
*
C*********************************************************************
C
      SUBROUTINE BINFIT(NPARM,PARM,F)
C
C---- SPECIFICATIONS.
      IMPLICIT DOUBLE PRECISION (A-Z)
      INTEGER I,NDATA,NPARM
      DIMENSION PARM(2)
      COMMON /BKCALC/ K(20,20),L(20,20),ZL,ZV
      COMMON /DATA/ T(200),P(200),X(200),Y(200)/NDATA/NDATA
      COMMON /RESULT/ GACAL(200),GAEXP(200)
C
C---- ASSIGN VALUES TO BLOCK 'COEF'.
      K(1,1)=0D0
      K(2,2)=0D0
      K(1,2)=PARM(1)/1D2
      K(2,1)=PARM(1)/1D2
      L(1,1)=0D0
      L(2,2)=0D0
      IF (NPARM.EQ.2) THEN
         L(1,2)=PARM(2)/1D2
         L(2,1)=PARM(2)/1D2
      ELSE
         L(1,2)=0D0
         L(2,1)=0D0
      END IF
C     WRITE (6,*) 'K12,L12=',K(1,2),L(1,2)
      WRITE (8,*) 'K12,L12=',K(1,2),L(1,2)
C
C---- CALCULATE OBJECTIVE FUNCTION. FIND GAMMA AT EACH POINT.
C
      F=0D0
      DO 1000 I=1,NDATA
```

```
        GACAL(I)=DEXP(K(1,2)/(1+((K(1,2)*X(I))/(L(1,2)*(1-X(I)))))**2)
        F=F+(GAEXP(I)-GACAL(I))**2
 1000 CONTINUE
C     WRITE (6,*) 'F=',F
      WRITE (8,*) 'F=',F
C
      RETURN
      END
*****************************************************************************
*
*                  PCONV(P,LIN,LOUT)
*
* SUBROUTINE FOR PRESSURE CONVERSIONS.
*
* VARIABLES:
*   P: PRESSURE.
*   LIN: INPUT UNITS.
*   LOUT: OUTPUT UNITS.
* LIN AND LOUT ARE CHARACTER*4 VARIABLES WHICH MUST BE ONE OF
* 'PSIA','MMHG',' ATM',' KPA',' ATM',' BAR'.
*
*****************************************************************************
C
      SUBROUTINE PCONV(P,LIN,LOUT)
      IMPLICIT DOUBLE PRECISION (A-Z)
      CHARACTER*4 LIN,LOUT
C
C---- CONVERT TO ATM.
C
      IF (LIN.EQ.'PSIA') P=P/14.696D0
      IF (LIN.EQ.'MMHG') P=P/760D0
      IF (LIN.EQ.' KPA') P=P/101.325D0
      IF (LIN.EQ.' MPA') P=P/101.325D0*1D3
      IF (LIN.EQ.' BAR') P=P/101.325D0*1D2
      IF (LIN.EQ.' ATM') P=P
C
C---- CONVERT TO DESIRED UNITS.
C
      IF (LOUT.EQ.'PSIA') P=P*14.696D0
      IF (LOUT.EQ.'MMHG') P=P*760D0
      IF (LOUT.EQ.' KPA') P=P*101.325D0
      IF (LOUT.EQ.' MPA') P=P*101.325D0/1D3
      IF (LOUT.EQ.' BAR') P=P*101.325D0/1D2
      RETURN
      END
```

Appendix G

Computer Program for P-T-x Correlation

In this Appendix, the program used to correlate the equilibrium values along the three-phase coexistence curve and to evaluate the binary parameters in the mixing rules is presented.

```
C
C---- SPECIFICATIONS.
C
      IMPLICIT DOUBLE PRECISION (A-Z)
      INTEGER I,IER,NDATA,IMIX,IOPT,NCOMP,IFIRST,IPAR
      CHARACTER LABEL*40,TUNIT*1,PUNIT*4,REF*80,COMP(2)*30,
     1          VVUNIT*10,VLUNIT*10,IEOS*3,ICALC*3,ANT*80,
     1          IFUNCT*5,ITYPE*1,VVVVP*80,CALC*3
      EXTERNAL BINFIT
      DIMENSION PARM(2),G(2),H(3),WORK(6),PROP(20),K1(20),K2(20),
     1          VL(200),VLP(200),VV(200),VVP(200),MW(2),XL(2),YV(2)
      DIMENSION XX(2),YY(20),Z(20),
     1          AIL(20),AIV(20),BIL(20),BIV(20),A(20),B(20),
     2          C(20),CIL(20),CIV(20),U(20),UIL(20),UIV(20),
     3          W(20),WIL(20),WIV(20),UL(200),WL(200),UV(200),WV(200)
      COMMON /BKCALC/ K(20,20),L(20,20),M(20,20),ZL,ZV
      COMMON /PROP/ TC(20),PC(20),AC(20),ZC(20)
      COMMON /EOS/ IEOS,ICALC,CALC,IFUNCT,ITYPE
      COMMON /DATA/ T(200),P(200),X(200),Y(200),NDATA,NCOMP
      COMMON /RESULT/ PP(200),YP(200),XP(200),ZLP(200),ZVP(200)
      COMMON /BKV/ V1S
      COMMON /ANTO/ ANTA,ANTB,ANTC
      COMMON /RVP/ RVPG(2),RVPB(2),RVPM(2)
      COMMON /NALP/ COEFN
C
C---- INPUT TYPE OF CALCULATION
C
      WRITE (8,*) 'CALCULATION TYPE - INPUT STRING (SV , SLV) :'
      READ (7,*) ICALC
C
C---- INPUT TYPE OF EQUATION OF STATE USE
C
      WRITE (8,*) 'EOS TYPE - INPUT STRING (PR , TPR)'
      READ (7,*) IEOS
C
C---- INPUT TYPE OF ALPHA TEMPERATURE FUNCTION USE
C
      WRITE (8,*) 'TYPE OF ALPHA FUNCT-INPUT STRING (SOAVE,SUGIE,NEW)'
      READ (7,*) IFUNCT
C
C---- INPUT TYPE OF MIXING RULE USE
C
      WRITE (8,*) 'MIXING RULE TYPE - INPUT STRING (C , A)'
      READ (7,*) ITYPE
C
C---- INPUT NUMBER OF PARAMETERS
C
      IF (ITYPE.EQ.'C') THEN
         WRITE (8,*) 'NO. OF PARAMETER (1 OR 2)'
         READ (7,*) IMIX
      ELSE
         IMIX=2
      ENDIF
C
C---- INITIAL KIJ AND/OR LIJ AND/OR MIJ GUESSES
```

```
C
      IF (ITYPE.EQ.'C') THEN
         IF (IMIX.EQ.1) THEN
            WRITE (8,*) 'INITIAL PARAMETER GUESSES (KIJ) :'
            DO 21 I=1,IMIX
              READ (7,*) PARM(I)
 21         CONTINUE
         ENDIF
         IF (IMIX.EQ.2) THEN
            WRITE (8,*) 'INITIAL PARAMETER GUESSES (KIJ , LIJ) :'
            DO 25 I=1,IMIX
              READ (7,*) PARM(I)
 25         CONTINUE
         ENDIF
      ELSE
         IF (ITYPE.EQ.'A') THEN
            WRITE (8,*) 'INITIAL PARAMETER GUESSES (LIJ , MIJ) :'
            DO 29 I=1,IMIX
               READ (7,*) PARM(I)
 29         CONTINUE
         ENDIF
      ENDIF
C
C---- SELECT SINGLE POINT CALCULATION OR ALL DATA POINT CALCULATION
C
      WRITE (8,*) 'SINGLE POINT (1) OR OPTIMIZATION (2):'
      READ (7,*) IOPT
C
C---- START
C
      IFIRST = 1
C
C---- READ IN DATA. PERFORM UNIT CONVERSIONS TO T IN K AND P IN ATM.
C
      READ (5,*) REF
      READ (5,*) COMP,LABEL
C
C
      CALC='NOR'
      NCOMP=2
      READ (5,*) V1S
      READ (5,*) ANT
      READ (5,*) ANTA,ANTB,ANTC
      READ (5,*) VVVVP
      READ (5,*) (RVPG(I),RVPB(I),RVPM(I),I=1,NCOMP)
C
C---- READ PURE COMPONENT PROPERTIES USING SUBROUTINE PURE
C
      DO 10 I=1,NCOMP
         CALL PURE(COMP(I),PROP)
         MW(I)=PROP(1)
         TC(I)=PROP(2)
         PC(I)=PROP(3)
         ZC(I)=PROP(4)
         AC(I)=PROP(5)
```

```
         CALL PCONV(PC(I),' ATM',' ATM')
 10    CONTINUE
 555   IPAR=1
       READ (5,*,END=999) NDATA
C
       IF (IFIRST.EQ.1) READ (5,*) TUNIT,PUNIT
       IF (IFIRST.EQ.1) IFIRST=IFIRST + 1
C
C---- INPUT THE DATA
C
       IF (ICALC.EQ.'SV') THEN
          READ (5,*) (T(I),P(I),Y(I),I=1,NDATA)
       ELSE
          READ (5,*) (T(I),P(I),X(I),I=1,NDATA)
       ENDIF
C
C---- PRINT OUT THE ORIGINAL DATA

C      IF(IPAR.EQ.1) THEN
C        WRITE(6,302) NDATA
C302     FORMAT(/'ORIGINAL ',I4,'    DATA'/)
C        IF (ICALC.EQ.'SV') THEN
C           WRITE(6,*)
C           WRITE(6,*) 'T-P-VAPOR MOLE FRACTION'
C           WRITE(6,*)
C           WRITE(6,*) '  ',TUNIT,'         ',PUNIT
C           WRITE(6,*)
C           WRITE(6,'(F7.2,F10.2,F13.6)') (T(I),P(I),Y(I),I=1,NDATA)
C        ELSE
C           WRITE(6,*)
C           WRITE(6,*) 'T-P-LIQUID MOLE FRACTION'
C           WRITE(6,*)
C           WRITE(6,*) '  ',TUNIT,'         ',PUNIT
C           WRITE(6,*)
C           WRITE(6,'(F7.2,F10.1,F13.4)') (T(I),P(I),X(I),I=1,NDATA)
C        ENDIF
C      ENDIF
C
C---- PERFORM UNIT CONVERSION
C
       DO 30 I=1,NDATA
          CALL PCONV(P(I),PUNIT,' ATM')
          CALL TCONV(T(I),TUNIT,'K')
 30    CONTINUE
C
C---- CALCULATE THE N VALUE IF TR .GE. 1.0
C
       IF (IFUNCT.EQ.'SUGIE') THEN
          TR=0.95D0
          PR=DEXP(RVPB(2)*(1D0/TR**RVPM(2)-1D0)+RVPG(2)*(TR**7-1D0))
          POT=PR/TR
          OMEGAC=0.4572D0
          ALPHA=ALPTR(OMEGAC,POT,1.D-6,ZLB,ZVB)
          COEFN=(DSQRT(ALPHA*TR)-1D0)/(1D0-DSQRT(TR))
          WRITE (6,*) 'COEFN---',COEFN
```

```
      ENDIF
C
C---- PERFORM CALCULATION
C
      IF (IOPT.EQ.2) THEN
         CALL ZXMIN(BINFIT,IMIX,4,300,3,PARM,H,G,F,WORK,IER)
      ELSE
         CALL BINFIT(IMIX,PARM,F)
      ENDIF
C
C---- CALCULATE THE REQUIRED DEVIATION
C
      AADP=000
      AADY=000
      AADX=000
C
C
      DO 1040 I=1,NDATA
         IF (ICALC.EQ.'SLV') THEN
            AADP=AADP+DABS(P(I)-PP(I))/P(I)/DFLOAT(NDATA)
            AADX=AADX+DABS(X(I)-XP(I))/DFLOAT(NDATA)
            GOTO 1040
         ENDIF
         AADY=AADY+DABS(Y(I)-YP(I))/DFLOAT(NDATA)
 1040 CONTINUE
C
C---- PRINT OUT RESULTS.
C
      WRITE (6,'(73(1H=))')
      WRITE (6,*)
      WRITE (6,*) '*** BINARY S-V OR S-L-V SYSTEM  *** '
      WRITE (6,*)
      WRITE (6,*) COMP
      WRITE (6,*) REF
      WRITE (6,*)
      WRITE (6,'(A31,F7.2)') 'SATURATED SOLID MOLAR VOLUME = ',V1S
      WRITE (6,*)
      WRITE (6,*) ANT
      WRITE (6,'(F7.4,F10.2,F10.2)') ANTA,ANTB,ANTC
      WRITE (6,*)
      WRITE (6,*) VVVVP
      WRITE (6,'(F10.5,2F10.5)') (RVPG(I),RVPB(I),RVPM(I),I=1,NCOMP)
      WRITE (6,*)
      WRITE (6,*) 'TEMPS IN K, PRESSURES IN ATM, VOLUMES IN ML/GMOL'
      WRITE (6,*) '------------ ------------------ ------------------'
      WRITE (6,*)
      IF (ICALC.EQ.'SV') WRITE (6,*) 'S-V CALCULATION'
      IF (ICALC.EQ.'SLV') WRITE (6,*) 'S-L-V CALCULATION'
      WRITE (6,*)
      IF (ITYPE.EQ.'C') THEN
        IF (IEOS.EQ.'PR') WRITE (6,*) 'USING PR  EOS'
     1                  ,' WITH CONVENTIONAL TYPE ',IMIX,' MIXING RULES.'
        IF (IEOS.EQ.'TPR') WRITE (6,*) 'USING TPR EOS'
     1                  ,' WITH CONVENTIONAL TYPE ',IMIX,' MIXING RULES.'
      ELSE
```

```
      IF (ITYPE.EQ.'A') THEN
         IF (IEOS.EQ.'PR') WRITE (6,*) 'USING PR  EOS'
     1             ,' WITH ADACHI TYPE ',IMIX,' MIXING RULES.'
         IF (IEOS.EQ.'TPR') WRITE (6,*) 'USING TPR EOS'
     1             ,' WITH ADACHI TYPE ',IMIX,' MIXING RULES.'
      ENDIF
     ENDIF
     WRITE (6,*)
     IF (ITYPE.EQ.'C') THEN
        WRITE (6,'(A20,G15.5)') 'K12 = ',PARM(1)
        IF (IMIX.EQ.2) WRITE (6,'(A20,G15.5)') 'L12 = ',PARM(2)
     ELSE
        IF (ITYPE.EQ.'A') THEN
           WRITE (6,'(A20,G15.5)') 'L12 = ',PARM(1)
           WRITE (6,'(A20,G15.5)') 'M12 = ',PARM(2)
        ENDIF
     ENDIF
     WRITE (6,*)
     IF (IFUNCT.EQ.'SOAVE') THEN
        WRITE (6,*) 'USING SOAVE TYPE ALPHA FUNCTION'
     ELSE
        IF (IFUNCT.EQ.'SUGIE') THEN
           WRITE (6,*) 'USING SUGIE TYPE ALPHA/TR FUNCTION'
        ELSE
           IF (IFUNCT.EQ.'NEW') THEN
              WRITE (6,*) 'USING NEW TYPE ALPHA FUNCTION'
           ENDIF
        ENDIF
     ENDIF
     WRITE (6,*)
     IF (ICALC.EQ.'SLV') THEN
        WRITE (6,'(A20,G15.5)') 'RMSD IN P = ',DSQRT(F/DFLOAT(NDATA))
     END IF
     WRITE (6,*)
     IF (ICALC.EQ.'SV') THEN
        WRITE (6,'(1(1X,A13,1X))') '%AAD IN Y'
        WRITE (6,'(G15.4)') AADY*1D2
     END IF
     IF (ICALC.EQ.'SLV') THEN
        WRITE (6,'(4(1X,A13,1X))') '%AAD IN P','%AAD IN X'
        WRITE (6,'(4G15.4)') AADP*1D2,AADX*1D2
     END IF
     WRITE (6,*)
     WRITE (6,'(73(1H-))')
     IF (ICALC.EQ.'SV') THEN
        WRITE (6,'(3X,A1,19X,A1,29X,A1)')
     1    'T','P','Y'
        WRITE (6,'(19X,9(1H-),6X,42(1H-))')
        WRITE (6,'(22X,A3,15X,A3,8X,A4,8X,A3)')
     1 'EXP','EXP','PRED','DEV'
     ELSE
        WRITE (6,'(3X,A1,19X,A1,38X,A1)')
     1    'T','P','X'
        WRITE (6,'(9X,30(1H-),9X,26(1H-))')
        WRITE (6,'(10X,A3,8X,A4,8X,A3,14X,A3,6X,A4,5X,A3)')
```

```
     1 'EXP','PRED','DEV','EXP','PRED','DEV'
      END IF
      WRITE (6,'(73(1H-))')
      IF (ICALC.EQ.'SV') THEN
         WRITE (6,'(F6.2,G25.4,3X,3F11.5)')
     1 (T(I),P(I),Y(I),YP(I),Y(I)-YP(I),I=1,NDATA)
      ELSE
      WRITE (6,'(F6.2,3G12.4,4X,3F9.4)')
     1 (T(I),P(I),PP(I),P(I)-PP(I),X(I),XP(I),X(I)-XP(I),I=1,NDATA
     2 )
      END IF
      WRITE (6,'(73(1H-))')
      WRITE (6,*)
      DO 111 I=1,NDATA
C        CALL TCONV(T(I),'K','C')
         CALL PCONV(P(I),' ATM',' MPA')
         CALL PCONV(PP(I),' ATM',' MPA')
  111 CONTINUE
      WRITE (6,*)
      IF (ICALC.EQ.'SV') THEN
         WRITE (6,*) NDATA
         WRITE (6,'(F13.6,F11.5,F13.6)')
     1   (Y(I),P(I),YP(I),I=1,NDATA)
         WRITE (6,*) NDATA
         WRITE (6,'(F13.6,F11.5,F13.6)')
     1   (YP(I),P(I),Y(I),I=1,NDATA)
      ELSE
         WRITE (6,*)
         WRITE (6,*)
         WRITE (6,*)
         WRITE (6,*) NDATA
         WRITE (6,'(F6.2,2F12.4)')
     1   (T(I),P(I),PP(I),I=1,NDATA)
         WRITE (6,*) NDATA
         WRITE (6,'(F6.2,2F12.4)')
     1   (T(I),PP(I),P(I),I=1,NDATA)
         WRITE (6,*)
         WRITE (6,*) 'X-P DATA'
         WRITE (6,*)
         WRITE (6,*) NDATA
         WRITE (6,'(F13.6,F12.4,F13.6)')
     1   (X(I),P(I),XP(I),I=1,NDATA)
         WRITE (6,*) NDATA
         WRITE (6,'(F13.6,F12.4,F13.6)')
     1   (XP(I),P(I),X(I),I=1,NDATA)
      END IF
      WRITE (6,*)
      WRITE (6,*)
      WRITE (6,*)
      IF (IOPT.EQ.2) THEN
         WRITE (6,*) 'STATISTICAL SUMMARY:'
         WRITE (6,*)
         WRITE (6,*) 'METHOD IS LEAST SQUARES FIT OF P=P(T,X)'
         WRITE (6,*) 'WITH',NDATA,'POINTS AND',IMIX,'PARAMETERS.'
         WRITE (6,*) 'CONVERGED TO',IDINT(WORK(3)),'DIGITS IN',
```

```
     1              IDINT(WORK(2)),'ITERATIONS.'
         WRITE (6,*)
         WRITE (6,'(A30,2G15.5)') 'PARAMETER VALUES: ',
     1        (PARM(I),I=1,IMIX)
         WRITE (6,'(A30,G15.5)') 'SUM OF SQUARED RESIDUALS: ',F
         WRITE (6,'(A30,2G15.5)') 'GRADIENT: ',(G(I),I=1,IMIX)
         WRITE (6,'(A30,3G15.5)') 'HESSIAN (SYMMETRIC MODE): ',
     ;        (H(I),I=1,IMIX*(IMIX+1)/2)
         WRITE (6,*)
       END IF
C
C---- PRINT OUT THE K VALUE IF REQUIRED
C
C      IF (IEOS.EQ.'PR') THEN
C      WRITE (6,*) 'K-VALUES:'
C      WRITE (6,*)
C      RMS=0D0
C      AAD=0D0
C      BIAS=0D0
C      DO 1100 I=1,NDATA
C         K(I)=Y(I)/X(I)
C         KP(I)=YP(I)/X(I)
C         DEV=(K(I)-KP(I))/K(I)
C         RMS=RMS+DEV**2
C         AAD=AAD+DABS(DEV)
C         BIAS=BIAS+DEV
C1100  CONTINUE
C      WRITE (6,'(A20,G15.5)') 'RMS = ',DSQRT(RMS/NDATA)*1D2
C      WRITE (6,'(A20,G15.5)') 'AAD = ',AAD/NDATA*1D2
C      WRITE (6,'(A20,G15.5)') 'BIAS = ',BIAS/NDATA*1D2
C      WRITE (6,*)
C      WRITE (6,'(5(4X,A2,4X))') 'X','Y','YP','K','KP'
C      WRITE (6,'(5F10.5)') (X(I),Y(I),YP(I),K(I),KP(I),I=1,NDATA)
C      WRITE (6,*)
C      WRITE (6,'(130(1H-))')
C      END IF
C
C---- PRINT OUT THE U AND W VALUE FOR TPR EQUATION OF STATE IF REQUIRED
C
C      IF (IEOS.EQ.'TPR') THEN
C      DO 3000 J=1,NDATA
C      XX(1)=X(J)
C      XX(2)=1D0-X(J)
C      YY(1)=YP(J)
C      YY(2)=1D0-YP(J)
C      DO 3001 I=1,2
C         TR=T(J)/TC(I)
C         PR=PP(J)/PC(I)
C         CALL EOSTPR(TR,PR,AC(I),A(I),B(I),U(I),W(I))
C         C(I)=(2D0-U(I))/4D0*B(I)
C3001  CONTINUE
C      CALL GEOMIX(A,XX,KA,AL,AIL,2,20)
C      CALL GEOMIX(A,YY,KA,AV,AIV,2,20)
C      CALL ARMIX(B,XX,L,BL,BIL,2,20)
C      CALL ARMIX(B,YY,L,BV,BIV,2,20)
```

```
C     CALL ARMIX(C,XX,L,CL,CIL,2,20)
C     CALL ARMIX(C,YY,L,CV,CIV,2,20)
C     UL(J)=2D0-4D0*CL/BL
C     WL(J)=2D0*(CL/BL)**2-1D0
C     UV(J)=2D0-4D0*CV/BV
C     WV(J)=2D0*(CV/BV)**2-1D0
C3000 CONTINUE
C     WRITE (6,*)
C     WRITE (6,*) 'U AND W VALUES:'
C     WRITE (6,*)
C     WRITE (6,'(6(5X,A2,5X))') 'X','Y','UL','WL','UV','WV'
C     WRITE (6,'(6G12.5)')(X(I),YP(I),UL(I),WL(I),UV(I),WV(I),I=1,NDATA)
C     WRITE (6,*)
C     WRITE (6,'(130(1H=))')
C     END IF
      GOTO 555
 999  WRITE (7,*) 'END OF DATA FILE'
      STOP
      END
C
C
C*********************************************************************
*
*                  BINFIT(IMIX,PARM,F)
*
* USED BY IMSL ROUTINE ZXMIN TO OBTAIN OBJECTIVE FUNCTION.
*
C*********************************************************************
C
      SUBROUTINE BINFIT(IMIX,PARM,F)
C
C---- SPECIFICATIONS.
C
      IMPLICIT DOUBLE PRECISION (A-Z)
      INTEGER I,NDATA,IMIX,NCOMP
      DIMENSION XD(2),YD(2),PARM(2),Z(20)
      CHARACTER*3 ICALC,IEOS,CALC
      CHARACTER*5 IFUNCT
      CHARACTER*1 ITYPE
      COMMON /BKCALC/ K(20,20),L(20,20),M(20,20),ZL,ZV
      COMMON /PROP/ TC(20),PC(20),AC(20),ZC(20)
      COMMON /DATA/ T(200),P(200),X(200),Y(200),NDATA,NCOMP
      COMMON /RESULT/ PP(200),YP(200),XP(200),ZLP(200),ZVP(200)
      COMMON /EOS/ IEOS,ICALC,CALC,IFUNCT,ITYPE
      COMMON /ANTO/ ANTA,ANTB,ANTC
      COMMON /RVP/ RVPG(2),RVPB(2),RVPM(2)
      COMMON /NALP/ COEFN
C
C---- ASSIGN VALUES TO BLOCK 'COEF'.
C
      IF (ITYPE.EQ.'C') THEN
         K(1,1)=0D0
         K(2,2)=0D0
         K(1,2)=PARM(1)
         K(2,1)=PARM(1)
```

```
            M(1,1)=0D0
            M(2,2)=0D0
            M(1,2)=0D0
            M(2,1)=0D0
            L(1,1)=0D0
            L(2,2)=0D0
            IF (IMIX.EQ.2) THEN
               L(1,2)=PARM(2)
               L(2,1)=PARM(2)
            ELSE
               L(1,2)=0D0
               L(2,1)=0D0
            END IF
         ELSE
            IF (ITYPE.EQ.'A') THEN
               K(1,1)=0D0
               K(2,2)=0D0
               K(1,2)=PARM(1)
               K(2,1)=PARM(1)
               M(1,1)=0D0
               M(2,2)=0D0
               M(1,2)=PARM(2)
               M(2,1)=0D0-(PARM(2))
               L(1,2)=0D0
               L(2,1)=0D0
               L(1,2)=0D0
               L(2,1)=0D0
            ENDIF
         ENDIF
C
C---- CALCULATE OBJECTIVE FUNCTION. FIND DEW POINT AT EACH POINT.
C
         F=0D0
         DO 41 I=1,NDATA
            P1S=10.**(ANTA-(ANTB/(T(I)+(ANTC))))/1.01325
            CALL PCONV(P1S,' ATM',' ATM')
            PP(I)=P(I)
            IF (ICALC.EQ.'SV') THEN
               YD(1)=Y(I)
               YD(2)=1D0-YD(1)
            ELSE
               XD(1)=X(I)
               XD(2)=1D0-XD(1)
               YD(1)=P1S
               YD(2)=1D0-YD(1)
            END IF
            CALL DEWP(XD,YD,T(I),PP(I),P1S,NCOMP)
            YP(I)=YD(1)
            XP(I)=XD(1)
            IF (ICALC.EQ.'SV') THEN
               F=F+(YP(I)-Y(I))**2
            ELSE
               F=F+((PP(I)-P(I))/P(I))**2
            END IF
   41    CONTINUE
```

```
      IF (ITYPE.EQ.'C') THEN
         IF (IMIX.EQ.1) THEN
            WRITE (8,*) 'K12=',K(1,2),'    OBJ=',F
         ELSE
            WRITE (8,*) 'K12=',K(1,2)
            WRITE (8,*) 'L12=',L(1,2),'    OBJ=',F
         END IF
      ELSE
         IF (ITYPE.EQ.'A') THEN
            WRITE (8,*) 'L12=',K(1,2)
            WRITE (8,*) 'M12=',M(1,2),'    OBJ=',F
         ENDIF
      ENDIF
C
      RETURN
      END
C-----------------------------------------------------------------------
C   DEW POINT PRESSURE CALCULATION                                      C
C                                                                       C
C   VARIABLES:                                                          C
C   T  :  TEMPERATURE       (INPUT)   P :  PRESSURE           (INPUT)   C
C   PP :  DEW PRESSURE      (OUTPUT)  X :  LIQUID COMPOSITON  (OUTPUT)  C
C   Y  :  VAPOR COMPOSITION (INPUT)   Y1:  CAL. VAPOR COMP.   (OUTPUT)  C
C   PS :  SOLID SATURATED PRESSURE  (INPUT)
C-----------------------------------------------------------------------
      SUBROUTINE DEWP (X1,Y1,T,PP,PS,NCOMP)
      IMPLICIT DOUBLE PRECISION (A-Z)
      INTEGER I,NCOMP,ITER,NDATA,INDEX
      CHARACTER*3 IEOS,ICALC,CALC
      CHARACTER*5 IFUNCT
      CHARACTER*1 ITYPE
      DIMENSION K1(20),K2(20),X1(2),Y1(2),FCL(2),FCV(2),PAR(1),WK(20)
      DIMENSION Z(20),YC(2)
      COMMON /BKCALC/ K(20,20),L(20,20),M(20,20),ZL,ZV
      COMMON /PROP/ TC(20),PC(20),AC(20),ZC(20)
C     COMMON /RESULT/ PP(200),YP(200),XP(200),ZLP(200),ZVP(200)
      COMMON /EOS/ IEOS,ICALC,CALC,IFUNCT,ITYPE
      COMMON /BKV/ V1S
      COMMON /NALP/ COEFN
C
C
C---- CALCULATE VAPOR MOLE FRACTION ASSUME SOLID IS PURE
C
C
      GASR=82.06
C     INDEX=1
 77   CALL PRTPR(Y1,T,PP,FCV,NCOMP,0)
      YC(1)=(PS/PP)*(DEXP((V1S*(PP-PS))/(GASR*T))/FCV(1))
      DELY=DABS(Y1(1)-YC(1))/Y1(1)
C     INDEX=INDEX+1
C     IF (INDEX.GT.800) GOTO 85
      Y1(1)=YC(1)
      Y1(2)=1D0-Y1(1)
      IF (DELY.GE.1.D-9) GOTO 77
 85   IF (ICALC.EQ.'SV') GOTO 70
```

```
C
C
C---- PERFORM DEW POINT CALCULATION
C
C
C---- IF NO LIQUID COMPOSITION VALUE AVAILABLE TO FIND THE INITIAL
C---- FIRST LET FUGACITIES COEFFICIENT OF LIQUID PHASE EQUAL ONE
C
      IF ( X1(1).LE.0D0.OR.X1(1).GE.1D0) THEN
        CALL PRTPR(Y1,T,PP,FCV,NCOMP,0)
        DO 50 I=1,2
 50     X1(I)=Y1(I)*FCV(I)
        XSUM=X1(1)+X1(2)
        X1(1)=X1(1)/XSUM
        X1(2)=X1(2)/XSUM
C
C---- CALL SUBROUTINE TO CALCULATE FUGACITY COEFFICIENT, 0 = VAPOR
C                                                       1 =LIQUID
C
        CALL PRTPR(X1,T,PP,FCL,NCOMP,1)
        X1(1)=Y1(1)*FCV(1)/FCL(1)
        X1(2)=Y1(2)*FCV(2)/FCL(2)
        XSUM=X1(1)+X1(2)
        X1(1)=X1(1)/XSUM
        X1(2)=X1(2)/XSUM
      END IF
C
C---- AFTER INITIAL GUESS, PERFORM CALCULATION
C
      ITER=0
100   ITER=ITER+1
      IF (ITER.GT.50) GOTO 1000
         CALL PRTPR(X1,T,PP,FCL,NCOMP,1)
         ZV=ZL
         CALL PRTPR(Y1,T,PP,FCV,NCOMP,0)
         X1(1)=Y1(1)*FCV(1)/FCL(1)
         X1(2)=Y1(2)*FCV(2)/FCL(2)
         XSUM=X1(1)+X1(2)
         F2=XSUM-1D0
         PP2=PP
         X1(1)=X1(1)/XSUM
         X1(2)=X1(2)/XSUM
         IF(DABS(XSUM-1D0).LT.1.D-9) GOTO 1000
         IF (ITER.EQ.1) THEN
            F1=XSUM-1D0
            PP1=PP2
            PP=PP1*.98D0
            GOTO 87
         ENDIF
         PP=(F1*PP2-F2*PP1)/(F1-F2)
         PP1=PP2
         F1=F2
C        INDEX=1
 87   CALL PRTPR(Y1,T,PP,FCV,NCOMP,0)
      YC(1)=(PS/PP)*(DEXP((V1S*(PP-PS))/(GASR*T))/FCV(1))
```

```
      DELY=DABS(Y1(1)-YC(1))/Y1(1)
C     INDEX=INDEX+1
C     IF (INDEX.GT.800) GOTO 100
      Y1(1)=YC(1)
      Y1(2)=1D0-Y1(1)
      IF (DELY.GE.1.D-9) GOTO 87
        GOTO 100
1000   CONTINUE
 70    RETURN
       END
*****************************************************************
*
*              PRTPR(X,T,P,FUGC,NCOMP,IST)
*
*   SUBROUTINE TO CALCULATE FUGACITY COEFFICIENT USING PR OR TPR EOS
* WITH KIJ AND/OR LIJ TYPE MIXING RULES.
*
* DEFINITION OF VARIABLES:
*   X(NCOMP): COMPOSITION FOR EACH COMPONENT IN LIQUID PHASE.
*   Y(NCOMP): COMPOSITION FOR EACH COMPONENT IN VAPOR PHASE.
*   T: TEMPERATURE.
*   P: PRESSURE.
*   FUGC(NCOMP): FUGACITY COEFFICIENT FOR EACH COMPONENT (OUTPUT).
*   NCOMP: NUMBER OF COMPONENTS. 20 MAXIMUM!
*
* IN COMMON BLOCK \PROP\ TC(3),PC(3),AC(3):
*   TC(3): CRITICAL TEMPERATURE FOR EACH COMPONENT.
*   PC(3):  CRITICAL PRESSURE FOR EACH COMPONENT.
*   AC(3): ACENTRIC FACTOR FOR EACH COMPONENT.
*
* IN COMMON BLOCK \BKCALC\ K(20,20),L(20,20),ZL,ZV :
*   K(20,20): KIJ VALUES.
*   L(20,20): LIJ VALUES.
*   ZL: LIQUID COMPRESSIBILITY FACTOR    (OUTPUT).
*   ZV: VAPOR COMPRESSIBILITY FACTOR     (OUTPUT).
*
*****************************************************************
C
      SUBROUTINE PRTPR(X,T,P,FUGC,NCOMP,IST)
      IMPLICIT DOUBLE PRECISION (A-H,O-Z)
      INTEGER I,NCOMP,IST,IMIX
      CHARACTER*3 IEOS,ICALC,CALC
      CHARACTER*5 IFUNCT
      CHARACTER*1 ITYPE
      REAL*8 K,L
      DIMENSION X(NCOMP),FUGC(NCOMP),Z(20)
     1          ,AIL(3),AIV(3),BIL(3),BIV(3),A(3),B(3),
     2           C(3),CIL(3),CIV(3),U(3),UIL(3),UIV(3),
     3           W(3),WIL(3),WIV(3)
      COMMON /PROP/ TC(20),PC(20),AC(20),ZC(20)
      COMMON /BKCALC/ K(20,20),L(20,20),M(20,20),ZL,ZV
      COMMON /EOS/ IEOS,ICALC,CALC,IFUNCT,ITYPE
      COMMON /RVP/ RVPG(2),RVPB(2),RVPM(2)
      COMMON /ANTO/ ANTA,ANTB,ANTC
      COMMON /NALP/ COEFN
```

```
C
C---- CALCULATE PURE COMPONENT A,B AND/OR C PARAMETERS.
C
C     WRITE (6,'(A8,A3,A2,A3)') 'PRTPR---',IEOS,'  ',ICALC
C     WRITE (6,*) 'IFUNCT---',IFUNCT
      DO 1000 I=1,NCOMP
         IF (IFUNCT.EQ.'SOAVE') THEN
            TR=T/TC(I)
            PR=P/PC(I)
            IF (IEOS.EQ.'TPR') THEN
               CALL EOSTPR(TR,PR,AC(I),A(I),B(I),U(I),W(I),I)
               C(I)=(2D0-U(I))/4D0*B(I)
            ELSE
               CALL EOSPR(TR,PR,AC(I),A(I),B(I),U(I),W(I),I)
            END IF
         ELSE
            IF (IFUNCT.EQ.'SUGIE') THEN
               TR=T/TC(I)
C              WRITE (7,*) 'TR=',TR
C              WRITE (6,*) 'TR=',TR
               IF (TR.GT.0.95D0) THEN
C                 WRITE (6,*)
C                 WRITE (7,*) 'COMPONENT IS SCF',I
C                 WRITE (6,*) 'COMPONENT IS SCF',I
                  PR=P/PC(I)
                  CALC='SCC'
               ELSE
C                 WRITE (6,*)
C                 WRITE (6,*) 'COMPONENT IS SUBCRITICAL',I
C                 WRITE (7,*) 'COMPONENT IS SUBCRITICAL',I
                  CALC='NOR'
C                 WRITE (6,*) 'RVP---',TR,RVPG(I),RVPB(I),RVPM(I)
                PR=DEXP(RVPB(I)*(1D0/TR**RVPM(I)-1D0)+RVPG(I)*(TR**7-1D0))
C                 WRITE (7,*) 'TEMP--',T
C                 WRITE (6,*) 'TEMP--',T
C                 WRITE (7,*) 'PR----',PR
C                 WRITE (6,*) 'PR----',PR
               ENDIF
               IF (IEOS.EQ.'TPR') THEN
                  CALL EOSTPR(TR,PR,AC(I),A(I),B(I),U(I),W(I),I)
                  C(I)=(2D0-U(I))/4D0*B(I)
               ELSE
                  CALL EOSPR(TR,PR,AC(I),A(I),B(I),U(I),W(I),I)
               END IF
            ELSE
               IF (IFUNCT.EQ.'NEW') THEN
                  TR=T/TC(I)
                  PR=P/PC(I)
                  IF (IEOS.EQ.'TPR') THEN
                     CALL EOSTPR(TR,PR,AC(I),A(I),B(I),U(I),W(I),I)
                     C(I)=(2D0-U(I))/4D0*B(I)
                  ELSE
                     CALL EOSPR(TR,PR,AC(I),A(I),B(I),U(I),W(I),I)
                  END IF
               ENDIF
```

```
*
* VARIABLES:
*   A(NCOMP): PURE COMPONENT PARAMETERS.
*   X(NCOMP): MOLE FRACTIONS OF EACH COMPONENT.
*   COEFA: INTERACTION COEFFICIENTS.(KIJ OR LIJ)
*   COEFB: INTERACTION COEFFICIENTS. (MIJ)
*   AMIX: MIXTURE PARAMETER (OUTPUT).
*   AI(NCOMP): THE DERIVATIVES D(N*A(I))/D(N(I)) (OUTPUT).
*   NCOMP: THE NUMBER OF COMPONENTS.
*   IXCOEF: ROW DIMENSION OF COEF IN THE CALLING PROGRAM.
*
**********************************************  **************************
C
      SUBROUTINE GEOMIX(A,X,COEFA,COEFB,AMIX,AI,NCOMP,IXCOEF)
      IMPLICIT DOUBLE PRECISION (A-Z)
      INTEGER I,J,NCOMP,IXCOEF
      CHARACTER*3 IEOS,ICALC,CALC
      CHARACTER*5 IFUNCT
      CHARACTER*1 ITYPE
      DIMENSION A(NCOMP),X(NCOMP),AI(NCOMP),COEF(20,20),COEFA(20,20)
      DIMENSION COEFB(20,20)
      COMMON /EOS/ IEOS,ICALC,CALC,IFUNCT,ITYPE
C
      AMIX=0D0
      DO 1001 I=1,NCOMP
         AI(I)=0D0
         DO 1001 J=1,NCOMP
            IF (ITYPE.EQ.'C') THEN
               COEF(I,J)=COEFA(I,J)
            ELSE
               IF (ITYPE.EQ.'A') THEN
                  COEF(I,J)=COEFA(I,J)+COEFB(I,J)*(X(I)-X(J))
               ENDIF
            ENDIF
            AMIX=AMIX+X(I)*X(J)*DSQRT(A(I)*A(J))*(1D0-COEF(I,J))
            AI(I)=AI(I)+2D0*X(J)*DSQRT(A(I)*A(J))*(1D0-COEF(I,J))
 1001 CONTINUE
      DO 1002 I=1,NCOMP
         AI(I)=AI(I)-AMIX
 1002 CONTINUE
C
      RETURN
      END
**********************************************************************
*
*            ARMIX(A,X,COEF,AMIX,AI,NCOMP,IXCOEF)
*
* SUBROUTINE FOR ARITHMETIC AVERAGE MIXING RULE.
*
* VARIABLES:
*   A(NCOMP): PURE COMPONENT PARAMETERS.
*   X(NCOMP): MOLE FRACTIONS OF EACH COMPONENT.
*   COEF(IXCOEF,NCOMP): INTERACTION COEFFICIENTS. (LIJ)
*   AMIX: MIXTURE PARAMETER (OUTPUT).
*   AI(NCOMP): THE DERIVATIVES D(N*A(I))/DN(I) (OUTPUT).
```

```
            SM=.37964D0+1.48503D0*AC-.16442D0*AC**2+.01667D0*AC**3
         END IF
         IF (IFUNCT.EQ.'SOAVE') THEN
            ALPHA=(1D0+SM*(1D0-DSQRT(TR)))**2
         ELSE
            IF (IFUNCT.EQ.'SUGIE') THEN
C              WRITE (6,*) 'EOSPR--OM',OMEGAC
C              WRITE (6,*) 'EOSPR--CALC',CALC
               IF (CALC.EQ.'SCC') THEN
                  ALPHA=(1D0+COEFN*(1D0-DSQRT(TR)))**2
               ELSE
                  POT=PR/TR
                  ALPHA=ALPTR(OMEGAC,POT,1.D-8,ZLB,ZVB)
               ENDIF
            ELSE
               IF (IFUNCT.EQ.'NEW') THEN
                  IF (I.EQ.1) THEN
                     ALPHA=1D0+1.125363D0*(1D0-TR**0.5D0)-0.1791811D0*(1D0-
     &                     TR)-0.002358876D0*(1D0-TR**2)

                     ALPHA=ALPHA**2
                  ELSE
                     ALPHA=1.007710D0*DEXP(0.5856143D0*(1D0-TR))
                  ENDIF
               ENDIF
            ENDIF
         ENDIF
C
C---- CALCULATE THE CONSTANTS
C
         IF (IFUNCT.EQ.'SOAVE') THEN
            A=ALPHA*OMEGAC*PR/TR**2
         ELSE
            IF (IFUNCT.EQ.'SUGIE') THEN
               IF (CALC.EQ.'SCC') THEN
                  A=ALPHA*OMEGAC*PR/TR**2
               ELSE
                  A=ALPHA*OMEGAC*PR/TR
               ENDIF
            ELSE
               IF (IFUNCT.EQ.'NEW') THEN
                  A=ALPHA*OMEGAC*PR/TR**2
               ENDIF
            ENDIF
         ENDIF
         B=OMEGBC*PR/TR
         W=2D0*((2D0-U)/4D0)**2-1D0
C
         RETURN
         END
*************************************************************************
*
*              GEOMIX(A,X,COEFA,COEFB,AMIX,AI,NCOMP,IXCOEF)
*
* SUBROUTINE FOR GEOMETRIC AVERAGE MIXING RULE.
```

```
      IF (IFUNCT.EQ.'SOAVE') THEN
         A=ALPHA*OMEGAC*PR/TR**2
      ELSE
         IF (IFUNCT.EQ.'SUGIE') THEN
            IF (CALC.EQ.'SCC') THEN
               A=ALPHA*OMEGAC*PR/TR**2
            ELSE
               A=ALPHA*OMEGAC*PR/TR
            ENDIF
         ELSE
            IF (IFUNCT.EQ.'NEW') THEN
               A=ALPHA*OMEGAC*PR/TR**2
            ENDIF
         ENDIF
      END IF
      B=OMEGBC*PR/TR
      W=-1D0
      RETURN
      END
*****************************************************************************
*
*                  EOSTPR(TR,PR,AC,A,B,U,W,I)
*
* SUBROUTINE TO CALCULATE THE CONSTANTS(A,B & C) FOR TRANSLATED PR EOS.
*
* YU'S VERSION, MODIFIED BY MIKE MARGERUM.
*
* VARIABLES:
*   TR: REDUCED TEMPERATURE.
*   PR: REDUCED PRESSURE.
*   AC: ACENTRIC FACTOR.
*   A,B,U,W: DIMENSIONLESS EOS CONSTANTS (OUTPUT).
*
*****************************************************************************
C
      SUBROUTINE EOSTPR(TR,PR,AC,A,B,U,W,I)
      IMPLICIT DOUBLE PRECISION (A-Z)
      INTEGER I
      CHARACTER*3 IEOS,ICALC,CALC
      CHARACTER*5 IFUNCT
      CHARACTER*1 ITYPE
      COMMON /EOS/ IEOS,ICALC,CALC,IFUNCT,ITYPE
C
C---- SET CRITICAL POINT VALUES.
C
      OMEGAC=0.45724D0
      U=1.5251D0+1.1146D0*AC+1.1538D0*AC**2
      OMEGBC=.3112D0/(2D0+U)
C     OMEGBC=.08835-.030051*AC-.0087911*AC*AC
C
C---- CALCULATE ALPHA OR ALPHA/TR
C
      IF (AC.LT..2D0) THEN
         SM=.37464D0+1.54226D0*AC-.26992D0*AC**2
      ELSE
```

```
C
      SUBROUTINE EOSPR(TR,PR,AC,A,B,U,W,I)
      IMPLICIT DOUBLE PRECISION (A-Z)
      INTEGER I
      CHARACTER*3 IEOS,ICALC,CALC
      CHARACTER*5 IFUNCT
      CHARACTER*1 ITYPE
      COMMON /EOS/ IEOS,ICALC,CALC,IFUNCT,ITYPE
      COMMON /NALP/ COEFN
C
C---- SET CRITICAL POINT VALUES.
C
      OMEGAC=0.4572400
      U=200
      OMEGBC=.077800
C
C
C---- CALCULATE ALPHA.
C
C
      IF (AC.LT..200) THEN
         SM=.37464D0+1.54226D0*AC-.26992D0*AC**2
      ELSE
         SM=.37964D0+1.48503D0*AC-.16442D0*AC**2+.01667D0*AC**3
      END IF
      IF (IFUNCT.EQ.'SOAVE') THEN
         ALPHA=(1D0+SM*(1D0-DSQRT(TR)))**2
      ELSE
         IF (IFUNCT.EQ.'SUGIE') THEN
C           WRITE (6,*) 'EOSPR--OM',OMEGAC
C           WRITE (6,*) 'EOSPR--CALC----',CALC
            IF (CALC.EQ.'SCC') THEN
               ALPHA=(1D0+COEFN*(1D0-DSQRT(TR)))**2
C              WRITE (6,*) 'ALPHA--SCC',ALPHA
C              WRITE (7,*) 'ALPHA--SCC',ALPHA
            ELSE
               POT=PR/TR
               ALPHA=ALPTR(OMEGAC,POT,1.D-8,ZLB,ZVB)
            ENDIF
         ELSE
            IF (IFUNCT.EQ.'NEW') THEN
               IF (I.EQ.1) THEN
                  ALPHA=1D0+1.125363D0*(1D0-TR**0.5D0)-0.179181ID0*(1D0-
     &                 TR)-0.002358876D0*(1D0-TR**2)

                  ALPHA=ALPHA**2
               ELSE
                  ALPHA=1.00771DD0*DEXP(0.5856143D0*(1D0-TR))
               ENDIF
            ENDIF
         ENDIF
      ENDIF
C
C---- CALCULATE THE CONSTANTS
C
```

```
          ENDIF
        ENDIF
 1000 CONTINUE
C
C---- CALCULATE MIXTURE'S A,B AND/OR C PARAMETERS
C
      IF (IEOS.EQ.'PR') THEN
         CALL GEOMIX(A,X,K,M,AL,AIL,NCOMP,NCOMP)
         CALL ARMIX(B,X,L,BL,BIL,NCOMP,NCOMP)
         UL=2D0
         WL=-1D0
         DO 1004 I=1,NCOMP
         UIL(I)=2D0
         WIL(I)=-1D0
 1004    CONTINUE
      ELSE
         CALL GEOMIX(A,X,K,M,AL,AIL,NCOMP,NCOMP)
         CALL ARMIX(B,X,L,BL,BIL,NCOMP,NCOMP)
         CALL ARMIX(C,X,L,CL,CIL,NCOMP,NCOMP)
         UL=2D0-4D0*CL/BL
         WL=2D0*(CL/BL)**2-1D0
         DO 1003 I=1,NCOMP
         UIL(I)=2D0-4D0*(CL/BL+CIL(I)/BL-BIL(I)*CL/BL**2)
         WIL(I)=2D0*CL/BL*(CL/BL+2D0*CIL(I)/BL-2D0*BIL(I)*CL/BL**2)-1D0
 1003    CONTINUE
      END IF
C
C---- CALCULATE MIXTURE'S COMPRESSIBILITY FACTOR.
C
      CALL ZEOS(AL,BL,UL,WL,Z,1)
      IF(IST.EQ.0) ZL=Z(2)
      IF(IST.EQ.1) ZL=Z(1)
C
C---- CALCULATE MIXTURE'S FUGACITY COEFFICIENTS
C
      DO 1002 I=1,NCOMP
         FUGC(I)=FGCOEF(AL,BL,UL,WL,AIL(I),BIL(I),UIL(I),WIL(I),ZL,1)
 1002 CONTINUE
      RETURN
      END
*****************************************************************************
*
*                  EOSPR(TR,PR,AC,A,B,U,W,I)
*
* SUBROUTINE TO CALCULATE THE CONSTANTS(A AND B) IN THE PR EOS.
*
* YU'S VERSION, MODIFIED BY MIKE MARGERUM.
*
* VARIABLES:
*   TR: REDUCED TEMPERATURE.
*   PR: REDUCED PRESSURE.
*   AC: ACENTRIC FACTOR.
*   A,B,U,W: DIMENSIONLESS EOS CONSTANTS (OUTPUT).
*
*****************************************************************************
```

```
*   NCOMP: THE NUMBER OF COMPONENTS.
*   IXCOEF: ROW DIMENSION OF COEF IN THE CALLING PROGRAM.
*
*****************************************************************
C
      SUBROUTINE ARMIX(A,X,COEF,AMIX,AI,NCOMP,IXCOEF)
      IMPLICIT DOUBLE PRECISION (A-Z)
      INTEGER I,J,NCOMP,IXCOEF
      DIMENSION A(NCOMP),X(NCOMP),AI(NCOMP),COEF(20,20)
C
      AMIX=0D0
      DO 1001 I=1,NCOMP
         AI(I)=0D0
         DO 1001 J=1,NCOMP
            AMIX=AMIX+X(I)*X(J)*(A(I)+A(J))/2D0*(1D0-COEF(I,J))
            AI(I)=AI(I)+2D0*X(J)*(A(I)+A(J))/2D0*(1D0-COEF(I,J))
 1001 CONTINUE
      DO 1002 I=1,NCOMP
         AI(I)=AI(I)-AMIX
 1002 CONTINUE
C
      RETURN
      END
*****************************************************************
*
*                  ZEOS(A,B,U,W,Z,ISTATE)
*
* THIS SUBROUTINE FINDS THE COMPRESSIBILITY FACTOR(S) FOR
* THE GENERIC CUBIC EQUATION OF STATE.
*
* VARIABLES:
*   A,B,U,W: DIMENSIONLESS PARAMETERS OF THE GENERIC CUBIC EOS.
*   Z(20): (OUTPUT) CALCULATED COMPRESSIBILITY FACTOR(S). SEE ISTATE.
*   ISTATE: (OUTPUT) IF SUPERCRITICAL, ISTATE=1, AND Z(1)=Z(2). IF NOT
*           SUPERCRITICAL, ISTATE=2, Z(1) IS THE LIQUID ROOT AND
*           Z(2) IS THE VAPOR ROOT.
*
* REQUIRED SUBROUTINE: RTCUB.
*
*****************************************************************
C
      SUBROUTINE ZEOS(A,B,U,W,Z,ISTATE)
      IMPLICIT DOUBLE PRECISION (A-Z)
      INTEGER ISTATE,NRT,NNEG
      DIMENSION RT(3),Z(20)
C
C---- CALCULATE ROOTS
C
      CALL RTCUB(U*B-B-1D0,
     1           (W-U)*B**2-U*B+A,-W*B**3-W*B**2-A*B,RT,NRT,NNEG)
C
C---- SELECT APPROPRIATE ROOT.
C
      IF (NRT.EQ.1) THEN
         ISTATE=1
```

```
         Z(1)=RT(1)
         Z(2)=RT(1)
      ELSE
         IF (NNEG.NE.0) THEN
            ISTATE=1
            Z(1)=RT(3)
            Z(2)=RT(3)
         ELSE
            ISTATE=1
            Z(1)=RT(1)
            Z(2)=RT(3)
         END IF
      END IF
      RETURN
      END
*****************************************************************************
*
*                  RTCUB (B,C,D,X,NROOT,NNEG)
*
* THIS SUBROUTINE FINDS THE REAL ROOT(S) THE CUBIC EQUATION:
*    X**3+B*X**2+C*X+D=0
*
* DEFINITION OF VARIABLES:
*   B,C,D: COEFFICIENTS OF THE CUBIC.
*   X(I): I'TH REAL ROOT OF THE CUBIC.
*   NROOT: NUMBER OF REAL ROOTS OF THE CUBIC.
*          IF MORE THAN 1, THE ROOTS WILL BE SORTED.
*   NNEG: NUMBER OF NEGATIVE ROOTS.
*
*****************************************************************************
C
      SUBROUTINE RTCUB (B,C,D,X,NROOT,NNEG)
      IMPLICIT DOUBLE PRECISION (A-Z)
      INTEGER I,J,NNEG,NROOT
      DIMENSION X(3)
C
C---- INITIALIZE QUANTITIES.
C
      NNEG=0
      P=(3D0*C-B**2)/3D0
      Q=(27D0*D-9D0*B*C+2D0*B**3)/27D0
      R=(P/3D0)**3+(Q/2D0)**2
C
C---CALCULATE ROOTS (SORTED), NUMBER OF ROOTS, NUMBER OF NEGATIVE ROOTS.
C
      IF (R.GE.0D0) THEN
         NROOT=1
         AU=DSIGN(DABS(-Q/2D0+DSQRT(R))**(1D0/3D0),-Q/2D0+DSQRT(R))
         BU=DSIGN(DABS(-Q/2D0-DSQRT(R))**(1D0/3D0),-Q/2D0-DSQRT(R))
         X(1)=AU+BU-B/3D0
         IF (X(1).LT.0D0) NNEG=1
      ELSE
         NROOT=3
         P1=DACOS(DSQRT(-Q**2/P**3*27D0/4D0))/3D0
         P2=DACOS(-1D0)*2D0/3D0
```

```
         DO 1000 I=1,3
            X(I)=-DSIGN(2D0,Q)*DSQRT(-P/3D0)*DCOS(P1+P2*DFLOAT(I))-B/3D0
            IF (X(I).LT.0D0) NNEG=NNEG+1
 1000    CONTINUE
C
C---- BUBBLE SORT.
C
         DO 1001 J=1,NROOT-1
         DO 1001 I=J+1,NROOT
            IF (X(J).GT.X(I)) THEN
               TEMP=X(I)
               X(I)=X(J)
               X(J)=X(I)
            END IF
 1001    CONTINUE
      END IF
C
      RETURN
      END
*****************************************************************************
*
*             FGCOEF(A,B,U,W,AI,BI,UI,WI,Z,ITY)
*
* THIS FUNCTION SUBROUTINE CALCULATES THE FUGACITY COEFFICIENT FOR THE
* GENERIC CUBIC EQUATION OF STATE. ALL PARAMETERS MUST BE INDEPENDENT
* OF DENSITY.
*
* VARIABLES:
*   FGCOEF: CALCULATED FUGACITY COEFFICIENT.
*   A,B,U,W: DIMENSIONLESS PARAMETERS OF THE GENERIC EOS.
*   AI,BI,UI,WI: D(N*PARAMETER)/D(NI).
*   Z: COMPRESSIBILITY FACTOR.
*   ITYPE: IF U**2-4*W=0, ITYPE=0. IF NOT, ITYPE=1.
*
*****************************************************************************
C
      FUNCTION FGCOEF(A,B,U,W,AI,BI,UI,WI,Z,ITY)
      IMPLICIT DOUBLE PRECISION (A-Z)
      INTEGER ITY
C
C---- CALCULATE FUGACITY COEFFICIENT. ACCOUNT FOR SPECIAL CASES.
C
      IF (A.EQ.0D0) THEN
         AIA=1D0
      ELSE
         AIA=AI/A
      END IF
      IF (B.EQ.0D0) THEN
         BIB=1D0
      ELSE
         BIB=BI/B
      END IF
      IF (U.EQ.0D0) THEN
         UIU=1D0
      ELSE
```

```
         UIU=UI/U
      END IF
      IF (ITY.EQ.0) THEN
         DID=1D0
         F1=-2D0/(2D0*Z+U*B)
      ELSE
         D=DSQRT(U**2-4D0*W)
         DID=(U*UI-2D0*(W+WI))/D**2
         F1=DLOG((2D0*Z+B*(U-D))/(2D0*Z+B*(U+D)))/B/D
      END IF
      F2=1D0/(Z**2+U*B*Z+W*B**2)
      FGCOEF=DEXP(BI/(Z-B)-DLOG(Z-B)+A*(2D0+AIA-BIB-DID)*F1
     1       +A*(Z*(1-BIB-DID)+U*B/2D0*(UIU-DID))*F2)
C     WRITE (6,*) 'FUGACITY COEFF.....',FGCOEF
C     WRITE (7,*) 'FUGACITY COEFF.....',FGCOEF
C
      RETURN
      END
*****************************************************************************
*
*                  PCONV(P,LIN,LOUT)
*
* SUBROUTINE FOR PRESSURE CONVERSIONS.
*
* VARIABLES:
*   P: PRESSURE.
*   LIN: INPUT UNITS.
*   LOUT: OUTPUT UNITS.
* LIN AND LOUT ARE CHARACTER*4 VARIABLES WHICH MUST BE ONE OF
* 'PSIA','MMHG',' ATM',' KPA',' ATM',' BAR'.
*
*****************************************************************************
C
      SUBROUTINE PCONV(P,LIN,LOUT)
      IMPLICIT DOUBLE PRECISION (A-Z)
      CHARACTER*4 LIN,LOUT
C
C---- CONVERT TO ATM.
C
      IF (LIN.EQ.'PSIA') P=P/14.696D0
      IF (LIN.EQ.'MMHG') P=P/760D0
      IF (LIN.EQ.' KPA') P=P/101.325D0
      IF (LIN.EQ.' MPA') P=P/101.325D0*1D3
      IF (LIN.EQ.' BAR') P=P/101.325D0*1D2
      IF (LIN.EQ.' ATM') P=P
C
C---- CONVERT TO DESIRED UNITS.
C
      IF (LOUT.EQ.'PSIA') P=P*14.696D0
      IF (LOUT.EQ.'MMHG') P=P*760D0
      IF (LOUT.EQ.' KPA') P=P*101.325D0
      IF (LOUT.EQ.' MPA') P=P*101.325D0/1D3
      IF (LOUT.EQ.' BAR') P=P*101.325D0/1D2
      RETURN
      END
```

```
C
C
*****************************************************************
*                            ALPTR
*
* Function subroutine to calculate ALPHA/TR to within TOL for any
* cubic EOS given OMEGAC (A at the critical point) and the ratio
* PRTR (Pr/Tr on the saturation curve at the Tr of interest).
* Also returns ZLB and ZVB (ZL-B and ZV-B) on the saturation curve.
* REQUIRES THE ROUTINES CUBRT AND SORT.
*****************************************************************
      FUNCTION ALPTR(OMEGAC,PRTR,TOL,ZLB,ZVB)
      IMPLICIT DOUBLE PRECISION (A-H,O-Z)
      DIMENSION ROOT(3)
C-----Check for valid OMEGAC!
      IF (OMEGAC.LT.0.42187500) THEN
         WRITE (6,*) '*** OMEGAC LESS THAN 0.421875 IN ALPTR ***'
         RETURN
      ENDIF
C-----Initialize quantities.
      DUMMY1=OMEGAC**(1D0/3D0)
      DUMMY2=DSQRT(4D0*OMEGAC-3D0*OMEGAC**(2D0/3D0))
      F=1D0-DUMMY1
      G=(DUMMY1+DUMMY2)/2D0
      H=(DUMMY1-DUMMY2)/2D0
      ALPTR=(1D0-F/(1D0-F)*DLOG(PRTR))
C-----Successive substitution to find alpha/Tr.
 1020 CONTINUE
         ALPTRN=ALPTR
C--------Find ZV-B and ZL-B by solving a cubic.
         CALL CUBRT(PRTR*(1D0-3D0*F)-1D0,
     &              PRTR**2*F**3-PRTR*(1D0-3D0*F-OMEGAC*ALPTRN),
     &             -PRTR**2*F**3,ROOT,NROOT,NNEG)
         ZLB=ROOT(1)
         ZVB=ROOT(3)
         IF (OMEGAC.EQ.0.42187500) THEN
C-----------Use this if OMEGAC=27/64 (ie. C=0, eg. VDW eos).
            ALPTR=(ZLB-ZVB+DLOG(ZVB/ZLB))/OMEGAC/PRTR/(ZVB-ZLB)*
     &           (ZLB+PRTR*(G-F))*(ZVB+PRTR*(G-F))
         ELSE
C-----------Use this if OMEGAC>27/64 (most equations of state).
            ALPTR=(H-G)*(ZLB-ZVB+DLOG(ZVB/ZLB))/OMEGAC/
     &            LOG((ZVB+PRTR*(G-F))*(ZLB+PRTR*(H-F))/
     &                (ZVB+PRTR*(H-F))/(ZLB+PRTR*(G-F)))
         ENDIF
C-----Check if converged.
      IF (DABS(ALPTRN-ALPTR).GE.TOL) GO TO 1020
C     WRITE (6,*) 'ALPTR.....',ALPTR
C     WRITE (7,*) 'ALPTR.....',ALPTR
      RETURN
      END
*****************************************************************
*                          CUBRT
*
* This subroutine finds the NROOT real roots X of the cubic equation
```

```
* X**3+B*X**2+C*X+D=0. It sorts the roots and returns the number of
* negative roots NNEG. Requires the subroutine SORT.
************************************************************************
      SUBROUTINE CUBRT(B,C,D,X,NROOT,NNEG)
      IMPLICIT DOUBLE PRECISION (A-H,O-Z)
      DIMENSION X(3)
C-----Initialize important quantities.
      NNEG=0
      P=(3D0*C-B**2)/3D0
      Q=(27D0*D-9D0*B*C+2D0*B**3)/27D0
      R=(P/3D0)**3+(Q/2D0)**2
C-----Calculate roots, NROOT, NNEG.
      IF (R.GE.0D0) THEN
         NROOT=1
         AU=DSIGN(DABS(-Q/2D0+DSQRT(R))**(1D0/3D0),-Q/2D0+DSQRT(R))
         BU=DSIGN(DABS(-Q/2D0-DSQRT(R))**(1D0/3D0),-Q/2D0-DSQRT(R))
         X(1)=AU+BU-B/3D0
         IF (X(1).LT.0D0) NNEG=1
      ELSE
         NROOT=3
         P1=DACOS(DSQRT(-Q**2/P**3*27D0/4D0))/3D0
         P2=DACOS(-1D0)*2D0/3D0
         DO 1000 I=1,3
            X(I)=-DSIGN(2D0,Q)*DSQRT(-P/3D0)*DCOS(P1+P2*DFLOAT(I))-B/3D0
            IF (X(I).LT.0D0) NNEG=NNEG+1
 1000    CONTINUE
         CALL SORT(X,3)
      END IF
      RETURN
      END
************************************************************************
*                              SORT
*
* Sorts an array into ascending numerical order using the heapsort
* algorithm. From "Numerical Recipes".
************************************************************************
      SUBROUTINE SORT(RA,N)
      IMPLICIT DOUBLE PRECISION (A-H,O-Z)
      DIMENSION RA(N)
      L=N/2+1
      IR=N
   10 CONTINUE
         IF (L.GT.1) THEN
            L=L-1
            RRA=RA(L)
         ELSE
            RRA=RA(IR)
            RA(IR)=RA(1)
            IR=IR-1
            IF (IR.EQ.1) THEN
               RA(1)=RRA
               RETURN
            ENDIF
         ENDIF
         I=L
```

```
      J=L+L
20    IF (J.LE.IR) THEN
         IF (J.LT.IR) THEN
            IF (RA(J).LT.RA(J+1)) J=J+1
         ENDIF
         IF (RRA.LT.RA(J)) THEN
            RA(I)=RA(J)
            I=J
            J=J+J
         ELSE
            J=IR+1
         ENDIF
      GOTO 20
      ENDIF
      RA(I)=RRA
   GOTO 10
   END
```